8

A Comparison of 3D Gait Models Based on the Helen Hayes Hospital Marker Set

Dudley Tabakin

Submitted to the Faculty of Health Sciences at the University of Cape Town in partial fulfilment of the requirements for the degree of Master of Science in Biomedical Engineering.

Cape Town

July, 2000

Declaration

I, DUDLEY RALPH TABAKIN, hereby declare that the work on which this thesis is based is my original work (except where acknowledgements indicate otherwise) and that neither the whole nor any part of it has been, is being or is to be submitted for any other degree in this or any other University.

I empower the University to reproduce for purpose of research, either the whole or part of the contents of this thesis in any manner.

Signed by candidate

Signature

10 JULY 2000

Date

Abstract

Three-dimensional motion capture equipment and the calculation of kinematics and kinetics are regularly used in the assessment of gait for clinical and operative intervention. Different laboratories use different commercially available gait analysis packages and these packages use different algorithms to determine the embedded joint axes, joint centres, joint angles, body segment parameters and resultant joint moments.

This study compares three commercial gait analysis packages, Vicon Clinical Manager (VCM), GaitLab 2.0 (GL) and Peak Motus 2000 (PM) with a standard model developed using the Vicon BodyBuilder (BB) software package. All these packages use the same modified Helen Hayes Hospital marker set for external marker placement. BB, GL and PM all use the same algorithms described by Vaughan *et al.* (1999) to calculate the gait parameters, while VCM uses algorithms described by Kadaba *et al.* (1990) and Davis *et al.* (1991). The gait parameters compared include: pelvic tilt, obliquity and rotation angles, hip and knee flexion-extension and abduction-adduction angles, ankle flexion-extension angles, and hip, knee and ankle flexion-extension moments. Twenty subjects ranging from age eight to fifty were analysed using the six camera Vicon motion analysis system and an AMTI force plate. The data were compared using a repeated measures analysis of variance and Scheffés *post-hoc* comparison at 10% increments in the gait cycle from 0% to 90%.

The results showed significant differences ($p<0.01$) between BB and VCM for the ankle flexion-extension angle and for the hip abduction-adduction angle from 30% to 60% of the gait cycle. The ankle angle in VCM displays less plantar flexion than BB, while the hip abduction-adduction angle shows greater adduction. Significant differences ($p<0.01$) were also noted at 50% and 60% of the hip flexion-extension moment, at 60% of the knee flexion-extension moment and at 50% of the ankle flexion-extension moment. Small differences were noted between BB and GL which were not statistically significant. Significant differences ($p<0.01$) were noted between BB and PM for the hip and knee flexion-extension moments, which occurred at approximately the same points as the differences between BB and VCM.

The differences between BB and VCM in joint angle can probably be explained by the different algorithms used to calculate the segment reference axes and joint centres. The differences in joint moments can be accounted for by the different joint centre calculations as well as the methods used to estimate body segment parameters. The body segment parameters will only have a large effect on the joint moments during the swing phase of the gait cycle. Filtering techniques may also compound the differences between BB and VCM. The different filtering techniques account for the small differences observed between BB and GL. The differences in joint moment calculations between BB and PM can be accounted for by the different methods of estimating the body segment parameters and possibly also the filtering techniques used by the different packages.

The gait clinician should realise that the different gait analysis software packages produce results which may be statistically different. The differences, particularly between BB and VCM for the ankle flexion-extension angle, must be taken into account when comparing data between laboratories that use different gait analysis software packages. If these differences are not noted, differing clinical decisions could be made with the same set of data, depending on the software package used.

Acknowledgements

The research that follows was completed with the support, encouragement and patience of a number of dynamic people. Thank you!

Professor C.L. Vaughan, head of the Department of Biomedical Engineering, UCT, for his guidance and patience as thesis supervisor and for organising financial assistance.

Professor Mike Lambert, BERU, UCT for assisting me with ideas for the statistical analysis of my data.

Geoff Shaw, Martin Lyster and Oxford Metrics, for allowing me to use the VCM gait analysis software package and assisting me with modelling in BodyBuilder.

Gary Scheirman, Suzanne Barnes and Peak performance Technologies, for allowing me to use and helping me with the Peak Motus 2000 gait analysis software package.

The staff and fellow students of the Department of Biomedical Engineering, UCT, for their ideas and input.

The staff and students at the Sports Science Institute of South Africa and BERU, UCT, for volunteering themselves and their children to act as subjects.

My parents and brothers who encouraged and supported my move to Biomedical Engineering and who continue to be enthusiastic about my future plans.

Table of Contents

List of Figures

List of Tables

Abbreviations

BB	BodyBuilder model development software from Oxford Metrics
GL	GaitLab 2.0 gait analysis software
VCM	Vicon Clinical Manager gait analysis software
PM	Peak Motus 2000 gait analysis software
PAT	Pelvic angle tilt
PAO	Pelvic angle obliquity
PAR	Pelvic angle rotation
HAF	Hip flexion-extension angle
HAA	Hip abduction-adduction angle
KAF	Knee flexion-extension angle
KAA	Knee abduction-adduction angle
AAF	Ankle flexion-extension angle
HMF	Hip flexion-extension moment
KMF	Knee flexion-extension moment
AMF	Ankle flexion-extension moment
AJC	Ankle joint centre
KJC	Knee joint centre
HJC	Hip joint centre
Nm	Newton metre
Hz	Hertz (cycles per second)
LL	Leg length
W	Weight

Chapter 1

Introduction

Walking is a cyclic pattern of body movements that is characterised by smooth regular and repeating movements (Rose and Gamble, 1994; Vaughan, 1996). Gait analysis is important for quantifying normal and pathological patterns of locomotion (Kadaba *et al.*, 1990; Grood and Suntay, 1983). It is the systematic measurement, description and assessment of the biomechanical parameters which characterise gait (Davis *et al.*, 1991).

The sequence of events that take place for walking to occur are summarised by Vaughan (1996) and Vaughan *et al.* (1992 and 1999):

1. Registration and activation of the instruction to walk in the central nervous system;
2. Transmission of the gait signals to the peripheral nervous system;
3. Contraction of muscles that develop tension;
4. Generation of forces at, and moments across the synovial joints;
5. Regulation of joint forces and moments by the rigid body segments based on their anthropometry;
6. Displacement of these segments in a manner that is recognised as functional gait; and
7. Generation of ground reaction forces.

The complete gait cycle is broken up into two phases, the stance phase and the swing phase. These two phases are further divided into smaller stages. Stance phase is the first part of the gait cycle and starts at heel strike, moves through to midstance, and ends at toe off. The stance phase of the gait cycle normally accounts for 60 % of the cycle. The swing phase of the gait cycle starts at toe off, moves through midswing and ends at heel strike, and this phase accounts for the remaining 40 % of the gait cycle (Vaughan *et al.*, 1992; Rose and Gamble, 1994).

The current methods of gait analysis include visual assessment, electrogoniometers,

electromyography, kinematic and kinetic analysis systems (Davis *et al.,* 1991; Kadaba *et al.,* 1990). Of these methods, the most commonly used is that of combined kinematic and kinetic systems. These systems require the measurement of four main components:

1. Ground reaction forces with a forceplate or pressure plate;
2. Kinematic data with cameras and markers, which provide segment displacements, joint angles, velocities and acceleration;
3. Anthropometric measurements of skeletal segments, which provide inertial properties of the segments; and
4. Electromyography, which provides information on muscle recruitment and activation.

By combining the ground reaction forces, kinematic data and anthropometric measurements, the resultant joint forces and moments can be derived. Vaughan *et al.* (1992) describe this approach as the inverse dynamics problem, in which the motion is defined in great detail and the forces causing that motion must be determined.

This study uses a motion capture technique. Between 1945 and 1947, Eberhardt and Inman developed the methods of three-dimensional analysis and for the first time used three cameras, generally viewing the object from the front, from one side and from above or below (Cappozzo and Paul, 1997). Since this early development, advances have been exponential with the introduction of the digital computer. Optoelectronic stereophotogrammetric systems have since been developed and the optimal estimation of bone position and the orientation of bones during movement based on surface marker positions have been established (Cappozzo and Paul, 1997). However, there is more than one method for estimating bone positions from surface markers and there are also at least two different configurations for surface marker placements in general clinical use. This study examines one surface marker set and compares the bone position estimation algorithms within the gait analysis software programs.

Real-time motion capture has now become a reality, and marker identification and three-dimensional marker reconstruction has become complex. In most cases, marker identification in the gait analysis laboratory is solved by using a multi-camera system of

three or more cameras. Each marker must be seen by at least two cameras in order to be reconstructed in three dimensions. Three-dimensional reconstruction is done using software which implements direct linear transformation methods or a forward intersection method (Furnée, 1997).

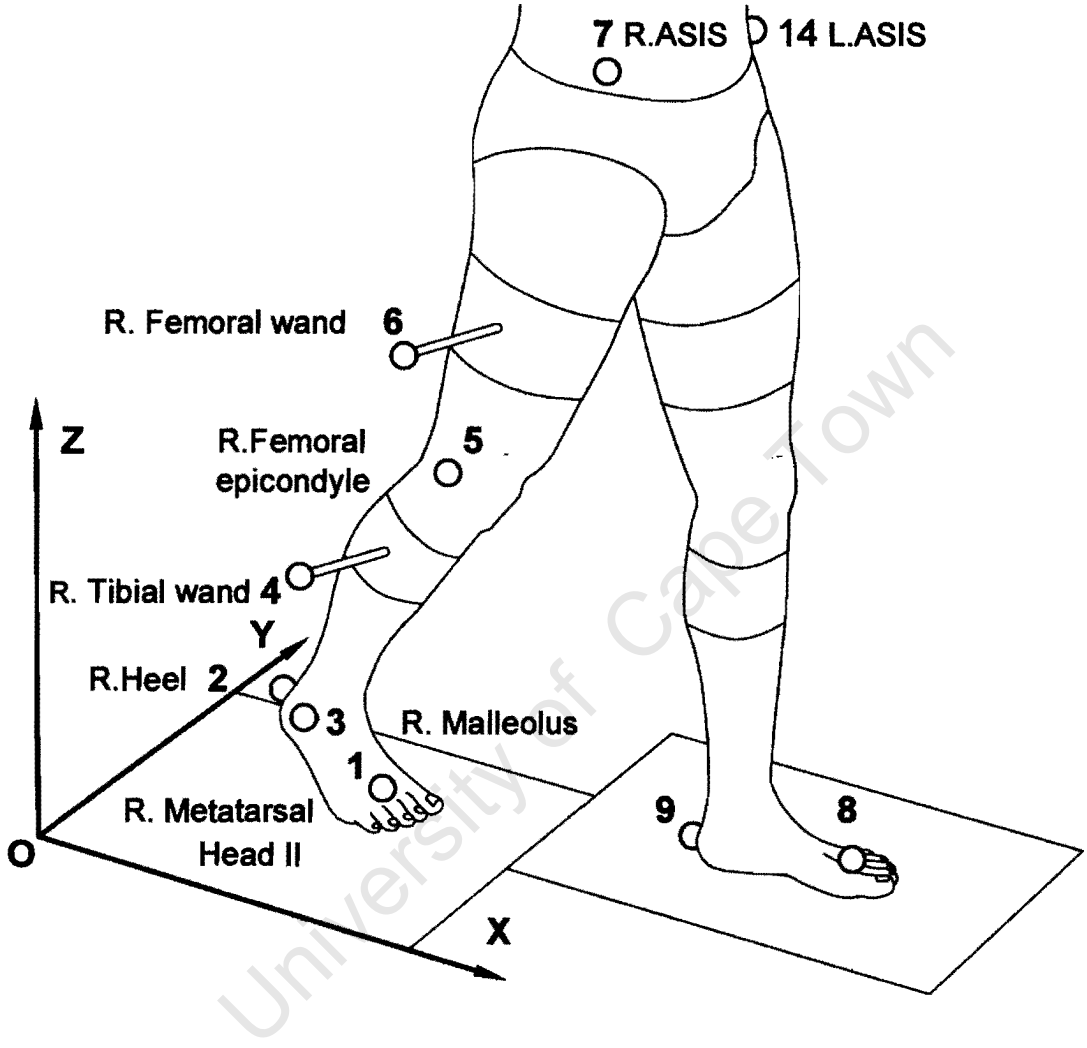

Figure 1.1 Helen Hayes Hospital Marker Set, seen from the front right side, from Vaughan *et al.* (1999)

The measurement of joint angle motion requires the tracking of closely spaced markers. The external marker system must be simple but still rigorous enough to define the relative motion of the rigid body segments in three dimensions (Kadaba *et al.*, 1990). One such commonly used set was developed at the Helen Hayes Hospital by Kadaba *et al.* (1990) and the modified version used in this study can be seen in Figures 1.1 and 1.2. This external marker set allows the calculation of an embedded bone axis and therefore an estimation of joint centres and segment orientations. Although the

Helen Hayes Hospital marker set is used in most commercial gait packages, the method of calculating the joint centres and segment orientations, as well as the resultant forces, moments and powers differ.

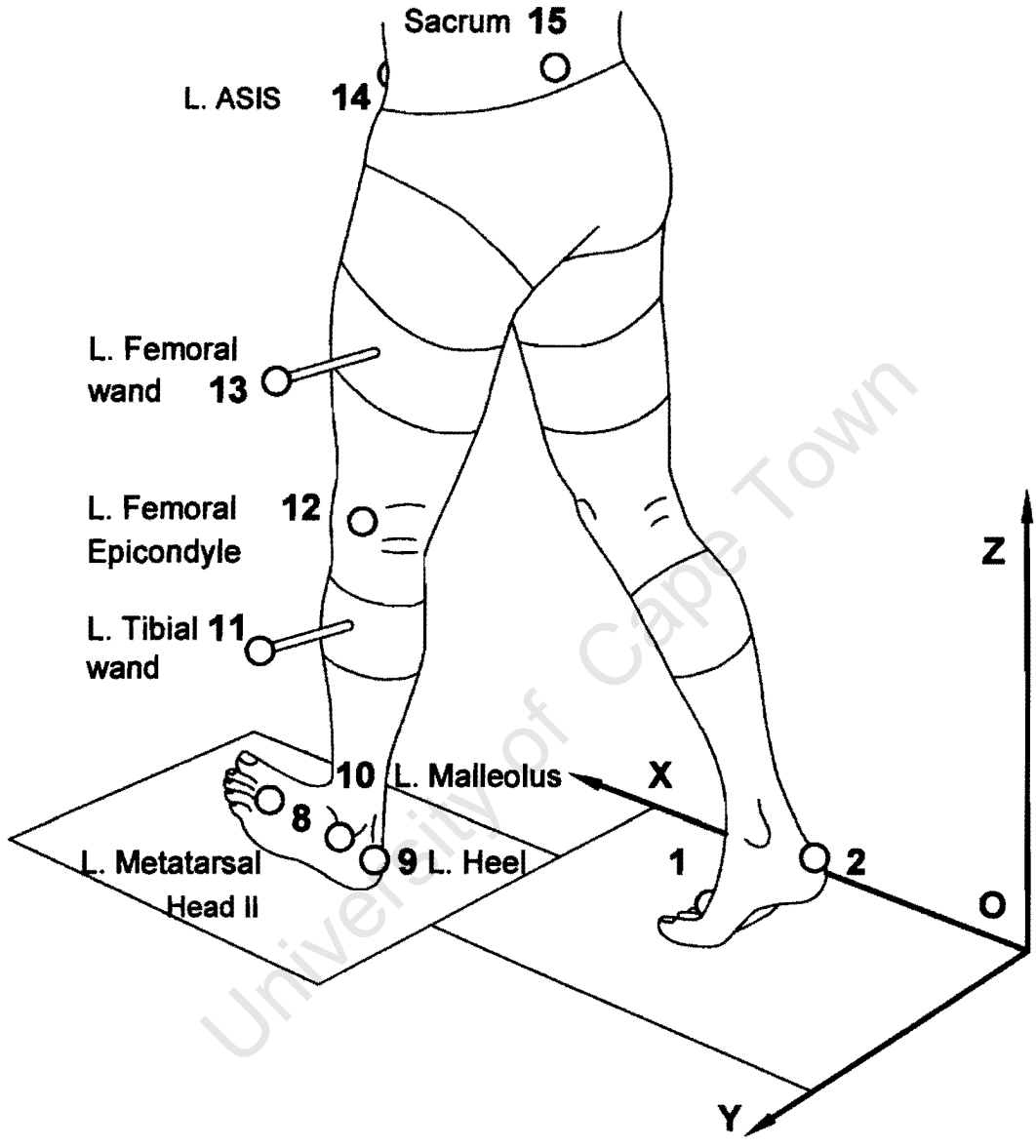

Figure 1.2 Helen Hayes Hospital Marker Set, seen from the back left side, from Vaughan *et al.* (1999)

The marker placement is important for defining segment orientations. Three non-colinear markers are needed to define a segment in three-dimensional space and with six degrees of freedom. In the modified Helen Hayes Hospital marker set used in this study (Figures 1.1 and 1.2), markers 7, 14 and 15 define the pelvis segment. The thigh segments are defined by the hip joint centres and markers 5 and 6, and 12 and 13 for the right and left thighs respectively. The calf segments are defined by the knee joint

centres and markers 3 and 4, and 10 and 11 respectively, while the foot segments are defined by markers 1, 2 and 3 for the right foot and 8, 9 and 10 for the left. This segment definition, along with the kinetic data obtained from a force platform, is required to calculate joint angles, segment orientations, resultant forces and moments and joint powers.

The fundamental objectives of the interpretation process of gait analysis are to identify the patient's gait attributes that are different from normal, suggest the possible cause of these abnormalities, and recommend clinical or operative treatment alternatives (Davis *et al.*, 1997). Davis *et al.* (1997) also describe the gait data, which are routinely made available to assist in clinical decision making. They are:

- Three-dimensional angles for each lower extremity joint as well as the pelvis and torso over the gait cycle;
- Three-dimensional joint moments, forces and powers over the gait cycle for each lower extremity joint;
- Step length and cadence;
- Video recordings; and
- EMG recordings of the gait cycle of the major lower extremity muscles.

The clinical application of gait analysis allows the clinician to quantitatively evaluate an individual's gait (Davis *et al.*, 1991). The results obtained from the various gait analysis models are often used in clinical assessments of pathological gait and decisions on operative intervention. However, different models use different mathematical algorithms. With this in mind, a question arises as to how comparable the various models are. If the results obtained using different models are not statistically different, then the models can be compared and clinical assessments and operative decisions may be vindicated. If however the difference in results is substantial, the results of some models may suggest one form of clinical intervention while others may suggest a completely different form of intervention.

In 1981 Brand and Crowninshield commented that gait analysis was then an evaluation tool and not a diagnostic tool. Although advances in technology have led to advanced

real-time data capture systems, little has changed in terms of the acceptance of gait analysis as a diagnostic tool. Davis *et al.* (1997) state that a fundamental problem of computerised gait analysis is the effective reporting of gait data that facilitate information integration and interpretation, and that inconsistencies in the reporting of gait data have contributed to the relatively limited acceptance of gait analysis as a clinical tool.

The accurate interpretation of gait data will require a standardisation or at least a close correspondence between the results obtained using the different gait analysis models. Effective application of any gait analysis method depends on the refinement of the instruments and technique involved, as well as the experience of the investigator (Chao, 1980).

Gait analysis models need to provide results, which are in agreement with each other before gait analysis can become more of a diagnostic tool. Therefore the purpose of this study was to compare the results from different commercially available gait analysis packages with the intention of considering whether clinical assessments and decisions to operate can be compared and justified using these different models.

Chapter 2

Literature Review

The simulation of human movement may be used to: understand neuromuscular disorders; make treatment decisions; improve athletic performance; understand posture and balance and evaluate muscle function (Barnes *et al.*, 1997).

Davis *et al.* (1991) explain that in gait analysis, kinematic and kinetic data are acquired and analysed to provide information which describes the fundamental gait characteristics and which is interpreted by the clinician to form an assessment.

The gait parameters, which include joint centres, segment orientations, joint angles, resultant joint forces and moments and joint powers are determined in the different gait analysis software packages using different mathematical algorithms. Potentially, these differences make it difficult for gait analysis to be compared between different gait laboratories. Some of the differences in the mathematical algorithms are presented below.

In their book *Dynamics of Human Gait*, Vaughan *et al.* (1999) describe human gait with a top down approach. The process starts as a nerve impulse in the central nervous system and ends with the generation of ground reaction forces. This approach is based on cause and effect.

Vaughan *et al.* (1999) describe the inverse dynamics approach by which the gait analyst may calculate the resultant forces and moments causing the motion. The inverse dynamics approach is used to calculate the gait parameters in all the gait analysis software programs compared in this study. Figure 2.1 illustrates this approach. The anthropometry, segment displacements and ground reaction forces are all measurable quantities.

Vaughan *et al.* (1999) describe how to combine these measurable quantities, so that the resultant forces and moments acting at the joints in the lower extremities may be calculated.

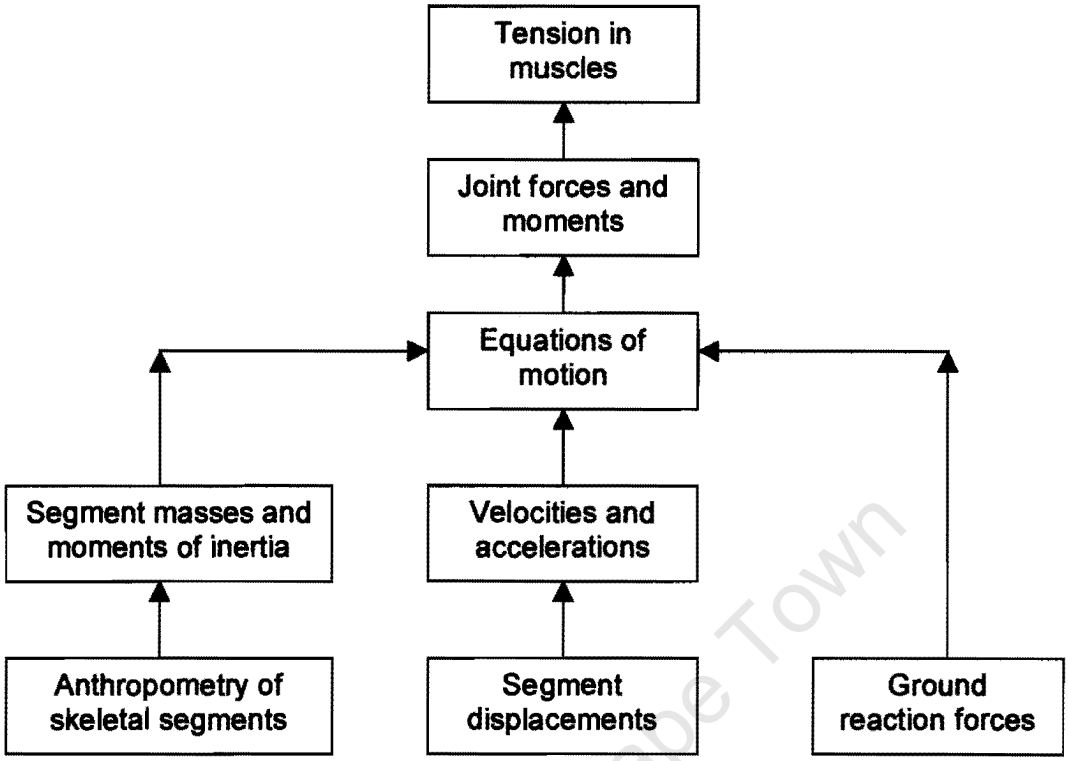

Figure 2.1 Flow chart of the inverse dynamics problem described by Vaughan *et al.* (1999)

2.1 Body Segment Parameters

The first step in a gait analysis model is to calculate the body segment parameters. Body segment parameters include the segment masses, segment centres of gravity and moments of inertia.

Vaughan *et al.* (1999) explain that first the analyst needs to measure body segment parameters, which are personalised for each subject. Body segment parameters include:

- The mass of the individual segments in kg;
- the centre of gravity location of the each segment relative to anatomical landmarks; and
- the moment of inertia of the segments (in $kg.m^2$) about three orthogonal axes.

The selection of individual segments is also important. Vaughan *et al.* (1999) choose a six-segment model, which includes the left and right thigh, calf and foot. An

assumption is made that the dimensions of these are rigid segments and do not change during the gait cycle. This model is chosen for simplicity, and as it is plain that the foot is not a rigid segment, it is realised that the model has its limitations. All the gait analysis packages compared in this study use the six-segment model.

There are various approaches that can be followed to estimate body segment parameters. Vaughan *et al.* (1999) describe some of these approaches:

- Cadaver averages;
- Reaction board;
- Mathematical modelling;
- Gamma ray, computed axial tomography or magnetic resonance imaging; and
- Kinematic measurements.

Each of these approaches has limitations. Vaughan *et al.* (1999) describe an approach for estimating body segment parameters, which they believe optimises the calculations. This technique has the following attributes:

- Personalised for individuals;
- Short time required to take measurements;
- Inexpensive and safe;
- Reasonably accurate.

The different gait analysis models use different approaches to estimate the body segment parameters. Vaughan *et al.* (1999) use a modelling procedure, which is based on a cadaveric study by Chandler *et al.* (1975). This approach can be seen in chapter three where it is used to estimate the body segment parameters in the BodyBuilder model. Davis *et al.* (1991) derive their body segment parameters based on a simple relationship described by Dempster *et al.* (1959).

The estimation of body segment parameters has a direct impact on the calculation of joint centres, segment masses and centres of gravity, which in turn affects the joint kinetics. As can be seen, there are different methods of determining these parameters. GaitLab 2.0 and the BodyBuilder model use the modelling procedure based on

assumption is made that the dimensions of these are rigid segments and do not change during the gait cycle. This model is chosen for simplicity, and as it is plain that the foot is not a rigid segment, it is realised that the model has its limitations. All the gait analysis packages compared in this study use the six-segment model.

There are various approaches that can be followed to estimate body segment parameters. Vaughan *et al.* (1999) describe some of these approaches:

- Cadaver averages;
- Reaction board;
- Mathematical modelling;
- Gamma ray, computed axial tomography or magnetic resonance imaging; and
- Kinematic measurements.

Each of these approaches has limitations. Vaughan *et al.* (1999) describe an approach for estimating body segment parameters, which they believe optimises the calculations. This technique has the following attributes:

- Personalised for individuals;
- Short time required to take measurements;
- Inexpensive and safe;
- Reasonably accurate.

The different gait analysis models use different approaches to estimate the body segment parameters. Vaughan *et al.* (1999) use a modelling procedure, which is based on a cadaveric study by Chandler *et al.* (1975). This approach can be seen in chapter three where it is used to estimate the body segment parameters in the BodyBuilder model. Davis *et al.* (1991) derive their body segment parameters based on a simple relationship described by Dempster *et al.* (1959).

The estimation of body segment parameters has a direct impact on the calculation of joint centres, segment masses and centres of gravity, which in turn affects the joint kinetics. As can be seen, there are different methods of determining these parameters. GaitLab 2.0 and the BodyBuilder model use the modelling procedure based on

Vaughan *et al.* (1999) while Vicon Clinical Manager and Peak Motus 2000 use the relationships described by Dempster *et al.* (1959).

2.2 Marker Positions

Cappello *et al.* (1997) suggest how marker points need to be selected:

1. Sufficient measurements of each marker should be available. The light reflected from the markers should be visible to sufficient cameras for identification.
2. The number of markers associated with each bone must be more than or equal to three.
3. The distance between markers and the offset of the marker from any line joining two others on the same bone must be sufficiently large to avoid error propagation from reconstructed marker co-ordinates to bone orientation.
4. The relative movement between markers and the underlying bone should be minimal.
5. Mounting the markers on the subject should be quick and easy.

A modified Helen Hayes Hospital marker set is used in this study and can be seen in Figures 1.1 and 1.2. This marker set has been modified from the marker sets described by Kadaba *et al.* (1990) and Davis *et al.* (1991). The modified Helen Hayes marker set makes use of the heel marker, while the original marker set does not describe the use of a heel marker. A common marker set is used in all the gait analysis software packages analysed in this study, therefore the variations which may exist because of the use of different marker sets is eliminated.

Vaughan *et al.* (1999) explain the advantages and disadvantages of the marker set used in this study. Advantages include: Markers are easy to track in three-dimensional space with video based kinematic systems; and provide more accurate orientation of the segment in three-dimensional space. Disadvantages are that the wands encumber the subject; and with jerky movement the wands will vibrate and move relative to the underlying skin.

Vaughan *et al.* (1999) continue to explain that one of the problems in capturing kinematic data is that the analyst is interested in the position of the underlying skeleton but he or she is only able to measure the positions of the external landmarks.

Cappello *et al.* (1997) state that reconstructed marker trajectories are not stationary with respect to the underlying bone, which is in contradiction with the objective of reconstructing a bone embedded reference axis and is the problem which has prevented motion analysis from supporting the clinical interpretations as it could. They describe two types of undesired movement: The error of marker co-ordinate reconstruction in the laboratory frame; and the relative movement between the marker and the underlying bone (skin movement artefacts). Segment embedded axis modelling procedures often do not accommodate these artefacts and assume the marker cluster to be rigid with the bone and not deformable.

Cappello *et al.* (1997) describe two methods of segment axis estimation from external markers. The first is a non-optimal estimation from three-marker clusters. A local reference frame can be defined starting with the co-ordinates of three non-collinear markers. This assumes that the position of the three markers is error free. The second method is the least squares estimation from a cluster of more than three markers, which attempts to account for the lack of accuracy in marker placement.

In a study described by Cappello *et al.* (1997), they conclude that even when four well distributed markers are selected to form a cluster, errors in bone orientation and position have a root mean square value in the order of 3° and 3 mm respectively and this requires attention to avoid excessive influence on the description of joint mechanics.

The gait models compared in this study use non-optimal methods to calculate the bone embedded axes. This method is used in the gait models, because of the problems with the number of markers needed. A large number of markers may cause subject encumbrance and may also violate one of Cappello's suggestions for marker placement, in that error propagation might occur because of confusion between the markers.

Errors occurring as a result of marker placement are therefore almost inevitable. However the focus of this study is not marker positioning and the gait parameters are calculated from a common marker set.

2.3 Segment Axes and Joint Centres

Grood and Suntay (1983) explain that the motions which occur in most anatomical joints involve three-dimensional movement, which is described by six independent co-ordinates or degrees of freedom. Three are translations and three are rotations. To construct a co-ordinate system for any joint system, it is necessary to specify: the cartesian co-ordinate system fixed in each bone, to describe its shape; the body fixed axes of the joint co-ordinate system and reference axes of the joint co-ordinate system used to describe the relative motion between the two bones; and the location of the translation reference points.

They suggest that it is convenient to establish the cartesian systems in each bone so that two of their axes correspond to the body fixed and reference axes of the joint co-ordinate system and to locate the origin of the cartesian systems coincident with the translation points or centres of gravity.

The purpose of a co-ordinate system is to allow the relative position between two bodies to be specified. The description of motion is the characterisation of how their relative position changes with time.

Davis *et al.* (1991) determine the instantaneous orientation of an orthogonal marker based, embedded co-ordinate system for each segment: trunk; pelvis; thighs; shanks; and feet. The Davis method of calculating the bone embedded co-ordinate system is described below. The pelvic co-ordinate system is constructed from the three-dimensional location vectors of the three pelvic markers (Right and Left anterior superior iliac spines (ASIS) and Sacrum). First two vectors are defined.

$$\mathbf{V}_1 = 0.5(\text{Right ASIS} + \text{Left ASIS}) - \text{Sacrum} \qquad 2.1$$

$$\mathbf{V}_2 = \text{Left ASIS} - \text{Right ASIS} \qquad 2.2$$

V_2 is then normalised to define a unit vector $\mathbf{u}_y$ and a third vector is computed:

$$\mathbf{V}_3 = \mathbf{V}_1 - (\mathbf{V}_1 \bullet \mathbf{u}_y)\,\mathbf{u}_y \qquad 2.3$$

V_3 is normalised to become unit vector $\mathbf{u}_x$ and finally unit vector $\mathbf{u}_z$ is computed from the cross product of $\mathbf{u}_x$ and $\mathbf{u}_y$. A similar process is repeated for each of the other body segments.

Davis *et al.* (1991) describe their approach for determining joint centres as follows. Each joint centre is calculated relative to the associated embedded co-ordinate system described above. The hip centre is located relative to the origin of the pelvic embedded co-ordinate system, the knee centre relative to the origin of the thigh embedded segment and the ankle relative to the origin of the shank embedded co-ordinate system.

The basis for the algorithm to locate the hip joint centre was developed at Newington Children's' Hospital in 1981 through radiographic examination of 25 hips. Three constants are produced for the model (Figure 2.2). $\theta = 28.4^{\circ}$ ($\pm 6.6^{\circ}$), $\beta = 18^{\circ}$ ($\pm 4^{\circ}$) and C, which is a function of leg length and can be predicted with the equation:

$$C = 0.115(\text{LegLength}) - 0.0153. \qquad 2.4$$

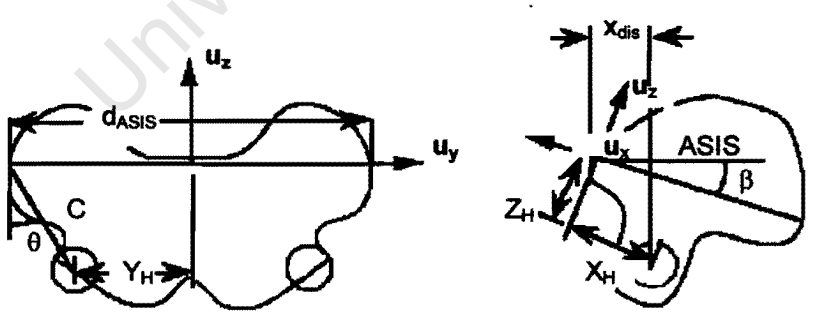

Figure 2.2 Geometry to locate the hip joint centre described by Davis *et al.* (1991)

The location of the hip joint centre in pelvic co-ordinates relative to the origin of the pelvic embedded co-ordinate system is therefore defined by Davis *et al.* (1991) as:

$$X_{HipJoint} = [-x_{dis} - r_{marker}] \cos(\beta) + C \cos(\theta)\sin(\beta) \quad 2.5$$

$$Y_{HipJoint} = S[C \sin(\theta) - d_{ASIS}/2] \quad 2.6$$

$$Z_{HipJoint} = [-x_{dis} - r_{marker}] \sin(\beta) - C \cos(\theta) \cos(\beta) \quad 2.7$$

Where: d_{ASIS} is the inter ASIS distance, x_{dis} is the anterior-posterior component of the ASIS distance, r_{marker} is the marker radius and S is +1 for the right side and –1 for the left. The knee centre is calculated based on the knee width measurement w_{knee} and the location of the ankle joint centre uses the same strategy as that for the knee.

Kadaba *et al.* (1990) use an empirical relation based on a pelvic radiograph study to estimate the location of the hip joint centre relative to the ASIS location and pelvic orientations. **IJK** represents the unit vectors of the embedded co-ordinates. For the pelvis, **J** is the unit vector along the line from right to left ASIS marker. **I** is perpendicular to **J**, pointing forward, and is in the plane defined by both ASIS and the sacral marker. The unit vector **K** is perpendicular to both **I** and **J**, defining a right-handed cartesian co-ordinate system. For the thigh, the unit vector **K** is in the direction from knee centre to hip centre, **J** is in the plane defined by the hip centre, knee centre and the thigh wand marker, in an orientation perpendicular to the **K** unit vector and points to the subjects left. **I** is calculated from the cross product of **J** and **K**. The shank unit vectors are defined identical to the thigh, with the knee centre, ankle centre and shank wand replacing those points used for the thigh. The foot has only two markers on it with no heel marker being necessary and therefore only one unit vector can be calculated and only two angular motions can be derived at the ankle joint. The unit vector is calculated from the line segment joining the ankle joint centre to the toe marker.

Vaughan *et al.* (1999) discuss modelling the human body as a series of interconnected rigid links in a standard biomechanical approach. A segment in three-dimensional space has six degrees of freedom, which means that six independent co-ordinates are needed to describe the segment's position in space.

Vaughan *et al.* (1999) describe a method of determining the embedded segment axes from the external marker positions which is described in chapter three. The method is

Fioretti *et al.* (1997) state that the expression "joint kinematics" alludes to the description of the relative movement between two adjacent bones. The methods of calculation must allow for comparison and generalisation of observations. They suggest the following requirements:

- Results must be repeatable and based on unambiguous definitions and consistently identifiable measurable quantities;
- The results should be expressed in established anatomical and physiological terminology; and
- The description of joint movements should be consistent with the descriptions already provided in the anatomical and physiological literature.

Chao (1980) explains that joint motions involved in daily activities are usually three-dimensional. When pathological changes occur in a joint, its deformity is often manifested in more than one plane. The ability to define joint orientation in three-dimensional space following the traditional rigid body theory is essential. Without a common definition of joint motion measurement, various experimental methods will be difficult to compare, thus making data sharing impossible.

Chao (1980) describes a method of determining Euler angle rotations and joint rotations using a triaxial goniometer. He states that to uniquely describe the relative angular orientation of two rigid bodies, connected by a joint, the use of Eulerian angles is the most convenient. Each segment has a set of unit vectors fixed to the reference frame of the body. The rotational sequence of motion follows the order of co-ordinate axes Z, y' and z''. Where y' and z'' are two intermediate axes remaining fixed to the moving body. The final position of the moving segment can be orientated relative to the fixed segment in terms of three Eulerian angles θ, ψ and ϕ.

Chao (1980) also comments that whenever the limb is allowed to move freely in three dimensions, the clinician is usually lost in defining the precise movement of the joint, and therefore a standardised joint motion definition must be established. Motion analysis has advanced in the two decades since Chao made these statements and the problem for the clinician now is not the definition of the movement. Chao's method of defining Euler angles is now one of a few different orientations and the problem for

clinicians today has more to do with how the different calculations compare to one another.

Grood and Suntay (1983) describe a method of three–dimensional joint motion which they feel will facilitate the communication between biomechanician and physician. They introduce a convenient co-ordinate system for describing three-dimensional motion along with its application to the human knee.

Grood and Suntay (1983) describe three unit base vectors, which define the axes as e_1, e_2 and e_3. Two of the axes are called body fixed axes, and are embedded in the two bodies whose relative motion is to be described. Their directions are specified by the vectors e_1 in the first body and e_3 in the second body. These two vectors are not necessarily perpendicular to each other. The fixed axes move with the respective bodies. The third axis is the common perpendicular axis between the two bodies and is described by the following equation:

$$e_2 = e_3 \times e_1 / |e_3 \times e_1| \qquad 2.8$$

e_2 is referred to as the floating axis (Figure 2.3).

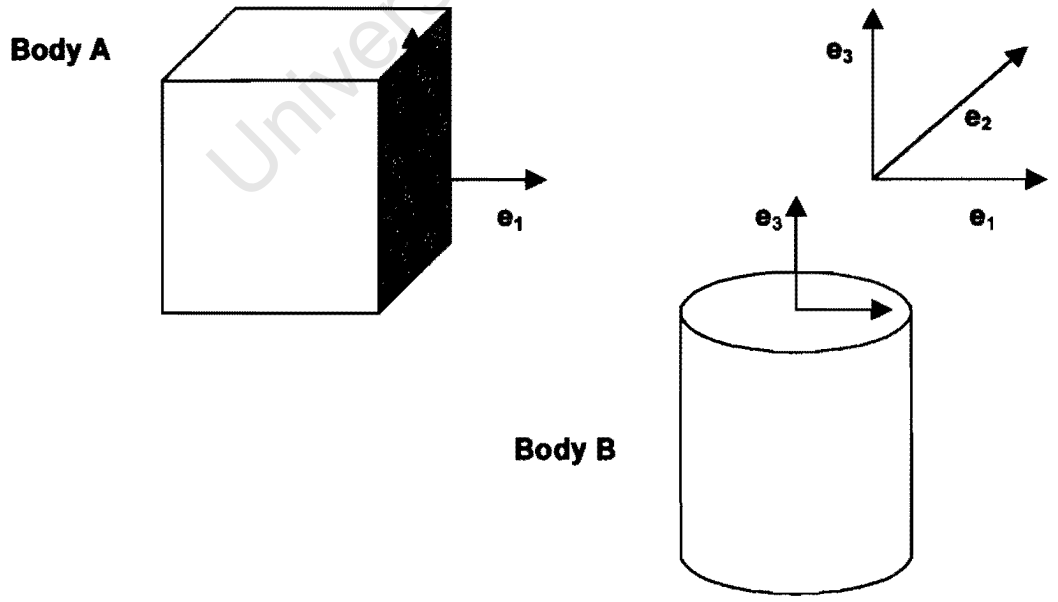

Figure 2.3 Definition of segment reference axis as described by Grood and Suntay (1983)

Grood and Suntay (1983) describe the first two joint angles (α and γ) as the rotation of the distal segment relative to the proximal segment about $\mathbf{e}_1$ and $\mathbf{e}_3$. The third relative rotation occurs about the floating axis and is measured as the angle, β between the two body fixed axes:

$$\cos \beta = \mathbf{e}_1 \bullet \mathbf{e}_3 \text{ (abduction-adduction)} \qquad 2.9$$

The Grood and Suntay (1983) definition of Euler angles is sequence independent. The relation between the angles, their joint co-ordinate system and conventional Euler angles is explained. For a given set of Euler angles, there is a unique set of axes corresponding to the joint co-ordinate system: a body fixed axis in the stationary segment; a body fixed axis in the moving segment; and a common perpendicular axis to these two. If the femur is assumed to be fixed and the tibia moving, then the joint co-ordinate system would correspond to a sequence of Euler rotations, first about the common x-axes, second about the rotated y axis in the tibia and third about the twice rotated z axis in the tibia.

Grood and Suntay (1983) argue that Euler angles, as described by the joint co-ordinate system, provide a precise mathematical description of clinical terminology for joint rotational motions.

Vaughan *et al.* (1999) use methods for calculating joint angles based on Chao (1980) and Grood and Suntay (1983). Each joint has a reference frame in the proximal and distal segments. For the hip joint these are the pelvis and thigh, for the knee joint they are the thigh and calf and for the ankle joint, the calf and foot. Joint angles are defined as a rotation of the distal segment relative to the proximal segment. The GaitLab 2.0, Peak Motus 2000 and BodyBuilder models use the methods described by Vaughan *et al.* (1999) to calculate the joint angles.

Vicon Clinical Manager uses the methods described by Kadaba *et al.* (1990) and Davis *et al.* (1991) to estimate joint angles and Euler angles. Kadaba *et al.* (1990) explain that orthopaedic angles specify the relative orientation of the distal moving segment with respect to the proximal reference frames. If **IJK** are the unit vectors of

the proximal reference segment, and $\mathbf{I}_3$ $\mathbf{J}_3$ $\mathbf{K}_3$ are the unit vectors in the distal embedded segments, then the rotational angles are calculated with the following equations:

$$\theta_2 = \sin^{-1}(-\mathbf{K}_3 \bullet \mathbf{J}) \qquad 2.10$$

$$\theta_1 = \sin^{-1}[(\mathbf{K}_3 \bullet \mathbf{I})/\cos(\theta_2)] \qquad 2.11$$

$$\theta_3 = \sin^{-1}[(\mathbf{I}_3 \bullet \mathbf{J})/\cos(\theta_2)] \qquad 2.12$$

For the ankle joint, the direction cosine matrix relating the foot frame and shank frame may be derived based on two orthopaedic angles. As is described above, the foot segment is defined with only one unit vector and therefore only two ankle rotations can be defined. The rotational angles of the foot are:

$$\theta_3 = \sin^{-1}(\mathbf{I}_3 \bullet \mathbf{J}) \qquad 2.13$$

$$\theta_1 = \sin^{-1}(\mathbf{K}_3 \bullet \mathbf{I}) \qquad 2.14$$

At each of the joints, flexion-extension is assumed as the first rotation, abduction-adduction is assumed to be the second rotation and the internal-external rotation takes place about the third rotated axis. They suggest that while it may be difficult to define the embedded axis exactly, it is necessary to be consistent in the definition so that it would be possible to compare data between different gait laboratories. (Kadaba *et al.*, 1990)

Davis *et al.* (1991) base their calculations of joint angles on the determination of Euler angles with a y-x-z axis rotation sequence (Kadaba *et al.*, 1990). The joint angles calculated correspond to flexion-extension, adduction-abduction and internal-external rotation.

Fioretti *et al.* (1997) discuss a study by Woltring (1994), in which a comparison is made of different methods for calculating a joint angle by various cardanic sequences applied to two different orientation matrices. Four methods are compared:

1. The cardanic conventions described by Grood and Suntay (1983).
2. The orthogonal projections of the orientation vector on the proximal bone embedded frame.

3. The non-orthogonal projections of the orientation vector on the joint axes defined by Grood and Suntay's cardanic conventions.
4. Joint angles obtained from a geometric approach.

The results showed that the joint angle curves have similar characteristics, demonstrating almost the same shape in time. They therefore state that it is difficult to claim superiority of one method over another and that the real difficulties lie in the experimental artefacts and errors.

Woltring (1994) describes a method of calculating joint angles and segment angles based on the concept of the attitude vector derived from Euler's theorem. He concludes that the attitude vector is better suited, than the Cardanic/Eulerian angles described by Chao (1980) and Grood and Suntay (1983), for representing three dimensional attitudes and rotations because of the orthogonality of the axes with respect to which its components are defined. Although this method is not used in any of the gait analysis software packages being studied, it is necessary to point out that other methods do exist and have their advantages and disadvantages.

2.5 Joint Kinetics

The calculation of joint kinetics is also an important aspect of gait analysis. Internal joint forces are transmitted by muscle action, tension in the ligaments and forces transmitted through the joint contact areas. (Rose and Gamble, 1994). Joint torques or moments may be thought of as the resultant effect of the forces exerted by the muscles crossing the joint. Vaughan (1996) refers to internal joint torques where the proximal segment exerts a torque on the distal segment. This convention is used for all kinetic calculations in all the gait models studied.

Davis *et al.* (1991) compute the three-dimensional joint moments using Newtonian mechanics, including angular accelerations and velocities and moments of inertia. The segmental mass, centre of mass location and segmental moments of inertia are approximated using the relationships of Dempster *et al.* (1959). A weighted least squares numerical differentiation scheme is used to compute the velocities and accelerations. Moment vectors are expressed relative to the embedded segment reference axes. This kinetic analysis is similar in to Vaughan *et al.* (1999) who use a

different approximation for body segment parameters and a finite difference theory to calculate derivatives.

Vaughan *et al.* (1996) agree that joint torques are subject to a variety of errors. The ground reaction forces make a significant contribution to the joint torques and are also the most reliable and accurate of the parameters, which are used to calculate joint torques. Segmental anthropometry and the segment accelerations are notoriously inaccurate but they do not make a large contribution to joint torques. The lever arms, the last parameter, have an important impact on joint torques and are very sensitive to marker placement on the skin and the biomechanical model chosen. Distal joint torques at the ankle therefore tend to be more reliable than proximal joint torques at the hip.

It is evident that although the ground reaction force data are generally accurate and the same for all gait analysis models, it is possible for variations between the models to be evident because of the different estimation methods used to calculate body segment parameters and the segment reference frames.

2.6 Filtering Techniques

All gait analysis models being compared in this study use some form of filtering, to smooth the raw displacement data before estimating the gait parameters. There are a number of different filtering techniques used in the different gait analysis models (Barth *et al.,* 1998). Vaughan (1982) discusses spline theory and digital filter theory which is used to filter raw displacement data, and finite difference theory which is used to find the first and second derivatives of the displacement-time data (velocity and acceleration). He compares the results of filtering from the different methods and concludes that the quintic spline is a good method to use for filtering, while a digital filter yields satisfactory results.

The Vicon Clinical Manager gait analysis model uses a Bezier spline interpolation (Hamming, 1983), which works by finding four valid sampled values, two either side of the required interpolation time. The Peak Motus 2000 model uses a 4^{th} order Butterworth filter (Hamming, 1983), while GaitLab 2.0 uses a 2^{nd} order low-pass

Butterworth filter (Vaughan, 1982) and the BodyBuilder model uses a five point weighted average filter (Lynn and Fuerst, 1989) to smooth the raw displacement data. These different methods may effect a difference between the different software packages for all gait parameters.

2.7 Statistical Analysis

Kadaba *et al.* (1989) and Growney *et al.* (1997) use a coefficient of multiple correlation (CMC) to describe the repeatability of kinematic and kinetic data. The CMC yields a measure of the repeatability of the gait cycle within a test day and between test days. Winter (1991) describes the coefficient of variation to test the repeatability of gait cycles and is the average standard deviation in the gait parameter divided by the average mean. These statistical comparisons are all coefficients. When the gait cycles are similar the coefficients tend to one and when they differ, these coefficients tend to zero. These methods do not compare the gait cycles at different time increments. This makes it difficult to assess where the differences in the gait cycle occur and what the causes of these differences are.

2.8 Summary of Literature

Software Package	Body Segment Parameters	Joint Centres	Joint Angles	Joint Kinetics	Filtering techniques
Vicon Clinical Manager	Dempster *et al.* (1959)	Davis *et al.* (1991), Kadaba *et al.* (1990)	Davis *et al.* (1991), Kadaba *et al.* (1990)	Davis *et al.* (1991)	Bezier spline interpolation.
Peak Motus 2000	Dempster *et al.* (1959)	Based on Vaughan *et al.* (1999)	Based on Vaughan *et al.* (1999)	Based on Vaughan *et al.* (1999)	4th order low pass Butterworth filter.
GaitLab 2.0	Vaughan *et al.* (1999)	Vaughan *et al.* (1999)	Grood and Suntay (1983), Chao (1980)	Vaughan *et al.* (1999)	2nd order low pass Butterworth filter.
Vicon BodyBuilder	Vaughan *et al.* (1999)	Vaughan *et al.* (1999)	Vaughan *et al.* (1999)	Vaughan *et al.* (1999)	Five-point weighted average filter.

Table 2.1 Summary of methods used by the different gait analysis packages

Chapter 3
Materials and Methods

3.1 Materials

The following materials are used to capture and process the gait data. The external marker data are captured with a Vicon 370, 6 camera motion analysis system and Vicon Workstation 3.0 motion analysis software from Oxford Metrics. Force plate data are captured from a six channel (508 by 464 mm) force plate from AMTI. The gait data are processed with GaitLab 2.0 gait analysis software from Kiboho publishers, Vicon Clinical Manager gait analysis software from Oxford Metrics, Peak Motus 2000, 3D Gait Analysis module from Peak Performance and Vicon Bodybuilder software version 3.52 for model development from Oxford Metrics. C3D files are converted to DST file format with the Rdata2 conversion program from Motion lab Systems.

The names and contact details of all the software vendors whose programs are used in this study are presented in Appendix D.

3.2 The BodyBuilder Model

A complete gait analysis model is developed using the Vicon BodyBuilder model development software, distributed by Oxford Metrics. The model uses the mathematical algorithms described by Vaughan *et al.* (1999). The model is described in two BodyBuilder executable files (Appendix B). The first is a parameter file, which includes subject constants such as the anthropometric parameters, sample frequency and established constants such as π and gravitational acceleration. A parameter file needs to be written for each subject, so that the different anthropometrics of the subjects can be entered.

The BodyBuilder model itself describes the mathematical algorithms that calculate the body segment parameters, bone embedded reference axes, the joint angles, Euler angles and resultant joint kinetics. The detailed model is presented in Appendix B, but

a general summary of the model will be described below.

A macro is a procedure that will be used repeatedly in the program and once defined can be called as many times as required. The BodyBuilder model begins with macro procedures to calculate vector and scalar products. A macro procedure to apply a filtering technique is also included in this section.

The vector (or cross) product is used to find the orthogonal result of two orthogonal vectors. The macro for a vector product takes the form:

$$\begin{aligned}\text{Cross product} = \quad & \{\mathbf{One}(Y)\times\mathbf{Two}(Z)-\mathbf{One}(Z)\times\mathbf{Two}(Y),\\ & \mathbf{One}(Z)\times\mathbf{Two}(X)-\mathbf{One}(X)\times\mathbf{Two}(Z),\\ & \mathbf{One}(X)\times\mathbf{Two}(Y)-\mathbf{One}(Y)\times\mathbf{Two}(X)\}\end{aligned} \qquad 3.1$$

where **One** and **Two** are two orthogonal vectors in the directions X, Y and Z.
The scalar (or dot) product is used to multiply vectors and takes the form:

$$\text{Dot product} = \{\mathbf{One}(X)\times\mathbf{Two}(X))+\mathbf{One}(Y)\times\mathbf{Two}(Y)+\mathbf{One}(Z)\times\mathbf{Two}(Z)\} \qquad 3.2$$

Where **One** and **Two** are vectors in the directions X, Y and Z. The last macro provides a weighted average filter technique which is used to filter the displacement data before further calculations are performed. The filter takes on the form:

$$x'_i = x_{i-2} + 3x_{i-1} + 4x_i + 3x_{i-1} + x_{i-2} \qquad 3.3$$

where x refers to unfiltered co-ordinate data and i refers to the *i*th sample frame. This filter is a five point weighted average filter and the function can be found in the BodyBuilder software package (Lynn and Fuerst, 1989).

Once the macros have been defined, the model continues with the calculation of body segment masses and moments of inertia based on the anthropometric measurements of the subject. Twenty anthropometric measurements are recorded for each subject immediately prior to the gait analysis being performed. These measurements are

chosen based on the method described by Vaughan *et al.* (1999). The anthropometric measurements are described in Table 3.1.

Parameter	Description
Total Body Mass	Measure the mass of the subject with all clothes except underwear removed.
ASIS Breadth	With a calliper, the distance between the anterior superior iliac spines is measured.
Thigh Length	With a calliper, the vertical distance between the superior point of the greater trochanter of the femur and the superior margin of the lateral tibia is measured.
Midthigh Circumference	With a tape measure perpendicular to the long axis of the leg at a point midway between the trochanteric and tibial landmarks, the circumference of the thigh is measured.
Calf Length	With a calliper, the vertical distance between the superior margin of the lateral tibia and the lateral malleolus is measured.
Calf Circumference	With a tape measure perpendicular to the long axis of the lower leg, the maximum circumference of the calf is measured.
Knee Diameter	With a calliper, the maximum diameter of the knee across the femoral epicondyles, is measured.
Foot Length	With a calliper, the distance from the posterior margin of the heel to the tip of the longest toe is measured.
Malleolus Height	With the subject standing, the vertical distance from the standing surface to the lateral malleolus is measured using a calliper.
Malleolus Width	With a calliper, the maximum distance between the medial and lateral malleoli is measured.
Foot Breadth	With a calliper, the breadth across the distal ends of metatarsal I and V is measured.

Table 3.1 Anthropometric measurements as described by Vaughan *et al.* (1999)

The segment masses are calculated using the prediction equations and theory described by Vaughan *et al.* (1999). A linear regression equation is used to predict the segment masses, which has the form:

$$\text{Segment mass} = C1(\text{Total body mass}) + C2(\text{Length})^3 + C3 \qquad 3.4$$

where C1, C2 and C3 are regression coefficients. The shapes of the thigh and calf are represented as cylinders:

$$\text{Mass of cylinder} = (\text{Density})/\ (\text{Length})(\text{Circumference})^2/4\pi \qquad 3.5$$

and a right pyramid represents the shape of the foot:

$$\text{Mass of pyramid} = (1/3)(\text{Density})(\text{Width})(\text{Height})(\text{Length}) \quad 3.6$$

The regression equations are based on six cadavers studied by Chandler *et al.* (1975).

The segment moment of inertia is related to body mass and the length of the segment squared. The linear regression equation for predicting segment moment of inertia has the form:

$$\text{Segment moment of inertia} = C4(\text{Total body mass})(\text{Length})^2 + C5 \quad 3.7$$

where C4 and C5 are regression coefficients. As in the segment mass calculations, the shape of the thigh and calf can be represented by cylinders while that of the foot is represented by a right pyramid. Therefore using the mathematical definition of moment of inertia and standard integrals:

$$\text{Moment of inertia of a cylinder about the flexion-extension axis} = (1/12)(\text{Mass})[(\text{Length})^2 + 0.076(\text{Circumference})^2] \quad 3.8$$

$$\text{Moment of inertia of a cylinder about the abduction-adduction axis} = (1/12)(\text{Mass})[(\text{Length})^2 + 0.076(\text{Circumference})^2] \quad 3.9$$

$$\text{Moment of inertia of a cylinder about the internal-external rotation axis} = (1/8\pi r^2)(\text{Mass})(\text{Circumference})^2 \quad 3.10$$

The next step in the model is to estimate the lower extremity joint centres (right and left hip, knee and ankle joints) and position of the left and right toes. The modified Helen Hayes Hospital marker set is described in chapter one and with Figures 1a and 1b. The three-step strategy described by Vaughan *et al.* (1999) to calculate the positions of the joint centres is followed. First three markers are selected from the segment of interest; then an orthogonal **uvw** reference axis is created based on the three markers and finally prediction equations are used to estimate the joint centres.

To create the **uvw** reference axes for the foot the origin of the axis is placed at the lateral malleolus marker. The three markers on the foot segment (Lateral malleolus, Heel and Metatarsal head II) will then form a plane (Figure 3.1). The **w** axis is perpendicular to this plane with its origin at the lateral malleolus marker. The **u** axis is parallel to a line between the heel and the second metatarsal head and the **v** axis is orthogonal to both the **u** and **w** axes, so that the **uvw** axes form a so-called right-handed system. Using this **uvw** system the prediction equations for the right ankle joint centre and the right longest toe can be described:

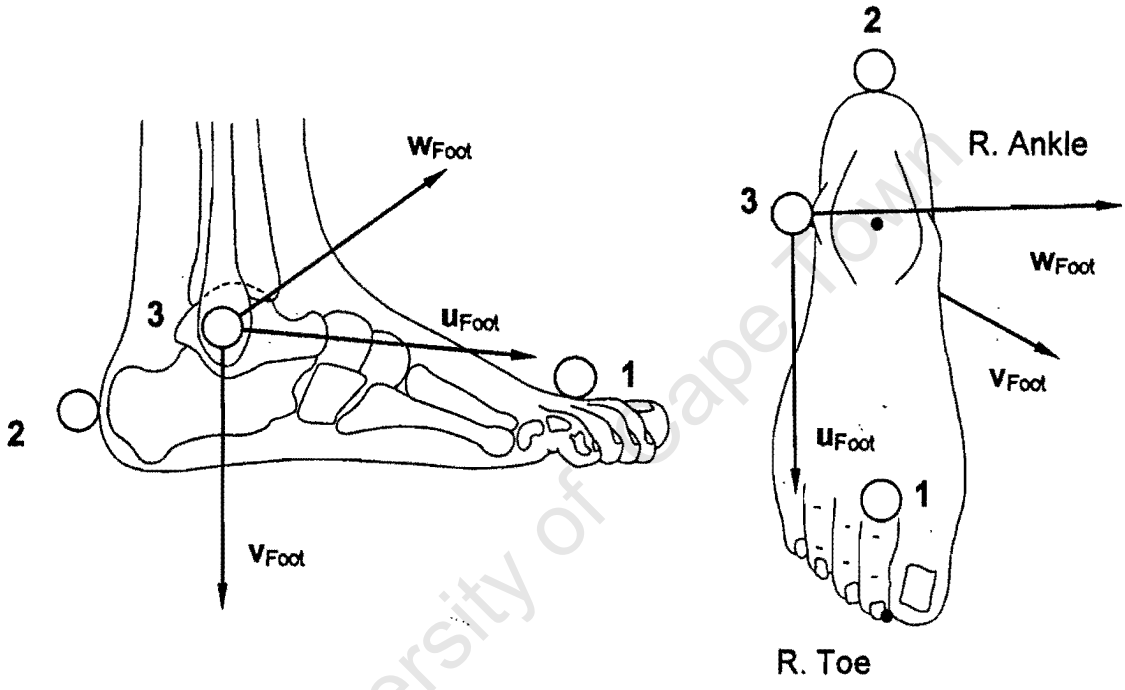

Figure 3.1 The **uvw** reference system used to define the foot as described by Vaughan *et al.* (1999)

$$\begin{aligned}\text{Ankle joint centre} = {} & \text{Lateral malleolus marker} \\ & + 0.016(\text{Foot length})\mathbf{u}_{foot} \\ & + 0.392(\text{Malleolus height})\mathbf{v}_{foot} \\ & + 0.478(\text{Malleolus width})\mathbf{w}_{foot} \end{aligned} \quad 3.11$$

$$\begin{aligned}\text{Toe point} = {} & \text{Lateral malleolus marker} \\ & + 0.742(\text{Foot length})\mathbf{u}_{foot} \\ & + 1.074(\text{Malleolus height})\mathbf{v}_{foot} \\ & - 0.187(\text{Malleolus width})\mathbf{w}_{foot} \end{aligned} \quad 3.12$$

To create the **uvw** reference axes for the calf, the origin is placed at the femoral epicondyle marker. The three markers on the calf (Femoral epicondyle, Tibial wand and Lateral Malleolus) now form a plane, the **w** axis is perpendicular to this plane (Figure 3.2). The **v** axis is parallel to the line between the lateral epicondyle marker and the lateral malleolus marker with its origin at the femoral epicondyle marker and the **u** axis is at right angles to the **v** and **w** axes, forming a right-handed system. The prediction equation for the right knee joint centre can now be described:

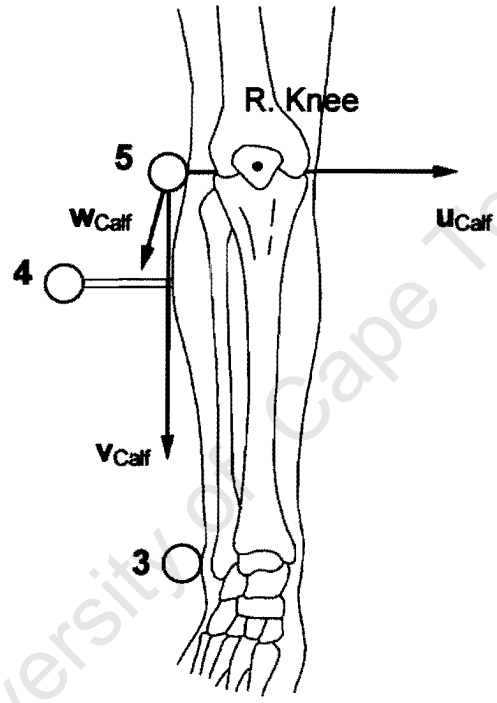

Figure 3.2 The **uvw** reference system used to define the calf as described by Vaughan *et al.* (1999)

$$\text{Knee joint centre} = \text{Femoral epicondyle marker} + 0.500(\text{Knee diameter})\mathbf{u}_{calf} \quad 3.13$$

There is no need to include the **w** and **v** axes in the prediction equation as the knee joint centre is assumed to be along the **u** axis.

When creating the **uvw** axes for the pelvis, we place the origin at the sacral marker. The three markers (Sacral, Left ASIS and Right ASIS) form a plane and the **w** axis is perpendicular to this plane (Figure 3.3). The **v** axis is parallel to the line between the

left and right ASIS's with its origin at the sacral marker and the **u** axis is at right angles to both the **v** and **w** axes and **uvw** thus form a right-handed system. The prediction equation for the left and right hip joints can be described:

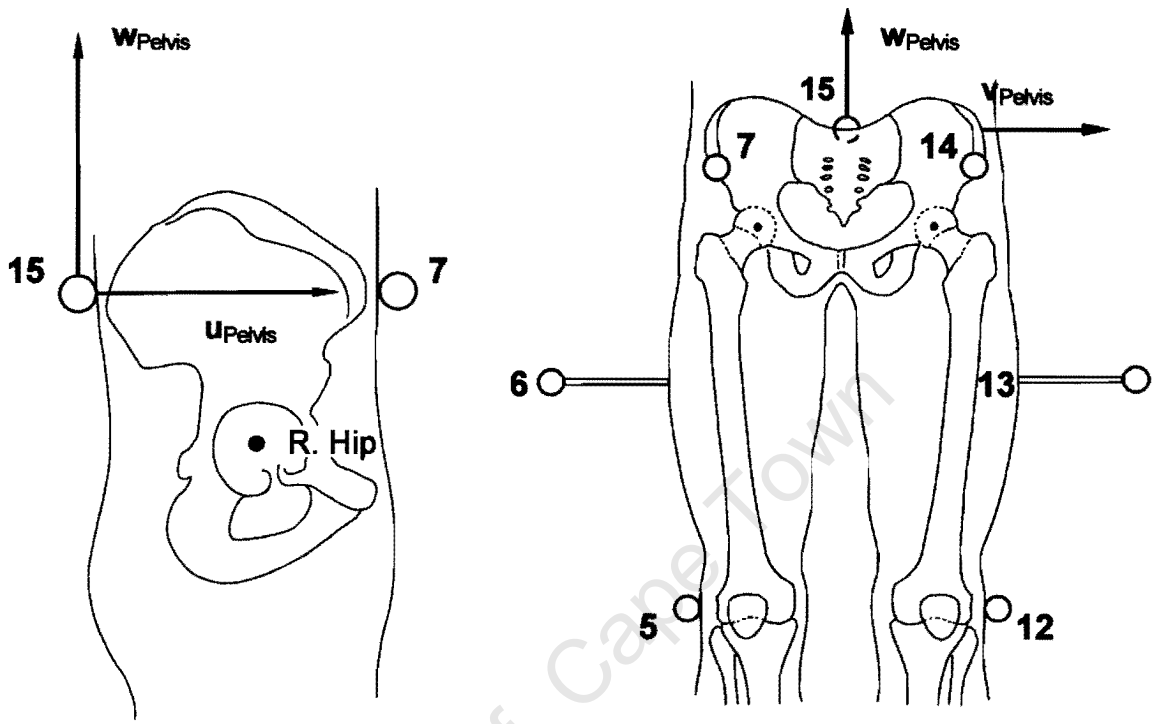

Figure 3.3 The **uvw** reference system used to define the pelvis as described by Vaughan *et al.* (1999)

$$\begin{aligned} \text{Hip joint centre} = \quad & \text{Sacral marker} \\ & + 0.598(\text{ASIS breadth})\mathbf{u}_{pelvis} \\ & \pm 0.344(\text{ASIS breadth})\mathbf{v}_{pelvis} \\ & - 0.290(\text{ASIS breadth})\mathbf{w}_{pelvis} \end{aligned} \qquad 3.14$$

The +/- differentiates between the left (+) and right (-) hips.

The coefficients in the prediction equations (3.11, 3.12 and 3.13) have been based on direct three-dimensional measurements of 12 normal subjects, while those for the hip joint (3.14) are based on stereo X-rays of a normal subject (Vaughan, 1983).

The model continues by defining the segment reference frames (xyz), which will describe how each segment is positioned relative to the global reference frame (XYZ). The origin of each reference frame (xyz) is at the segment's centre of gravity. The

description of the segment reference frames can be found in Vaughan *et al.* (1999). The pelvis segment reference frame is described based on the pelvis **uvw** axis described above, with the x axis pointing vertically up along the **w** axis, the y axis being along the **u** axis and pointing anteriorly and the z axis pointing to the subject's left along the **v** axis (Figure3.4).

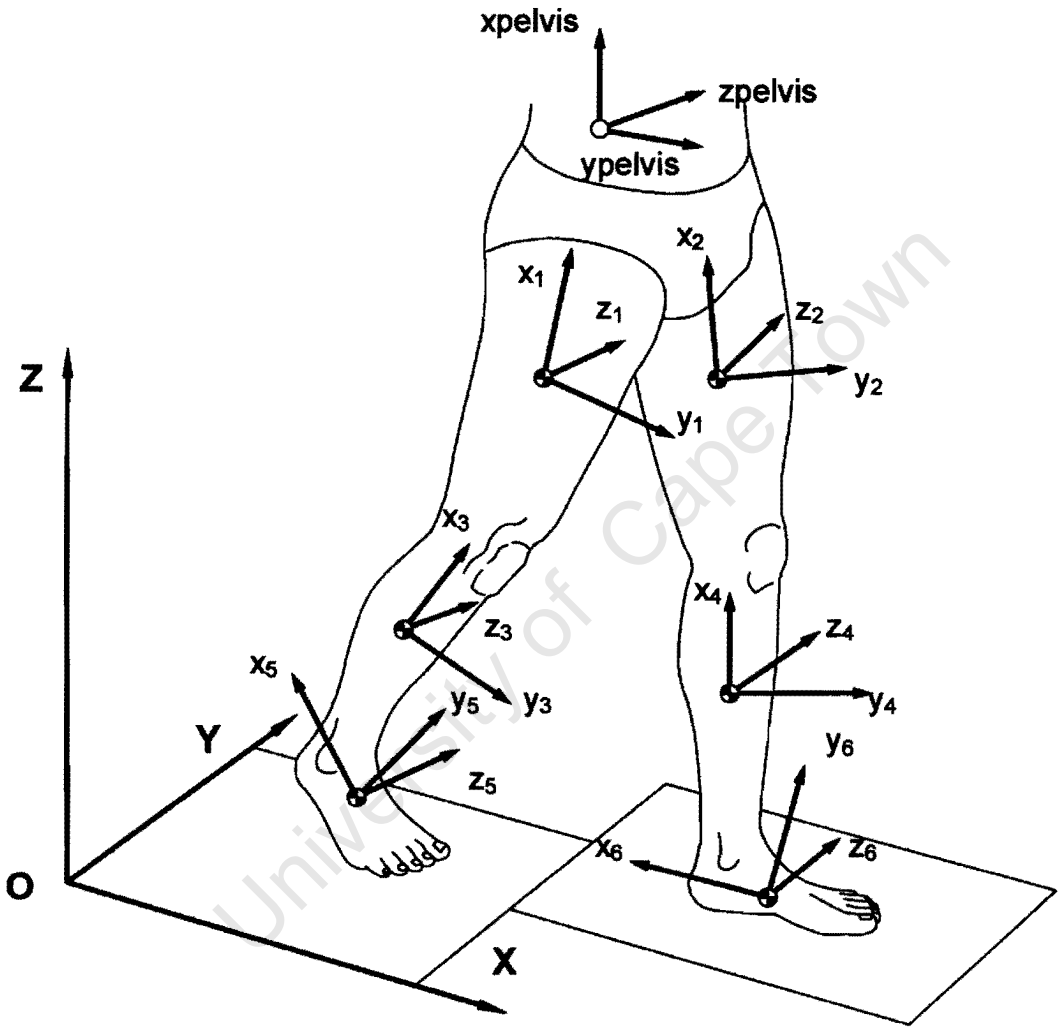

Figure 3.4 The segment reference frames from Vaughan *et al.* (1999). 1 and 2 are the right and left thigh, 3 and 4 are the right and left calf, 5 and 6 are the right and left foot respectively

In the thigh segments, the x axis runs from the knee joint centre to the hip joint centre. The hip joint, knee joint and thigh wand describe the xz plane. The y axis is at right angles to the xz plane and points anteriorly. The z axis is perpendicular to the x and y axes by the right-handed screw rule and points to the subject's left (Figure 3.4).

In the calf segments, the x axis again runs distal to proximal from the ankle joint centre to the knee joint centre. The knee and ankle joints and the tibial wand form the xz plane. The y axis is once again at right angles to the xz plane and points anteriorly, while the z axis is perpendicular to the x and y axes by the right-handed screw rule and points to the subject's left (Figure 3.4).

In the foot segments, the x axis is directed from the toe point to the heel marker. The xy plane is formed by the ankle joint, toe position and heel marker, and the z axis is at right angles to the xy plane and points to the subject's left. The y axis is obtained from the right-handed screw rule and points up (Figure 3.4).

Using the data from Chandler *et al.* (1975), the equations for formulating the segment centres of gravity are derived (Appendix B). The linear velocities and accelerations for each segment centre of gravity are also calculated. The velocities of the segment centres of gravity are the first derivatives of the segment centre of gravity displacement calculations, while the accelerations are the second derivative of the segment displacements.

Once the reference axes have been defined, the joint angle calculations are completed. The joint angle calculations include the three pelvis rotations, tilt, obliquity and rotation, the right and left, hip and knee angles around the three reference axes, xyz, namely flexion-extension, abduction-adduction and internal-external rotation and the ankle plantar-dorsi flexion, varus-valgus and inversion-eversion angles. As each joint has a reference frame embedded in its proximal and distal segment, the joint angles are defined as a rotation of the distal segment relative to the proximal one.

The angle rotations can be defined as (Figure 3.5):

- flexion-extension and plantar-dorsi flexion take place about the mediolateral axis of the proximal segment;
- internal-external rotation take place about the longitudinal axis of the distal segment; and
- abduction-adduction take place about the floating axis which is at right angles to the other two axes.

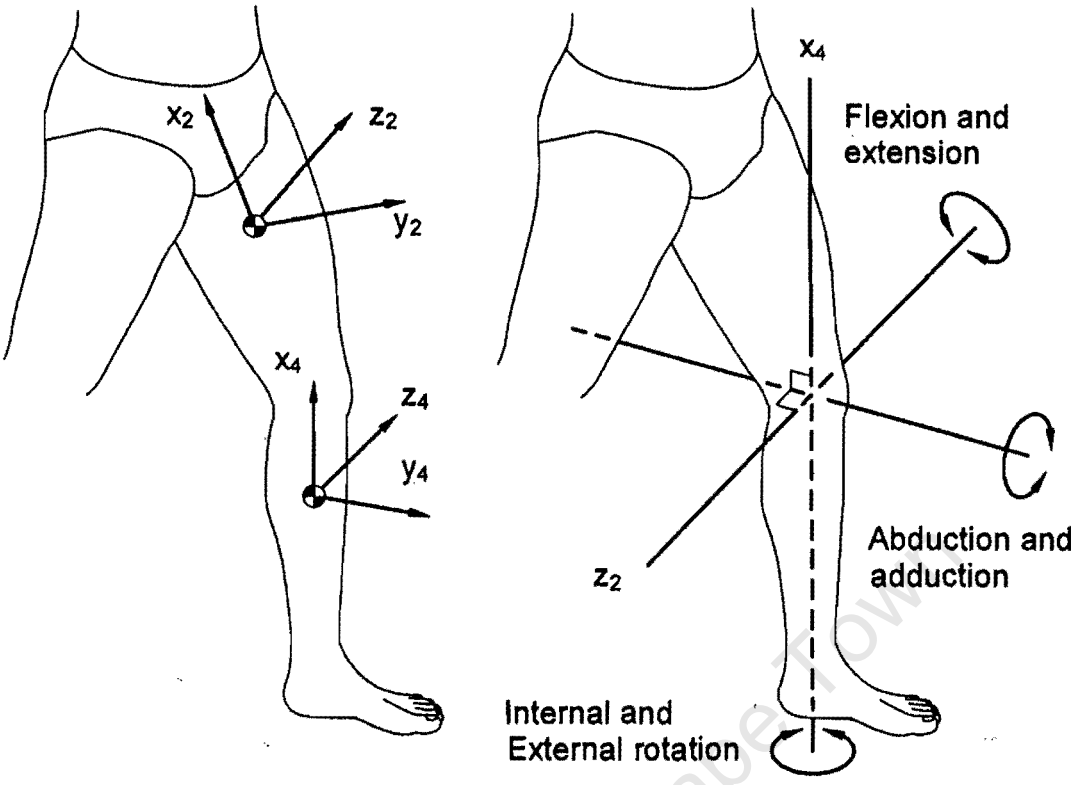

Figure 3.5 Joint angle rotations for the left knee described by Vaughan *et al.* (1999)

Euler angles are then calculated. Each segment's position is defined by six co-ordinates: the xyz co-ordinates, which define the position of the segment's centre of gravity; and three Euler angles. To calculate the Euler angles, the segment's centre of gravity is moved to coincide with the global reference origin, a line of nodes is defined at right angles to both the global Z axis and the segment z axis, and the segment's reference axis is then rotated from the global reference axis to its original position (Vaughan *et al.*, 1999). The three Euler angles are:

1. ϕ about the global Z axis.
2. θ about the line of nodes.
3. ψ about the segment z axis.

With these Euler angles, the angular velocities and accelerations of each segment are calculated. These parameters are needed for the calculation of angular momentum, which in turn are required to calculate the joint moments.

Finally, the joint kinetics can be calculated by integrating the six-parameter data from the force plate. The six parameters are three vector forces in the direction of the global X, Y and Z axes, and three vector moments about the global X, Y and Z axes. The joint kinetics calculated include: right hip and knee internal-external rotation, flexion-extension and abduction-adduction moments, right ankle inversion-eversion, plantar-dorsi flexion and varus-valgus moments.

In the BodyBuilder model, the first step is to extract the three-dimensional forces and moments from the force plate and filter the ground reaction force data to match the ground reaction force data inputs used in the other models. The force plate data needed to be filtered as the AMTI six channel force plate makes use of an external amplifier. 60 Hz inteference from the Vicon cameras is picked up in the cables which run from the force plate to the amplifier. Another filter is also applied to the force plate data by setting all force plate data to zero when the force in the vertical direction is less than 10 Newton. This filter decreases the amount of noise experienced when the subject is not on the force plate and only allows the ground reaction forces to be taken into account when the vertical force is more than 10 Newton.

The point at which the ground reaction forces acts is calculated. This point is known as the centre of pressure and can be found by manipulating the equation for moment calculations Moment = Force × (lever arm). In this case the lever arm will provide the resultant global X and Y positions of the centre of pressure. The centre of pressure data are calculated after the initial three point weighted average filter has been run, to ensure filtered centre of pressure data.

Using a free body diagram (Figure 3.6) as a guide, Newton's second law of motion is applied to each segment. Newton's second law of motion applied to linear systems can be summed up with the equation:

$$\text{Sum of the forces} = (\text{Mass})(\text{Acceleration}) \qquad 3.15$$

And applied to angular system:

Sum of the moments = (Moment of Inertia)(Angular acceleration) 3.16

Using Newton's equations 3.15 and 3.16 the ankle joint kinetics are calculated.

$$F_{AnkleX} = m_{RFootCG}\ddot{X}_{RFootCG} - F_{PlateX} \quad 3.17$$

$$F_{AnkleY} = m_{RFootCG}\ddot{Y}_{RFootCG} - F_{PlateY} \quad 3.18$$

$$F_{AnkleZ} = m_{RFootCG}(\ddot{Z}_{RFootCG} + 9.81) - F_{PlateZ} \quad 3.19$$

Where m is the mass of the segment, $\ddot{X}\ddot{Y}\ddot{Z}$ are the segment's accelerations in the XYZ global directions and F_{Plate} is the ground reaction force in the XYZ directions.

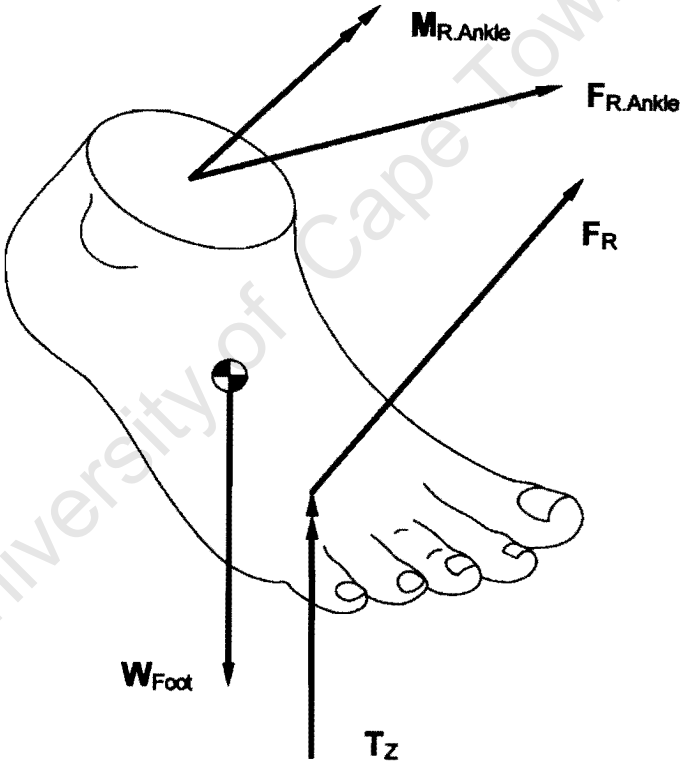

Figure 3.6 Free body diagram of the foot from Vaughan *et al.* (1999)

The proximal and distal moment arms are then calculated:

$$P_{Prx} = \text{Ankle joint centre} - \text{Foot CG} \quad 3.20$$

$$P_{Dis} = P_{Plate} - \text{Foot CG} \quad 3.21$$

Where $\mathbf{P}_{Plate}$ is a vector representing the centre of pressure applied to the force plate. The residual moment is calculated:

$$\mathbf{M}_{Res} = \mathbf{T}_{Plate} + (\mathbf{P}_{Prx} \times \mathbf{F}_{Ankle}) + (\mathbf{P}_{Dis} \times \mathbf{F}_{Plate}) \quad 3.22$$

Where $\mathbf{T}_{Plate}$ is the vector representing the moment about the z axis. Newton's law is now applied for angular systems and:

$$\mathbf{M}_{AnkleX} = H_x - \mathbf{i}_{Foot} \bullet \mathbf{M}_{Res} \quad 3.23$$

$$\mathbf{M}_{AnkleY} = H_y - \mathbf{j}_{Foot} \bullet \mathbf{M}_{Res} \quad 3.24$$

$$\mathbf{M}_{Ankle\,Z} = H_z - \mathbf{k}_{Foot} \bullet \mathbf{M}_{Res} \quad 3.25$$

Where H is the angular momentum and **ijk** are the segment's reference axis unit vectors. The resultant forces and moments are, however now based on the global reference frame and they will have more relevance when expressed in terms of a body based co-ordinate system. The same axes, which are used to define joint angles, are used here.

Forces:

- A mediolateral force along the mediolateral axis of the proximal segment.
- A proximal distal force along the longitudinal axis of the distal segment.
- An anterior/posterior force along the floating axis perpendicular to the mediolateral and longitudinal axes.

Moments:

- A flexion/extension moment about the mediolateral axis of the proximal segment.
- An internal/external rotation moment about the longitudinal axis of the distal segment.
- An abduction/adduction moment about a floating axis perpendicular to the mediolateral and longitudinal axes. (Figure 3.5)

$$\mathbf{F}_{Ankle.PrxDis} = \mathbf{F}_{Ankle} \bullet \mathbf{i}_{Foot} \quad 3.26$$

$$\mathbf{F}_{Ankle.MedLat} = \mathbf{F}_{Ankle} \bullet \mathbf{k}_{Calf} \quad 3.27$$

$$\mathbf{F}_{Ankle.AntPos} = \mathbf{F}_{Ankle} \bullet \mathbf{l}_{ankle} \quad 3.28$$

$$\mathbf{M}_{Ankle.InvEve} = \mathbf{M}_{Ankle} \bullet \mathbf{i}_{Foot} \quad 3.29$$

$$\mathbf{M}_{Ankle.PlaDor} = \mathbf{M}_{Ankle} \bullet \mathbf{k}_{Calf} \quad 3.30$$

$$\mathbf{M}_{Ankle.VarVal} = -\mathbf{M}_{Ankle} \bullet \mathbf{l}_{Ankle} \quad 3.31$$

where l is the joint abduction-adduction axis.

The BodyBuilder model can be viewed in Appendix B and details of the kinetic calculations are taken from Vaughan *et al.* (1999). The above explanation, although directly related to the BodyBuilder model, serves as an example of the normal modelling procedure in all gait analysis models.

3.3 Calibration Procedure

The quality of data for gait analysis requires that the cameras are positioned with great care and that the calibration procedure is accurately performed. The cameras need to be positioned so that they give the best possible view of the markers during the trial. The six cameras of the Vicon 370 motion capture system are set up around the laboratory walkway. Three cameras are positioned behind the subjects as they walk in the positive global X direction. Two cameras are positioned in front of the subjects and one camera is positioned to the left of the subjects. All the cameras are approximately four metres away from the walkway strip. Figure 3.7 shows the layout of the gait analysis laboratory in Cape Town, South Africa.

Each camera is then checked to ensure that all the markers are detectable in the camera's field of view, and that the camera volume will ensure more than one gait cycle can be captured. The cameras are adjusted until the volume of walkway for each camera is as large as possible.

The calibration procedure is done in two steps. First a static calibration is performed to determine the global XYZ axes of the walkway, and then a dynamic calibration is performed, to calibrate the walkway volume.

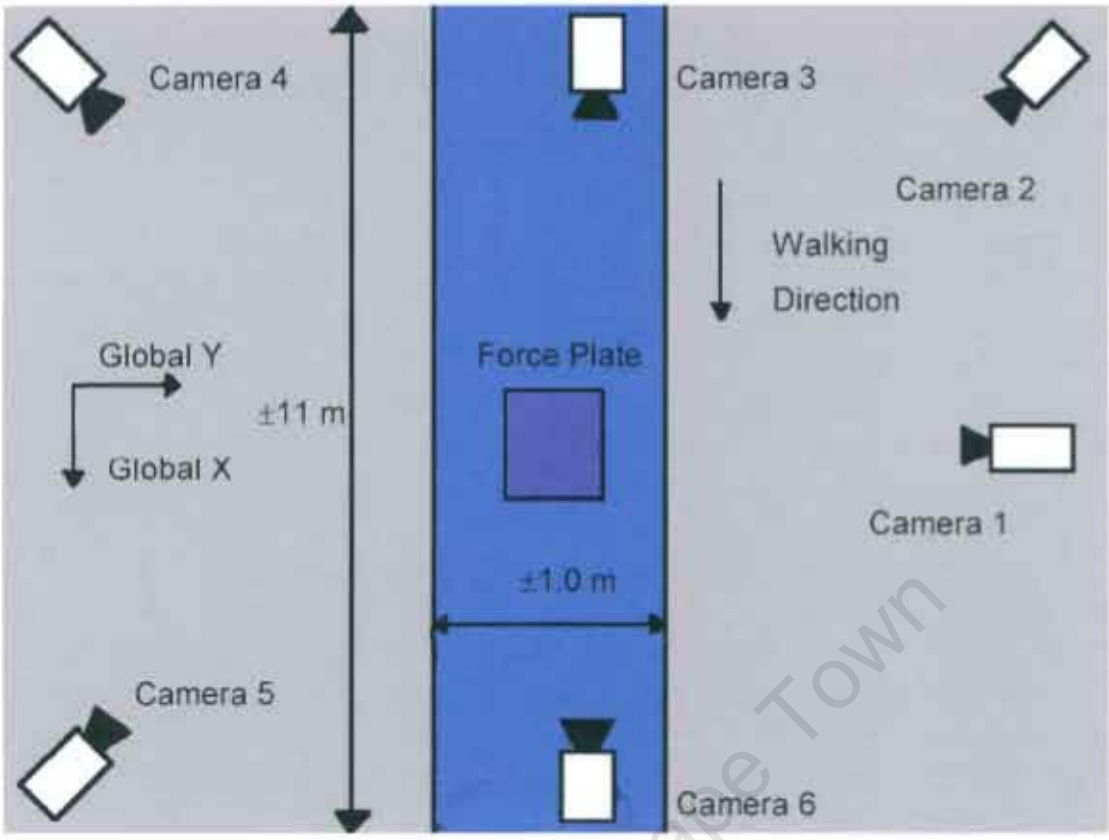

Figure 3.7 Layout of the gait analysis laboratory in Cape Town, South Africa

The Clinical L-Frame from Oxford Metrics is fitted onto the corner of the force plate with the arms parallel to the sides of the plate. The frame is used for the static calibration process. The Clinical L-Frame consists of reflective markers positioned on two arms. The origin of the frame is at its axis where the two arms meet. The matrix below defines the exact positions of the markers on the Clinical L-Frame. The X axis is the direction of walking anterior-posterior, while the Y axis is the mediolateral axis and the Z axis is the vertical axis. The measurements are displayed in millimetres.

[X	Y	Z]
[88.0	9.5	61.5]
[300.0	9.5	61.5]
[439.0	9.5	61.5]
[9.5	483.0	61.5]

The dynamic calibration is performed by waving a wand which has two 50 mm markers attached 500mm apart. The wand is moved throughout the walkway in an attempt to calibrate the entire measurement volume.

Once calibration is completed, the Vicon Workstation 3.0 software reports the calibration residual errors for each camera. To ensure accurate measurement by the cameras, the calibration procedure is repeated before each subject trial until a residual error of less than 1.5 mm is recorded for each camera.

3.4 Data Capture Procedure

Twenty subjects are recruited so that the different gait models can be compared and evaluated with variable data. The subjects are recruited from students, staff and children involved with or affiliated to the Sports Science Institute of South Africa in Cape Town, South Africa. Nine adult male, six adult female and five male adolescents are used as subjects, so that a wide range of heights and body masses can be assessed (Table 3.2).

Subject	Gender	Age (years)	Height (cm)	Body Mass (kg)
1	Male	18	180.0	138.5
2	Male	24	179.0	90.0
3	Female	19	165.4	60.2
4	Male	22	174.5	78.0
5	Female	33	163.0	73.0
6	Male	28	166.0	62.0
7	Male	8	128.0	26.5
8	Male	25	183.0	74.0
9	Female	23	174.0	59.0
10	Male	13	154.4	39.6
11	Female	26	164.0	67.0
12	Female	29	160.0	71.5
13	Female	26	169.0	63.5
14	Male	17	184.5	71.3
15	Male	50	200.0	97.0
16	Male	29	183.0	75.0
17	Male	22	169.0	65.5
18	Male	10	136.6	56.5
19	Male	10	148.0	35.0
20	Male	9	137.0	29.6
Mean		22.1	165.9	66.6
SD		9.9	18.1	25.1

Table 3.2 Subject gender, age, height and body mass

Marker trajectory data are captured with the Vicon 370, six-camera motion analysis system and Vicon Workstation 3.0 software at a capture frequency of 60 Hz. The ground reaction force data are captured with the AMTI six-channel force plate at a capture frequency of 120 Hz. All subjects are tested in the gait analysis laboratory of the University of Cape Town, located at the Sports Science Institute of South Africa in Cape Town.

The first step in the data capture procedure is to record the 20 anthropometric parameters for each subject as mentioned above. All data are collected with the subjects wearing running shorts, bare chested except for the female subjects. The subjects walked barefoot. Once the anthropometric data are recorded, retro-reflective markers are attached to the subject according to the marker positions of the modified Helen Hayes Hospital marker set (Figures 1a and 1b). The retro-reflective markers are all 25mm spheres covered in 3M retro-reflective tape. The wand markers are attached to 50mm stalks, which in turn are attached to flexible rubber bases. The markers are attached using clear double-sided tape, while the wand marker bases are attached with micropore strapping tape. All markers are attached directly to the skin.

As the wand markers are not attached to bony landmarks, it is necessary to follow a protocol for attaching the markers. The tibial wand is attached by first attaching the femoral epicondyle marker and the lateral malleolus marker and then finding the midpoint on a line between these two markers. The femoral wand is placed at the midpoint on a line between the superior point of the greater trochanter and the femoral epicondyle. It is important that the wands are on the line between their relevant markers, so that they define the segment xz planes correctly. As data are being compared between gait analysis models and not subjects, a line of sight method is used to place the femoral and tibial wands.

With the markers firmly in place, the subject stands on the force platform facing in the global positive X direction. A static trial is then recorded and checked to ensure that all markers are visible. The markers are then labelled using the Vicon Workstation software.

The subjects are instructed to walk naturally in the global positive X direction along the gait laboratory walkway. The laboratory walkway is approximately 11 metres long and 1 metre wide (Figure 3.7). The AMTI force plate is sunk into the floor at the same level as the walkway and is 6 metres from the start of the walkway in the global positive X direction. The force plate surface is covered in the same colour carpeting as the rest of the walkway and is indistinguishable from the rest of the walkway, unless a close inspection is performed (Figure 3.7). The carpet covering has no significant effect on the force plate signals (Whittle and Ferris, 1993). The subjects are given a starting position from which they walk. They repeat the walks until two trials are captured in which they place their right foot cleanly on the force plate. The subjects' starting position is changed in order to assist in stepping on the force plate without requiring them to target the platform. However, it has been suggested that targeting of the force plate does not significantly affect the results (Grabiner *et al.*, 1995).

The force plate and camera data are synchronised by the Vicon Workstation 3.0 software program. The Workstation 3.0 system reconstructs the markers in three dimensions from the individual camera data. The file output is in the C3D file format which is a binary file containing reconstructed video data, analogue data and anthropometric parameters.

3.5 Data Processing

Before the raw marker trajectory data and ground reaction force data can be processed, it is necessary to arrange the files according to the input format needed for each gait analysis software package. The formats are listed in Table 3.3 below:

Software Package	File Format
BodyBuilder (BB)	C3D
Vicon Clinical Manager (VCM)	C3D
GaitLab 2.0 (GL)	DST format, ASCII based format
Peak Motus 2000 (PM)	Comma delimited ASCII format

Table 3.3 Gait analysis software file formats

The ground reaction force data are filtered using the weighted three-point average technique, before it is included in the required file format. For the BodyBuilder model this filtering is performed as part of the model calculations, while for the other models

the ground reaction force data first had to be extracted.

The GaitLab 2.0 model requires the data to be converted to the DST file format. The files are converted from C3D to DST format using the software program Rdata2 version 2.406 developed by Edmund Cramp of Motion Lab Systems (Appendix D). The force plate data are, however, filtered separately and then the filtered results are included in the DST file. Peak Motus 2000 requires the marker trajectory and ground reaction force data to be saved as comma delimited ASCII files. The marker trajectories and filtered ground reaction forces are then entered into Peak Motus 2000 as two separate, although synchronised, ASCII files (Figure 3.8).

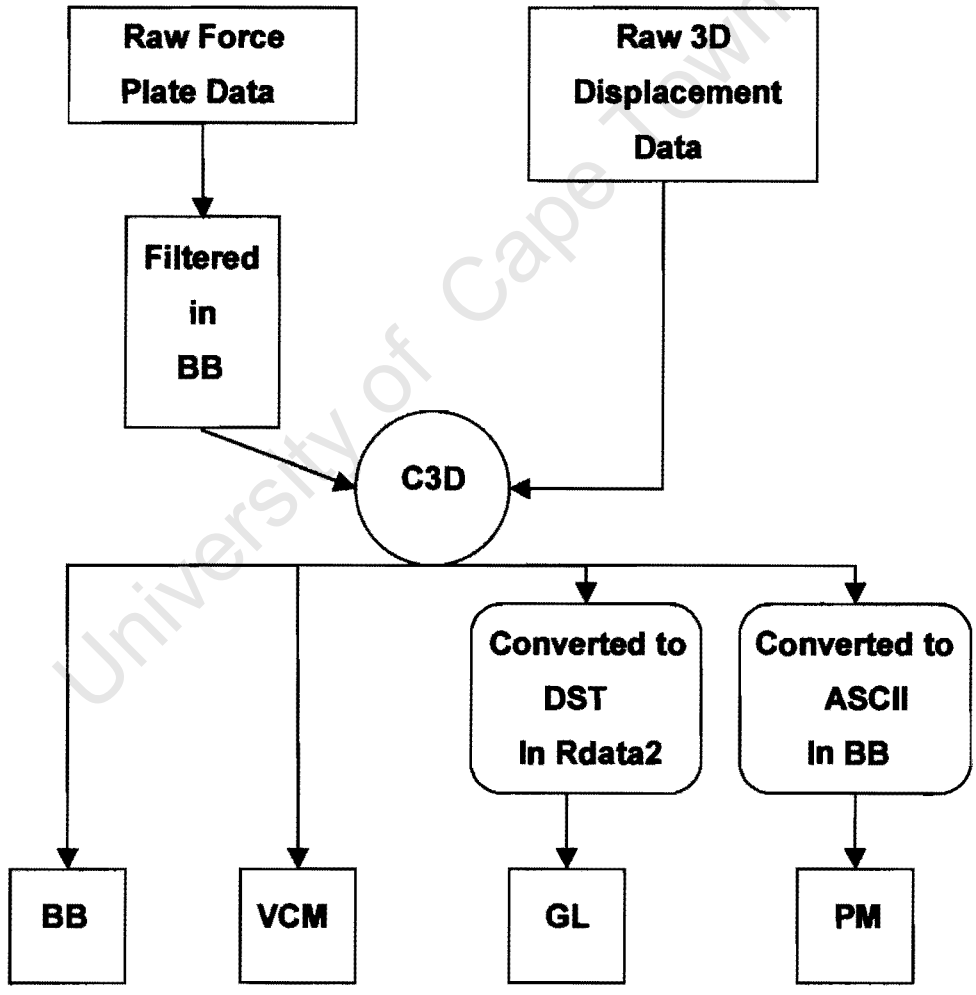

Figure 3.8 Flow chart of the pre-processing procedure for each gait analysis software package

The files are now ready to be processed using the four gait analysis software packages. Eleven gait parameters are chosen to compare the different models. The eleven parameters are the most common gait parameters examined by clinicians:

- Pelvic Tilt, Obliquity and Rotation angles (3)
- Hip Flexion-Extension and Abduction-Adduction angles (2)
- Knee Flexion-Extension and Abduction-Adduction angles (2)
- Ankle Plantar-Dorsiflexion angle (1)
- Hip and Knee Flexion-Extension moments (2)
- Ankle Plantar-Dorsiflexion moments (1)

BodyBuilder version 3.52 is used to process the data with the BodyBuilder model. The BodyBuilder model described in the section above uses mathematical algorithms described by Vaughan *et al.* (1999). The BodyBuilder model uses a five point weighted average filter described in equation 3.3, to filter the raw displacement data.

In Vicon Clinical Manager version 1.37, the C3D file is processed directly after entering the required anthropometric data and calculating the offset angle for the ankle from the static trial. This is all calculated in the VCM package. The processed files are saved as GCD files, which are ASCII files. The ankle plantar-dorsiflexion angles are reported with dorsiflexion positive, while the abduction-adduction angles are reported with adduction as positive and the flexion-extension moments for the hip and the knee are reported with extension positive, while all the moments are calculated normalised to body weight. The above mentioned angles and moments are reported differently to the other models where the ankle plantar flexion angle is positive, the abduction angle is positive and the flexion moment is positive and moments are reported as Newton metres and are not normalised with body weight. The GCD files are therefore transformed so that they have the same format as the other models. The Vicon Clinical manager model uses mathematical algorithms described by Kadaba *et al.* (1990) and Davis *et al.* (1991) and a Bezier spline interpolation (Hamming, 1983) is used to filter the raw displacement data.

The DST files are processed by GaitLab 2.0. As the anthropometric parameters form part of the DST file format, the anthropometric data for these trials are entered into the Rdata2 program. The results of these trials are once again saved in the DST file format. GaitLab 2.0 uses mathematical algorithms described by Vaughan *et al.* (1999), some of which are based on the work of Chao (1980) and Grood and Suntay

(1983) and a low pass digital filtering technique described by Vaughan (1982) to filter the raw displacement data.

The Peak Motus 2000 trials are processed using the ASCII comma delimited files as input. The results are exported into comma delimited ASCII files. The anthropometric data are entered as part of the gait analysis procedure, which is incorporated in the software. Peak Motus 2000 uses mathematical algorithms taken from Vaughan *et al.* (1992) and a 4^{th} order Butterworth low pass digital filter (Hamming, 1983) to filter the raw displacement data.

3.6 Interpolation of Results

The gait parameters from Vicon Clinical Manager are reported in 51 time increments as a percent of gait cycle from 0% to 100% in 2% steps. This reporting format is preferred for the data analysis, so that all the data can be compared as a percentage of the gait cycle. For this reason, the results from the other gait models have to be interpolated so that they will also consist of 51 time increments.

Because of the large variation in subject heights there is a large variation in step length and cadence between the subjects. The interpolation, therefore, also allows for inter-subject analysis.

In order to compare the data, a MATLAB program is used to interpolate the original data, to be incorporated into 51 time increments. The MATLAB program uses a simple spline interpolation function which can be seen in Appendix C. Seven of the twenty gait cycles are also measured from toe off to toe off instead of heel strike to heel strike and these cycles are rearranged so that they can be compared with the gait cycles of the other subjects.

The moment calculations for all subjects are also normalised so that they can be compared. The subject variabilty in height and weight must be taken into account. Therefore the joint moments are normalised by dividing the resulting moment in Nm

by the result of Body Weight × Leg Length which also has dimensions Nm. The moments are therefore dimensionless.

3.7 Statistical Analysis

The aim of this study is to compare the different gait analysis models. In order to do this a method has to be found by which the gait cycles processed using the different models can be compared on a general basis and at specific points in the gait cycle. One model is chosen as the base model, against which the other models can be compared. The BodyBuilder model is therefore chosen as the base model and each of the other models is compared directly to this model and not to each other.

A mean value for each of the 51 time increments in the gait cycle over the twenty subjects is calculated and the graphs of these means for the BodyBuilder model are plotted against those of Vicon Clinical Manager, GaitLab 2.0 and Peak Motus 2000.

A more in-depth analysis is then carried out by dividing the gait cycle into 10% stages from 0% to 90% and comparing the data for the 20 subjects. A repeated measures analysis of variance is used to compare the data at each of the 10% stages of the gait cycle for each gait parameter. Scheffés *post-hoc* test is used to compare each of the models individually to the BodyBuilder model at each of the ten time increment. The data are compared for significance at both the $p=0.05$ and $p=0.01$ levels.

Chapter 4

Results

The results of the study described in chapter three are presented below. The results of the statistical analysis are first pointed out in general, highlighting the significant differences which are observed. The results of the subject means from each software package, Vicon Clinical Manager (VCM), GaitLab 2.0 (GL) and Peak Motus 2000 (PM) are then plotted alongside the results of the subject means obtained by the BodyBuilder model (BB) and the statistical results of each parameter are presented.

4.1 Statistical Analysis

Table 4.1 below displays the results of the analysis of variance and Scheffés *post-hoc* comparison, which is performed on each parameter separately. In the table NS means "not significant", * represents $0.05 > p > 0.01$ and ** represents $p < 0.01$.
The parameters are defined as:

PAT	Pelvic Angle Tilt
PAO	Pelvic Angle Obliquity
PAR	Pelvic Angle Rotation
HAF	Hip Angle Flexion-Extension
HAA	Hip Angle Abduction-Adduction
KAF	Knee Angle Flexion-Extension
KAA	Knee Angle Abduction-Adduction
AAF	Ankle Angle Flexion-Extension
HMF	Hip Moment Flexion-Extension
KMF	Knee Moment Flexion-Extension
AMF	Ankle Moment Flexion-Extension

Table 4.1 shows no significant differences between BodyBuilder and the other three models for pelvic tilt and rotation and hip and knee flexion-extension angles at all of the 10% gait cycle increments at which they are compared. Pelvic obliquity, shows a highly significant difference ($p<0.01$) between BB and VCM at 0% of the gait cycle and a smaller significance ($0.05>p>0.01$) at the same point in the cycle for the comparison between BB and GL.

Parameter	Comparison	% Gait Cycle									
		0	10	20	30	40	50	60	70	80	90
PAT	VCM	NS	NS	NS	NS	NS	NS	NS	NS	NS	NS
	GL	NS	NS	NS	NS	NS	NS	NS	NS	NS	NS
	PM	NS	NS	NS	NS	NS	NS	NS	NS	NS	NS
PAO	VCM	**	NS	NS	NS	NS	NS	NS	NS	NS	NS
	GL	*	NS	NS	NS	NS	NS	NS	NS	NS	NS
	PM	NS	NS	NS	NS	NS	NS	NS	NS	NS	NS
PAR	VCM	NS	NS	NS	NS	NS	NS	NS	NS	NS	NS
	GL	NS	NS	NS	NS	NS	NS	NS	NS	NS	NS
	PM	NS	NS	NS	NS	NS	NS	NS	NS	NS	NS
HAF	VCM	NS	NS	NS	NS	NS	NS	NS	NS	NS	NS
	GL	NS	NS	NS	NS	NS	NS	NS	NS	NS	NS
	PM	NS	NS	NS	NS	NS	NS	NS	NS	NS	NS
HAA	VCM	NS	NS	NS	**	**	**	**	NS	NS	NS
	GL	NS	NS	NS	NS	NS	NS	NS	NS	NS	NS
	PM	NS	NS	NS	NS	NS	NS	NS	NS	NS	NS
KAF	VCM	NS	NS	NS	NS	NS	NS	NS	NS	NS	NS
	GL	NS	NS	NS	NS	NS	NS	NS	NS	NS	NS
	PM	NS	NS	NS	NS	NS	NS	NS	NS	NS	NS
KAA	VCM	NS	NS	NS	NS	NS	NS	NS	NS	*	NS
	GL	NS	NS	NS	NS	NS	NS	NS	NS	NS	NS
	PM	NS	NS	NS	NS	NS	NS	NS	NS	NS	NS
AAF	VCM	**	**	**	**	**	**	**	**	**	**
	GL	NS	NS	NS	NS	NS	NS	NS	NS	NS	NS
	PM	NS	NS	NS	NS	NS	NS	NS	NS	NS	NS
HMF	VCM	NS	NS	NS	NS	NS	**	**	NS	NS	NS
	GL	NS	NS	NS	NS	NS	NS	NS	NS	NS	NS
	PM	NS	NS	NS	NS	*	**	**	NS	NS	**
KMF	VCM	NS	NS	NS	NS	NS	NS	**	NS	NS	NS
	GL	NS	NS	NS	NS	NS	NS	NS	NS	NS	NS
	PM	NS	NS	NS	NS	NS	NS	**	**	NS	NS
AMF	VCM	NS	NS	NS	NS	NS	**	NS	NS	NS	NS
	GL	NS	NS	NS	NS	NS	NS	NS	NS	NS	NS
	PM	NS	NS	NS	NS	NS	NS	NS	NS	NS	NS

Table 4.1 Repeated measures analysis of variance. Scheffés *post-hoc* comparison, comparing VCM, GL and PM to BB. NS means "not significant", * represents $0.05 > p > 0.01$ and ** represents $p < 0.01$

The hip abduction-adduction angle shows a highly significant difference between BB and VCM for the 30% to 60 % gait cycle increments. The ankle flexion-extension angle shows a highly significant difference between BB and VCM for all of the gait cycle increments at which they are compared. The hip flexion-extension moment shows a highly significant difference between BB and VCM at the 50% and 60% increments and between BB and PM at the 50%, 60% and 90% increments with a significant difference being displayed at the 40% increment. Knee flexion-extension moments display a highly significant difference between BB and VCM at 60% of the gait cycle and between BB and PM at 60% and 70% of the gait cycle. Finally the ankle flexion-extension moment shows a significant difference between BB and VCM at 50% of the gait cycle.

Table 4.2 shows the mean differences, maximum differences and standard deviations between the BodyBuilder model and all of the other models. The difference between BB and VCM for the ankle flexion extension angle can be seen to be the largest, with a mean difference of 6.7^0 and a maximum difference of 9.7^0

Gait Parameter	BB-VCM Mean	Max	SD	BB-GL Mean	Max	SD	BB-PM Mean	Max	SD
PAT (^{0})	0.1	0.2	0.1	0.1	0.3	0.1	0.1	0.3	0.1
PAO (^{0})	0.4	1.0	0.3	0.4	0.8	0.2	0.4	1.0	0.2
PAR (^{0})	0.1	0.3	0.1	0.0	0.2	0.0	0.2	0.6	0.1
HAF (^{0})	0.8	1.9	0.5	0.1	0.4	0.1	0.2	0.5	0.1
HAA (^{0})	1.0	1.7	0.5	0.4	0.7	0.1	0.1	0.5	0.1
KAF (^{0})	2.0	5.3	1.2	1.3	3.5	1.0	1.0	2.5	0.8
KAA (^{0})	0.9	2.8	0.8	0.7	1.0	0.1	0.2	1.2	0.3
AAF (^{0})	6.7	9.7	1.4	0.2	0.7	0.1	0.8	2.5	0.7
HMF	0.02	0.06	0.02	0.01	0.05	0.01	0.03	0.06	0.02
KMF	0.01	0.03	0.01	0.00	0.01	0.00	0.01	0.03	0.01
AMF	0.00	0.02	0.00	0.00	0.00	0.00	0.00	0.00	0.00

Table 4.2 Mean differences and standard deviations between BB and the other three models

4.2 Graphical Results

4.2.1 Pelvic Tilt

Figure 4.1 plots the means of the pelvic tilt angles. In Figure 4.1 only small visible differences can be noticed between BB and the other three models. The largest calculated mean difference between the models is found between BB and PM, and is only 0.1^0, with a maximum difference of 0.3^0 (Table 4.1). However the pelvic tilt angle has a large variability in relation to its range of motion (Figure A.1 in Appendix A).

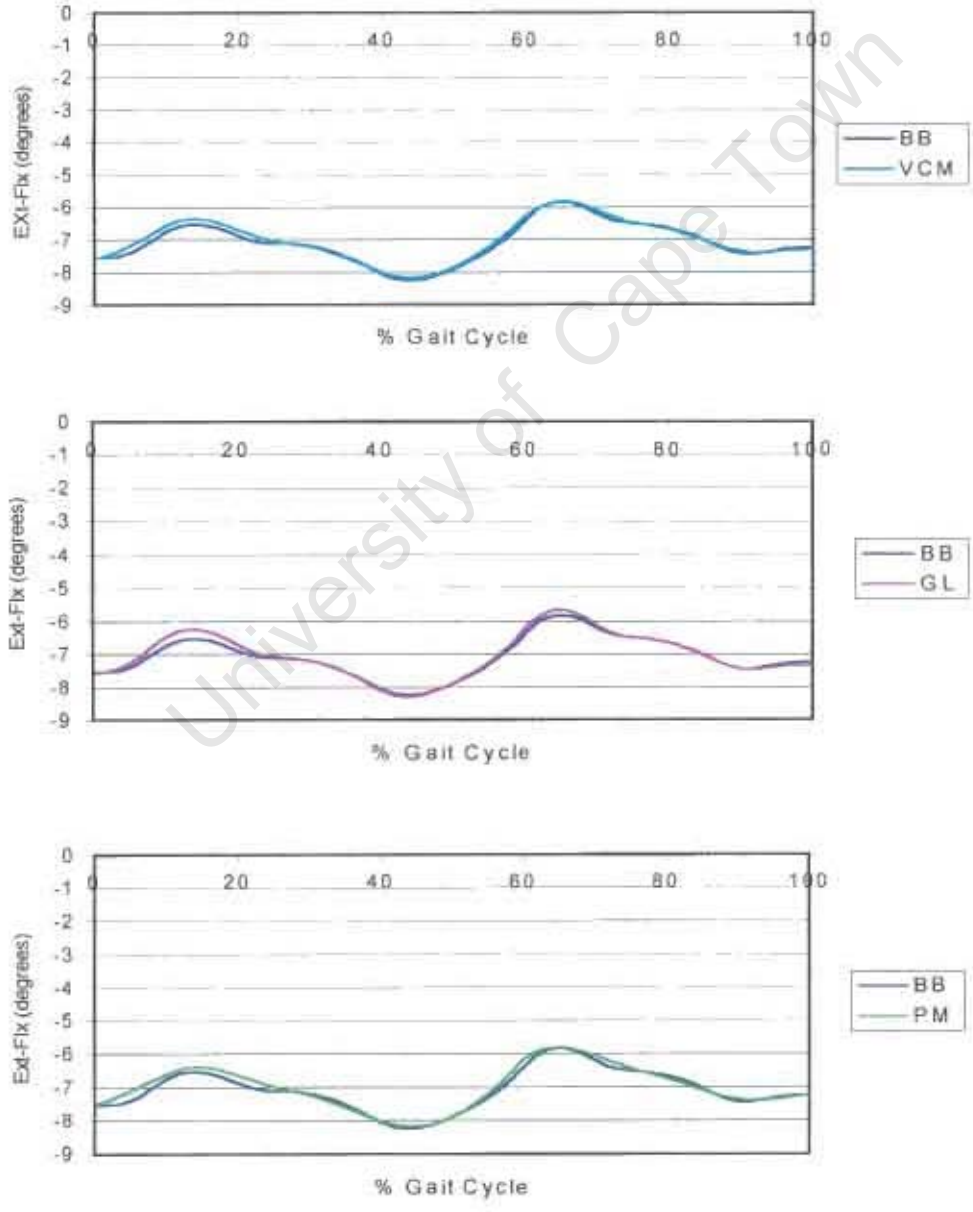

Figure 4.1 Plot of pelvic tilt subject means for BB vs VCM, GL and PM

4.2.2 Pelvic Obliquity

Figure 4.2 plots the means of the pelvic obliquity angles. A significant difference ($p<0.01$) can be seen between BB and VCM at 0% and 100% (assumed to be the same point) of the gait cycle. A smaller significant difference ($0.05>p>0.01$) is found between BB and GL at 0%. A small difference can also be seen between BB and PM at 0%. However Scheffés *post-hoc* comparison (Table 4.1) does not show this difference to be significant, as it is between BB and the other two models. For the rest of the cycle small differences can be seen at 10% and 50% of the cycle but these differences are not found to be significant.

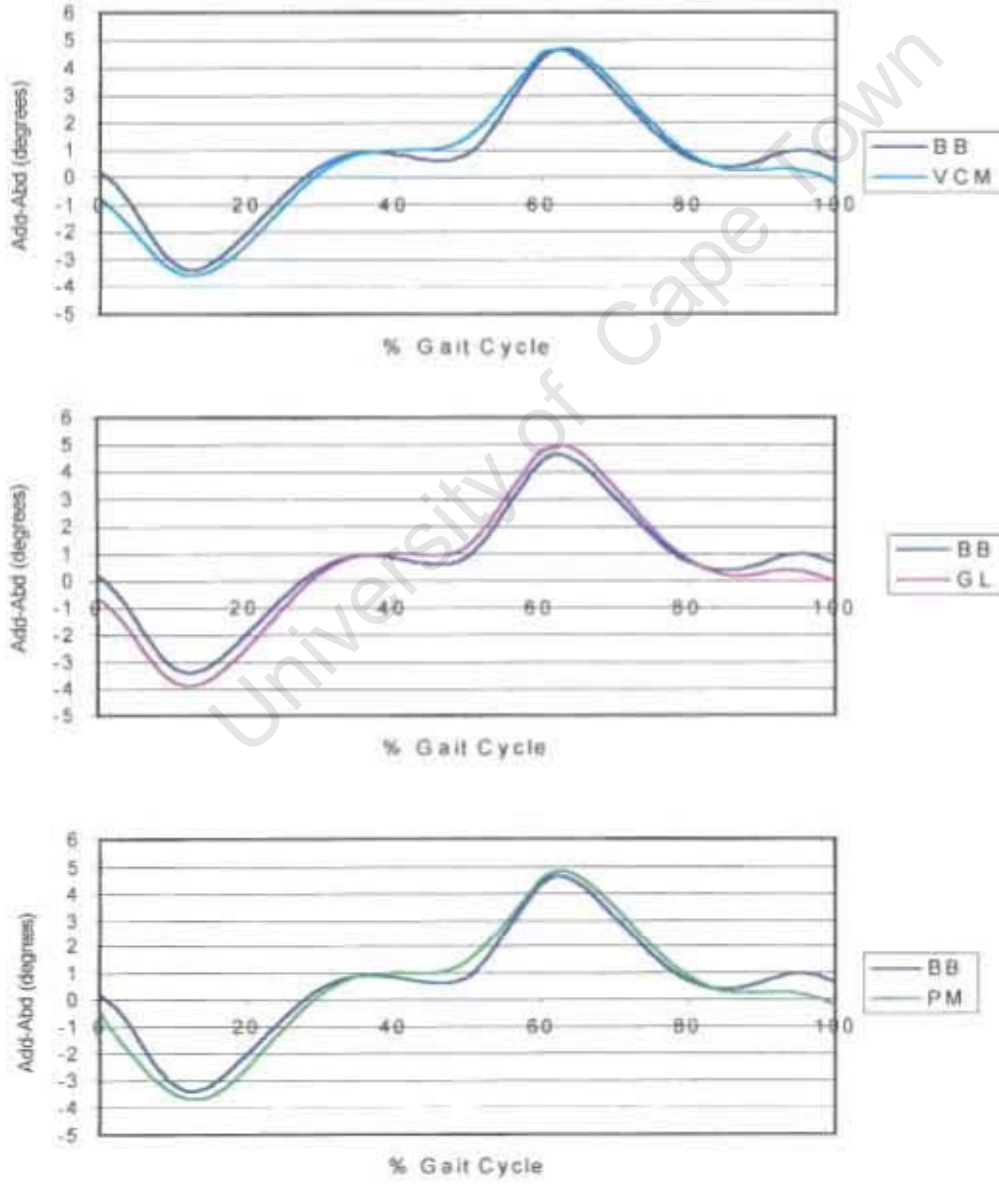

Figure 4.2 Plot of pelvic obliquity subject means for BB vs VCM, GL and PM

4.2.3 Pelvic Rotation

In Figure 4.3, it can be seen that only very small differences exist between BB and the other three models for the pelvic rotation angle, and no significant difference are found. The biggest mean difference over the entire cycle is found between BB and PM (Table 4.2) and is as little as 0.2^0, with a maximum of 0.6^0. The range of the pelvic angles in all cases tilt, obliquity and rotation is small and therefore the visible differences, prove to be only small angle differences. The pelvic angles are also subject to a large variability (Figures A.1, A.2 and A.3 in Appendix A) which will prevent the observed differences from being significant.

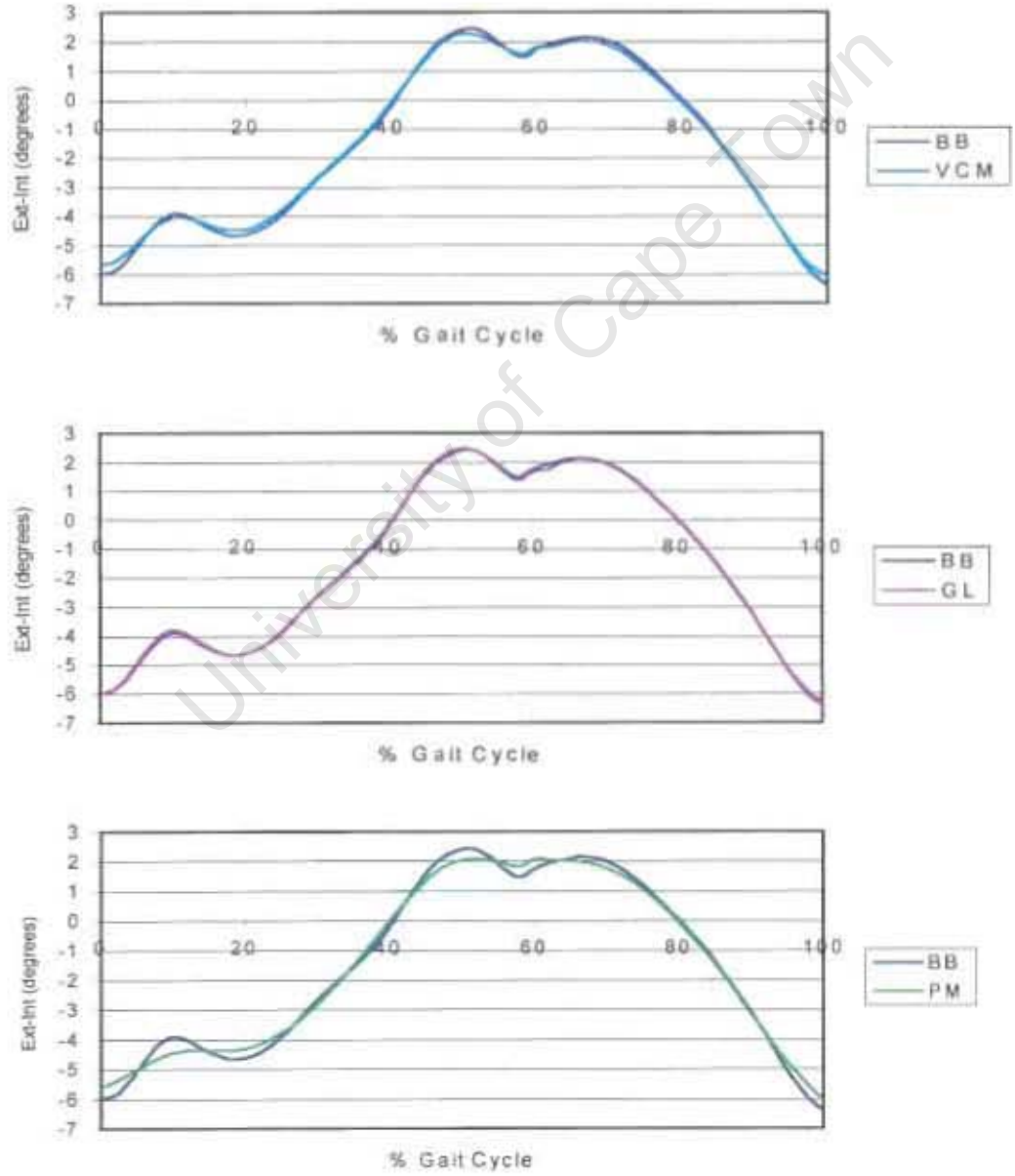

Figure 4.3 Plot of pelvic rotation subject means for BB vs VCM, GL and PM

4.2.4 Right Hip Angle (Flexion-Extension)

Figure 4.4 plots the means of the hip flexion-extension angles. Very little visible difference can be seen between BodyBuilder and the other models for the right hip angle. It is noted that the subject mean from the Vicon Clinical Manager model has a very small offset. The VCM model shows larger flexion and less extension than the BB model. However, this difference is not significant. This difference can also be seen in the mean of the differences to be 0.8^0 with a maximum difference of 1.9^0 (Table 4.2).

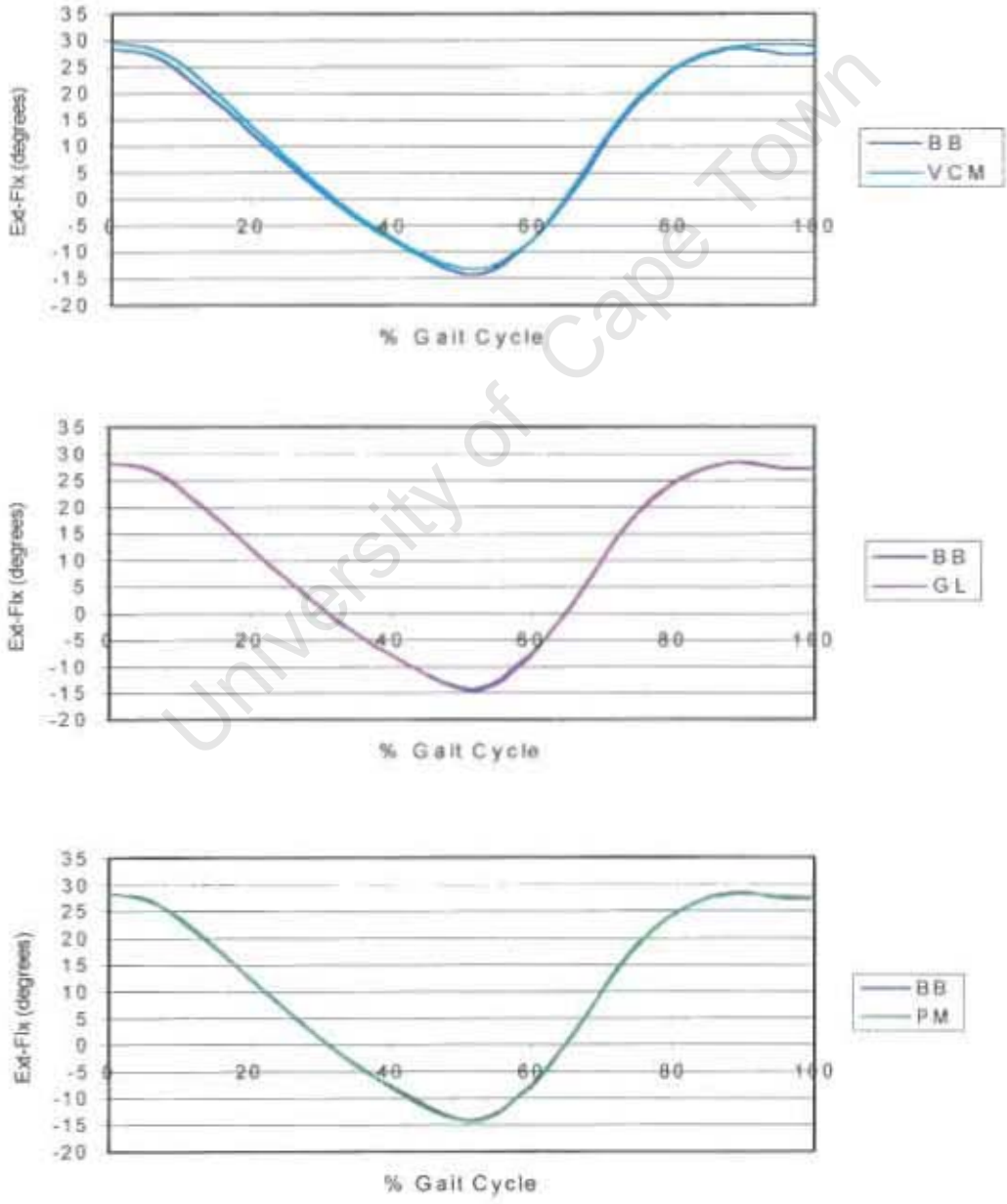

Figure 4.4 Plot of hip flexion-extension angle subject means for BB vs VCM, GL and PM

4.2.5 Right Hip Angle (Abduction-Adduction)

Figure 4.5 plots the means of the hip abduction-adduction angle. In the plots of the hip abduction-adduction angle an obvious offset can be seen between BB and VCM, with the VCM model calculating the angle with more adduction and less abduction than the BB model. This difference is found to be significant ($p<0.01$) at 30%, 40%, 50% and 60% of the gait cycle (Table 4.1). A small offset can be seen between BB and GL (GL showing slightly higher abduction angles), but this is not found to be significant.

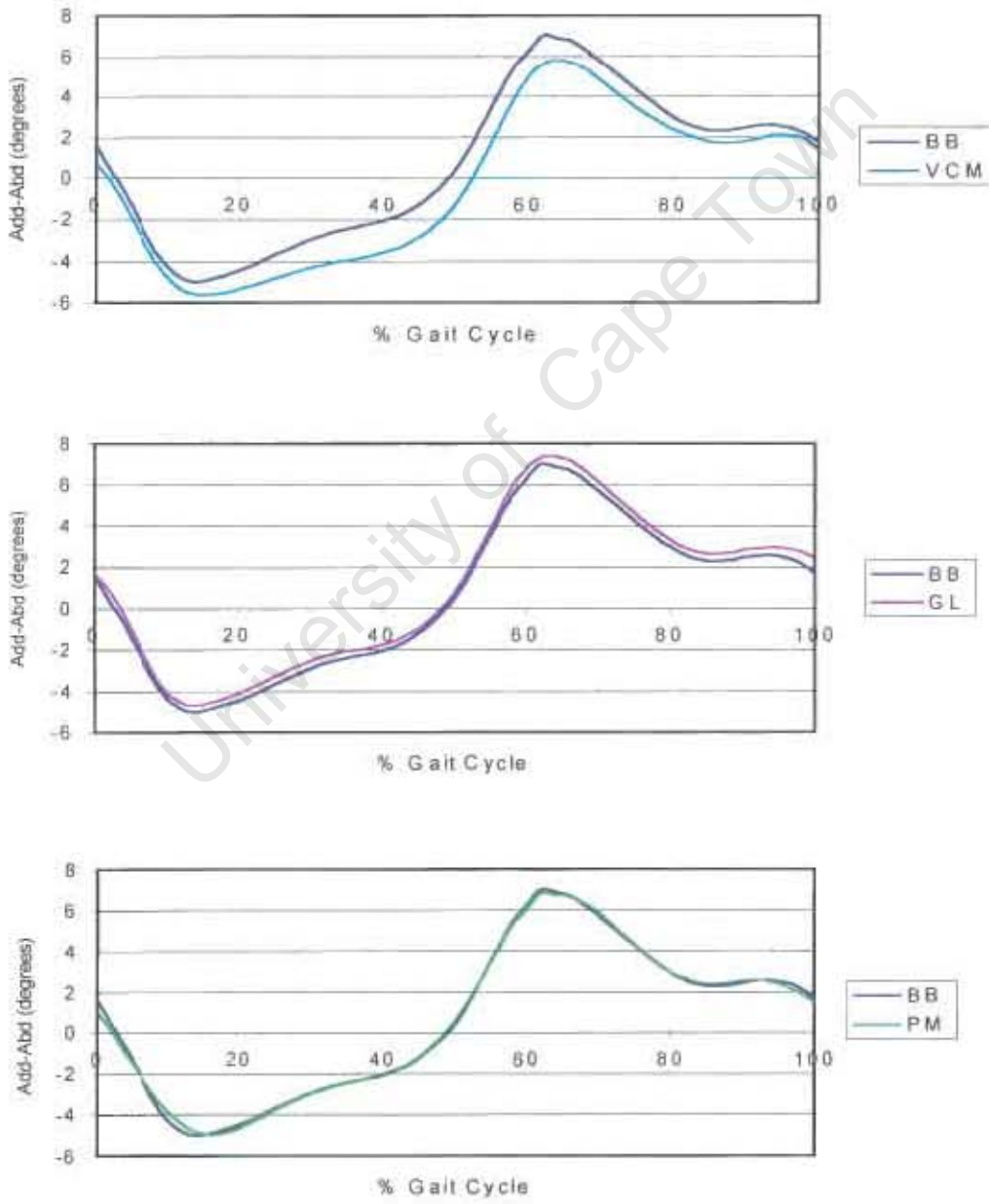

Figure 4.5 Plot of hip abduction-adduction angle subject means for BB vs VCM, GL and PM

4.2.6 Right Knee Angle (Flexion-Extension)

Figure 4.6 plots the means of the knee flexion-extension angles which are seen to be very similar. Once again it is noted that the VCM model has an angle offset, showing larger angles of flexion than BB. The maximum difference occurs at approximately mid-swing, while another difference can be seen after heel strike. The GL and PM models also show slight differences to BB after heel strike and during the swing phase, although these models display less flexion than BB after heel strike and more flexion during swing phase.

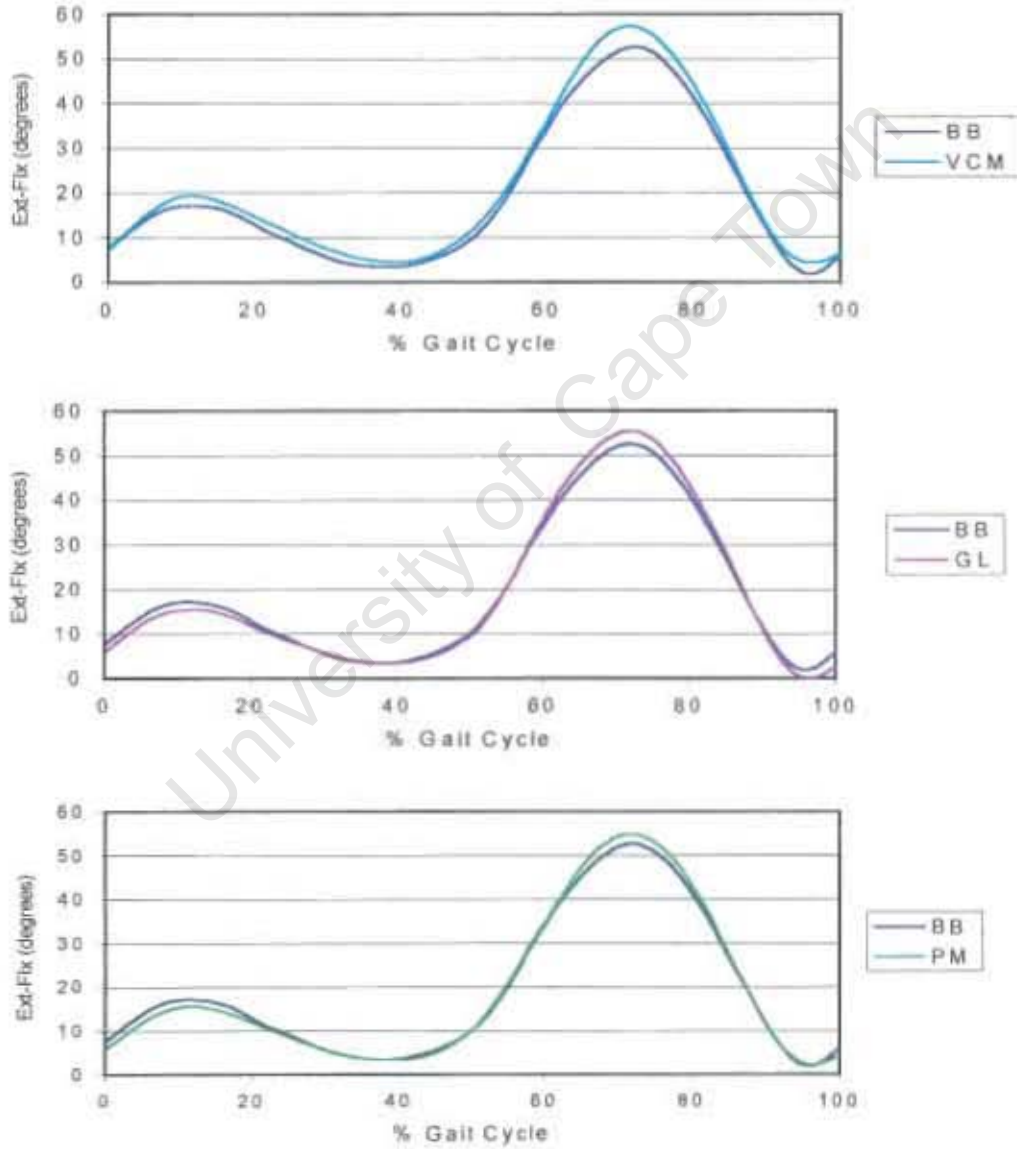

Figure 4.6 Plot of knee flexion-extension angle subject means for BB vs VCM, GL and PM

4.2.7 Right Knee Angle (Abduction-Adduction)

Figure 4.7 plots the means of the knee abduction-adduction angles which show some marked differences, particularly when comparing VCM to BB, with a maximum difference being noted at 80% of the gait cycle. This difference shows a low level of significance ($0.05>p>0.02$) at 80% (Table 4.1), although no significant differences are noted in any of the other cases. The GaitLab 2.0 model shows a small offset from the BodyBuilder model, which is not found to be significant, although the angle shows a large variability (Figure A.7 in Appendix A).

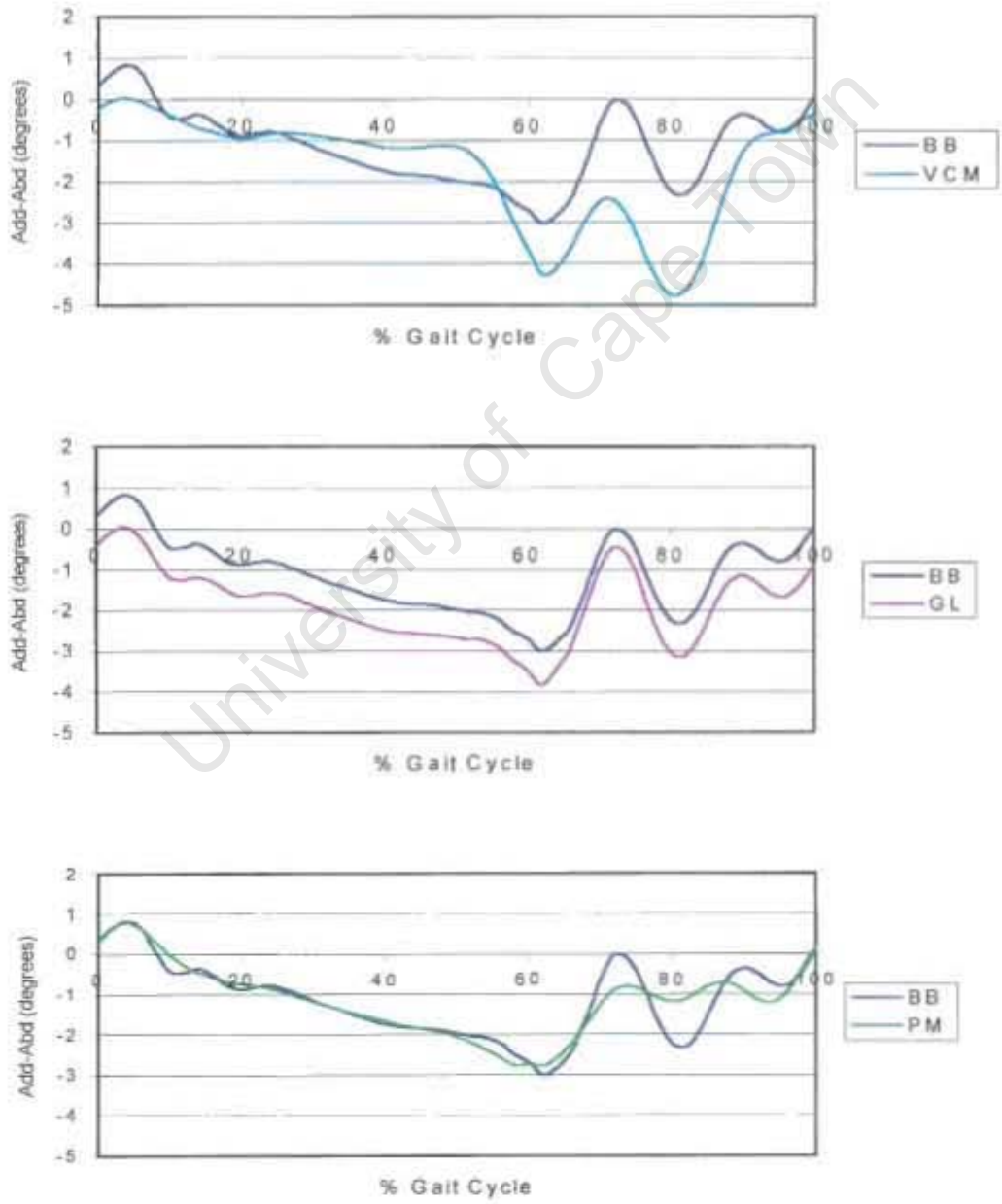

Figure 4.7 Plot of knee abduction-adduction angle subject means for BB vs VCM, GL and PM

4.2.8 Right Ankle Angle (Flexion-Extension)

Figure 4.8 plots the means of the ankle dorsi-plantar flexion angles. A large angle offset is observed between BB and VCM. VCM displays higher ankle dorsiflexion and lower plantar flexion angles than BB, with a maximum difference of 9.7^0 at the approximate point of toe off (60%) and a mean difference of 6.7^0 over the entire cycle (Table 4.2). Scheffés *post-hoc* comparison shows a significant difference between VCM and BB ($p<0.01$) at all ten gait cycle increments at which the models are compared. The differences between BB and GL and between BB and PM for the ankle angle can be seen to be very small and are not found to be statistically different (Table 4.1).

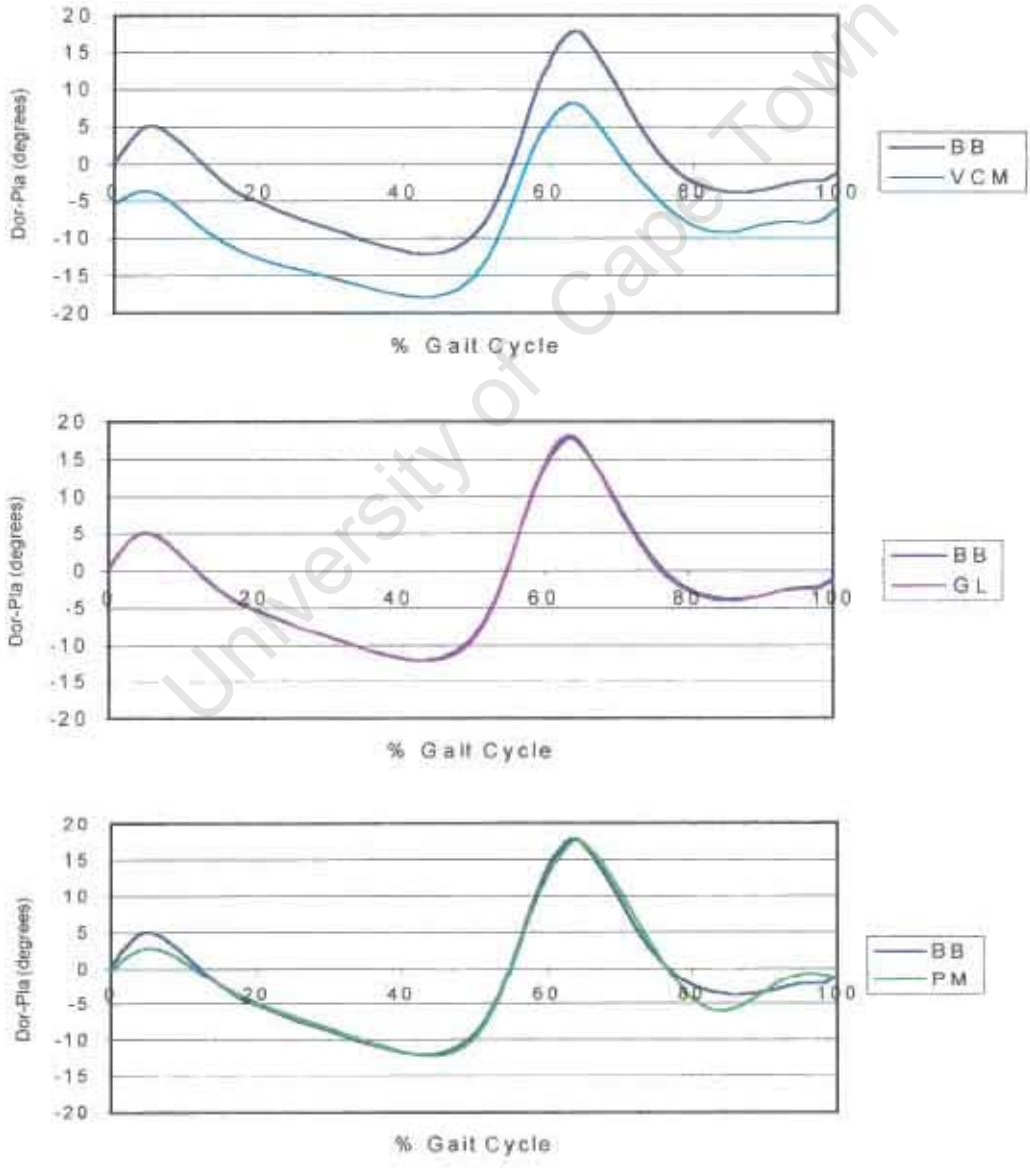

Figure 4.8 Plot of ankle dorsi-plantar flexion angle subject means for BB vs VCM, GL and PM

4.2.9 Right Hip Moment (Flexion-Extension)

Figure 4.9 plots the hip flexion-extension moments which illustrates the significant differences ($p<0.01$) between BB and VCM at 50% and 60% of the gait cycle (Table 4.1). The plot of BB vs GL shows small but non-significant differences. A significant difference ($0.05>p>0.01$) at 40% and highly significant differences ($p<0.01$) at 50%, 60% and 90% of the gait cycle, are observed between BB and PM. A visible difference can also be seen between BB and the other three models at about 95% of the cycle, with the BB model presenting a smaller extension moment.

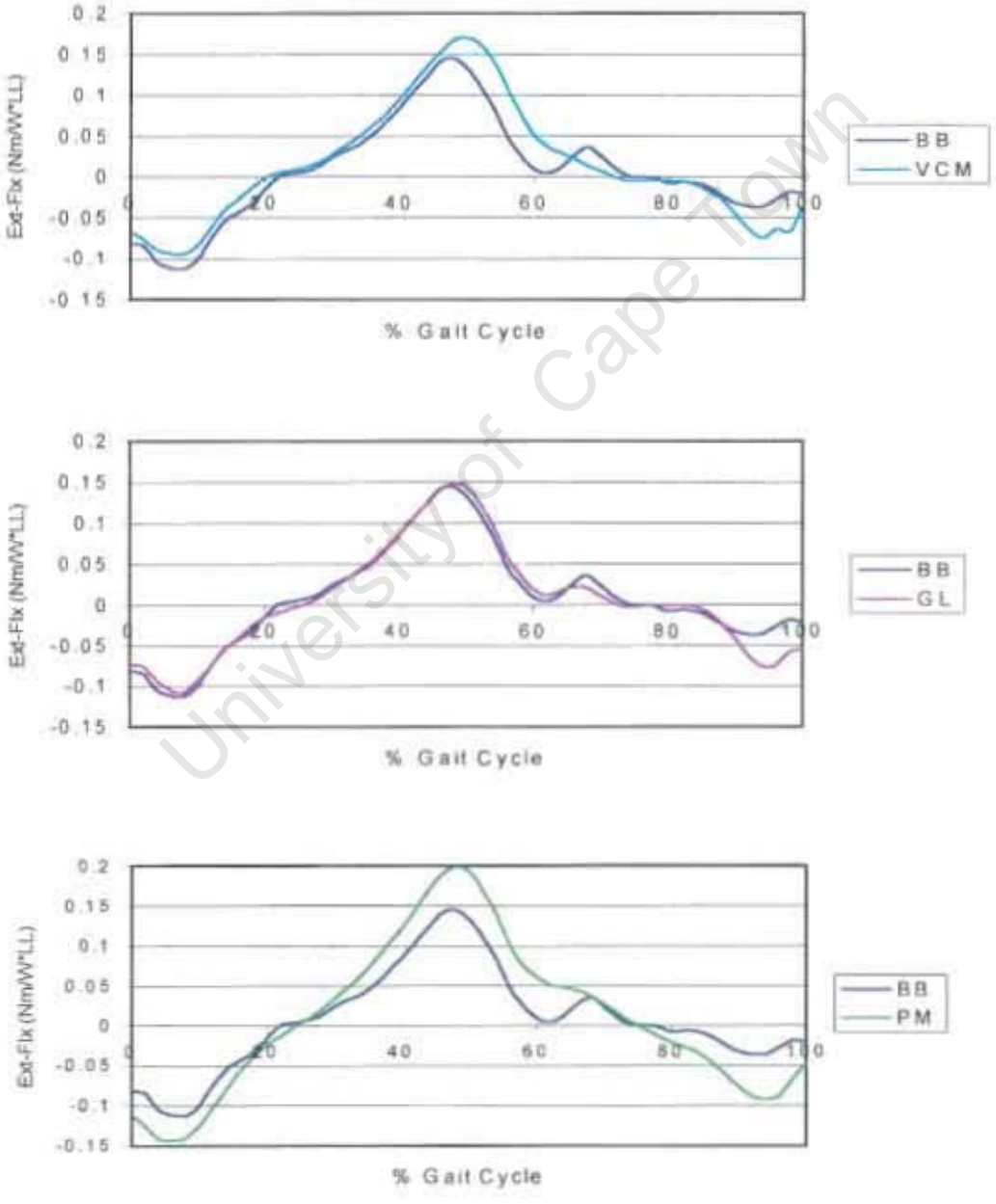

Figure 4.9 Plot of hip flexion-extension moments subject means for BB vs VCM, GL and PM

4.2.10 Right Knee Moment (Flexion-Extension)

Figure 4.10 plots the mean knee flexion-extension moment. A highly significant difference ($p<0.01$) can be seen between BB and VCM at 60% of the cycle and once again differences are noted at about 95% of the cycle (Table 1). No significant differences can be seen between BB and GL, although a large difference is observed at about 95% of the gait cycle. Significant differences ($p<0.01$) can be seen between BB and PM at 60% and 70% of the cycle with another large difference being evident at 95% of the cycle. No tests of significance are done at the 95% increment of the gait cycle. At approximately 95%, the BB model displays a smaller flexion moment than the other three models.

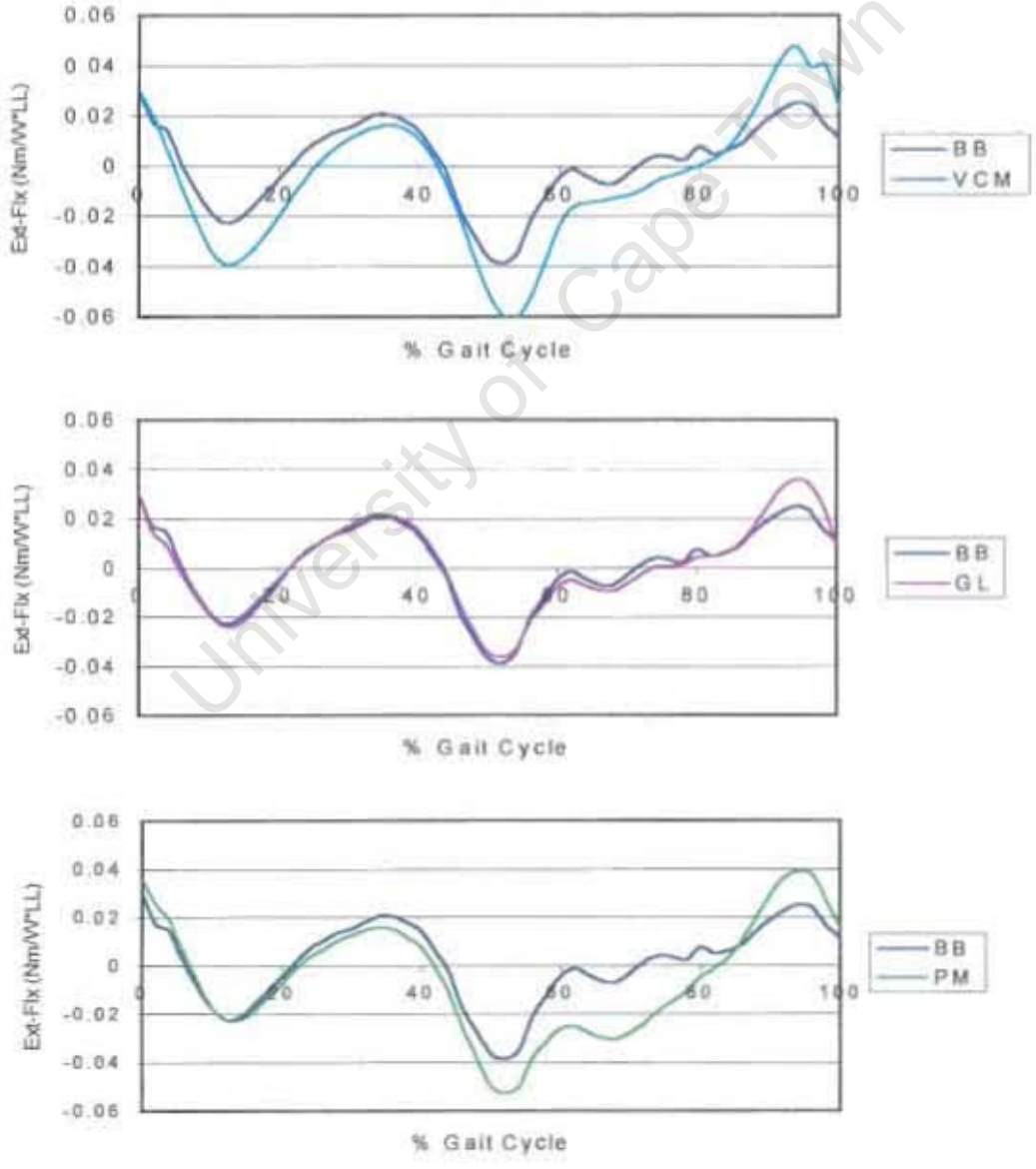

Figure 4.10 Plot of knee flexion-extension moments subject means for BB vs VCM, GL and PM

4.2.11 Right Ankle Moment (Flexion-Extension)

Figure 4.11 plots the mean results of the ankle dorsi-planter flexion moments. A difference can be seen between BB and VCM. The VCM model shows a higher ankle dorsi-flexion moment than the BB model along the entire gait cycle. This difference is only found to be significant ($p<0.01$) at the 50% increment of the gait cycle. The figure shows very small differences between BB and GL and between BB and PM.

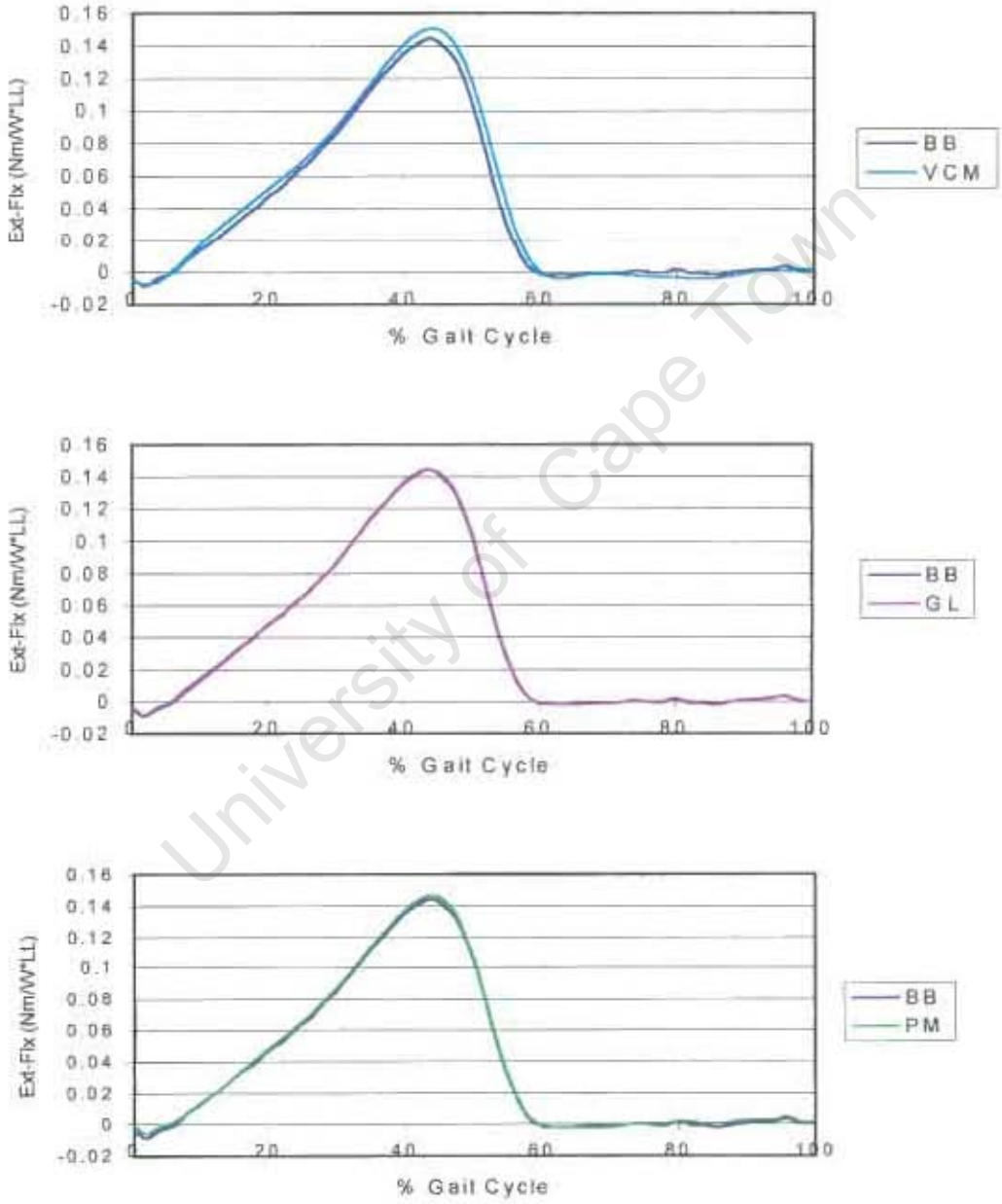

Figure 4.11 Plot of ankle dorsi-plantar flexion moments subject means for BB vs VCM, GL and PM

4.3. Summary of results

In general, the BodyBuilder model produces similar results to all three of the other models. The Vicon Clinical Manager model shows the greatest differences from the BodyBuilder model. Highly significant differences ($p<0.01$) can be seen between BB and VCM for the ankle dorsi-plantar flexion angle (over the entire cycle) and the hip abduction-adduction angle (from 30% to 60% of the gait cycle). Significant differences can also be observed between BB and VCM and between BB and PM at a few specific points along the gait cycle for the hip, knee and ankle flexion-extension moments.

Chapter 5

Discussion

The results section pointed out the differences that are found between the BodyBuilder model and Vicon Clinical Manager, GaitLab 2.0 and Peak Motus 2000. In general all the gait analysis models produce similar results. The graphs produced by all of these packages display the expected results for the different parameters, which describe the gait cycle.

This study is able to eliminate the differences, which may occur with marker placement, by adopting the commonly used Helen Hayes Hospital marker set (Figures 1.1 and 1.2). The same subject data from the same trial is also processed by each gait analysis software package.

The results of this study can be compared with normal adult gait data of Kadaba *et al.* (1989 and 1990) and other normal data presented on the clinical gait analysis website (http://guardian.curtin.edu.au/cga/data/index.html). The range of motion for both joint angles and moments at each joint is similar to these other studies. The pelvic rotation angle in this study does display a strange "kink" at 60 % of the gait cycle and it is not symmetrical about the zero line. The reason for this is that 7 of the 20 gait cycles analysed are taken from toe off to toe off and the processed results are then rearranged (heel strike to heel strike) so that they could be compared with the gait cycles of the other subjects.

Significant differences are observed between the models at particular gait cycle increments, using a repeated measures analysis of variance and Scheffés *post-hoc* test. There are many possibilities for these differences, which will be discussed in more detail below. In broad terms, these differences may be accounted for by the different methods used to estimate body segment parameters, estimate joint centres and segment axes, calculate joint angles, calculate joint kinetics, filter raw displacement data and statistically compare the models.

5.1 Estimating Body Segment Parameters

Body segment parameters are estimated based on the measurement of anthropometric data from the subject. These anthropometric measurements, which are described in chapters two and three, are necessary for the calculation of joint centres, segment moments of inertia, segment masses and segment centres of gravity. These calculated parameters are subsequently used to estimate the segment velocities and accelerations and finally the net joint moments.

5.1.1 Anthropometric Measurements

In BodyBuilder, GaitLab 2.0 and Peak Motus 2000, the 20 anthropometric parameters described in chapter three are measured. In VCM the anthropometric parameters measured are body mass, height, leg length, knee width and ankle width. VCM also estimates the hip joint centre based on the ASIS breadth and the leg length, while the other models estimate this center based only on the ASIS breadth.

These differences may lead to a small difference in joint centre positioning which will compound as the model progresses toward calculating the joint moments. The joint centre calculations only use the direct anthropometric measurements described above, while the joint moments are calculated based on the segment moments of inertia, segment centres of gravity and segment masses.

The different needs for anthropometric measurements, from the different models, are assumed to have little effect on the differences observed in the joint angle calculations.

5.1.2 Body Segment Parameters

The estimation of body segment parameters in the models studied are based on Chandler *et al.* (1975) and Dempster *et al.* (1959). The BodyBuilder and GaitLab 2.0 models estimate body segment parameters based on data from cadaveric studies performed by Chandler *et al.* (1975). Therefore the estimation of body segment

parameters should not have any influence over the differences encountered between the BodyBuilder model and GaitLab 2.0.

The body segment parameters estimated in Vicon Clinical Manager and Peak Motus 2000 are approximated based on the relationships of Dempster *et al.* (1959). As discussed above, the body segment parameters are the basis for calculating the segment velocities, accelerations and joint kinetics.

The segment mass is used in the calculation of joint forces, while the segment centre of gravity is needed to calculate the segment velocities and accelerations which are also used to calculate the joint forces. This can be seen when recalling Newtons Laws:

$$\Sigma \text{ Forces} = \text{Segment Mass} \times \text{Segment Acceleration} \qquad 5.1$$

The moment of inertia estimations are then used to calculate the segmental momentum which in turn has an influence on the joint moments.

In all models the lower extremities are divided into six segments, with the thigh and tibia segments being defined as a cylinder and the foot segments as a right pyramid (chapter three). Therefore the segment masses and moments of inertia are in general defined in the same manner, only with differing estimation algorithms.

Significant differences are noted between BodyBuilder and VCM and between BodyBuilder and Peak Motus 2000 for the knee and hip flexion-extension moments. On closer inspection, it can be seen that these differences occur at approximately the same stage in the gait cycle (between 40% and 60% for hip moment and between 60% and 70% for knee moment, Table 4.1). The only major difference between BB and PM for calculating gait parameters is in the prediction of these body segment parameters.

The influence of the body segment parameters on the joint moment calculations during the stance phase is, however, assumed to be small. Davis (1994a) in the Biomch-L archives performed an assessment of the contribution of different errors on

the overall uncertainty of a calculated value for a joint moment. He concludes that BSP and acceleration data have little effect on the overall uncertainty of the hip moment during the stance phase of gait, accounting for less than 2% of the total uncertainty. Davis (1994b) performs a complete error analysis of a simplified case of the foot in contact with the ground and finds that even when the error associated with BSP's is set to zero, little effect on the overall uncertainty in joint moment is observed.

During the swing phase of the gait cycle (60%-100%) the inertial and acceleration parameters are the only ones affecting the joint moments, as the ground reaction forces are zero. Therefore, during this phase of the gait cycle the difference in BSP estimation between the different gait analysis packages will account for differences observed in the joint moments (Table 4.1).

5.2 Estimation of Segment Axes and Joint Centres

5.2.1 Segment Reference Axes

The definition of the segment axes in BodyBuilder, GaitLab 2.0 and Peak Motus 2000 are described by Vaughan *et al.* (1999), while the segment axes in Vicon Clinical Manager are described by Kadaba *et al.* (1990) and Davis *et al.* (1991).

The pelvis, thigh and shank segments are all defined similarly for all of the models. Differences are however observed in the definition of the foot segment reference axes. In BB, GL and PM the foot segment reference axes are defined using the three markers on the foot; lateral malleolus, 2nd metatarsal head and heel (chapter three). In VCM the heel marker is not used in the foot segment axis definition. Therefore the foot segment in VCM is defined with only one unit vector from the lateral malleolus to the 2nd metatarsal head.

The segment orientation is likely to have a large effect on the gait parameters relating to the ankle. This effect can be seen when comparing the BB model to VCM, where the ankle flexion-extension angle is found to be significantly different ($p<0.01$) over the entire gait cycle. The fixed segment axis in the BodyBuilder model is defined

along the line from the heel marker to the 2nd metatarsal head (chapter three) (Vaughan *et al.*, 1999), while in the VCM model (Kadaba *et al.* 1990 and Davis *et al.* 1991) the fixed axis is defined along a line from the ankle joint centre to the 2nd metatarsal head, as no heel marker is necessary. A static trial is used in VCM to calculate an offset angle to compensate for this. The coordinate system in the foot is rotated by this offset angle before the ankle angles are calculated. This angle offset is however constant and therefore the differences in segment axis definitions between the models still exist. The fixed axis in the BB model, places the foot in a more dorsiflexed position than the VCM model and therefore the ankle angle will show more plantar flexion in BB. Figure 5.1 describes the segment axes in the BB model.

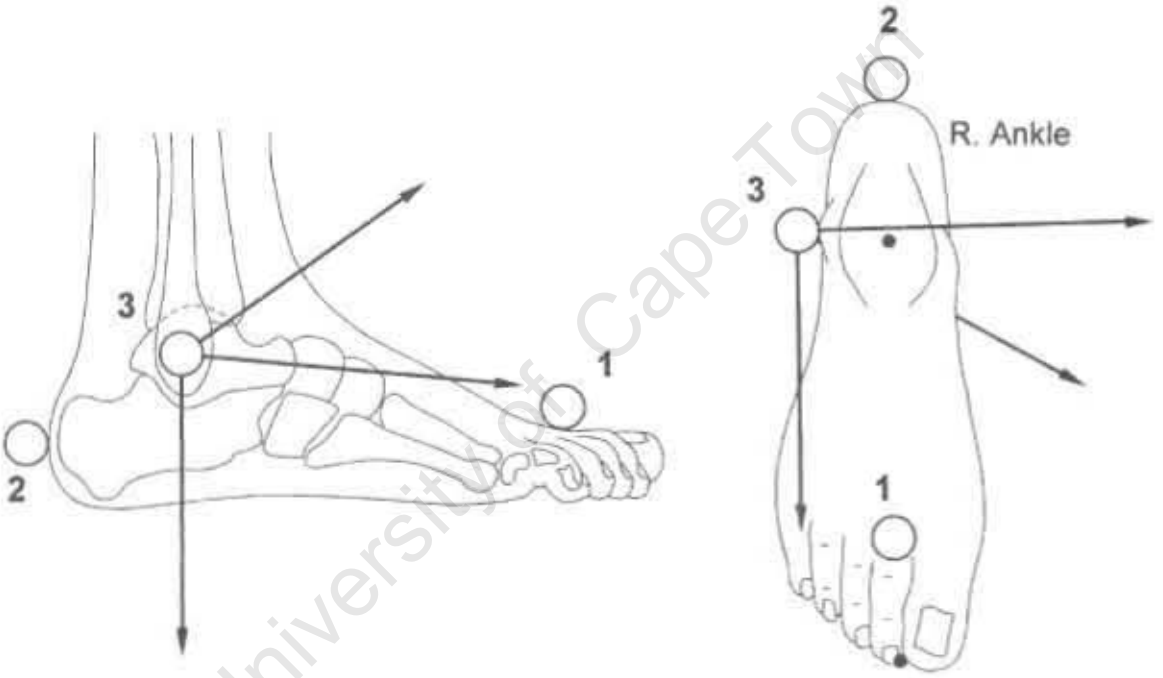

Figure 5.1 Segment axes defined in the BodyBuilder model

The significant difference ($p<0.01$) observed at 0% of the cycle in the pelvic obliquity angle may also be affected by the definition of the segment reference frame. The pelvis segment in both BB and VCM is however defined in a similar manner and the difference is only significant at 0% of the cycle and therefore is more likely influenced by other factors such as filtering and joint center estimation.

5.2.2 Joint Centre Estimation

In chapters two and three, two different methods for estimating joint centres are presented. GaitLab 2.0, BodyBuilder and Peak Motus 2000 use the same method described by Vaughan *et al.* (1999), while Vicon Clinical Manager uses methods described by Davis *et al.* (1991) and Kadaba *et al.* (1990). It is therefore expected that differences, which exist between BodyBuilder and GaitLab 2.0 and between BodyBuilder and Peak Motus 2000, are not influenced by the segment axes and joint centre estimations. However, differences which exist between BodyBuilder and Vicon Clinical Manager are likely affected by the different methods used to calculate joint centres.

The results of the repeated measures analysis of variance and Scheffés *post-hoc* test showed that there are significant differences ($p<0.01$) between BodyBuilder and Vicon Clinical Manager at 30%, 40%, 50% and 60% of the gait cycle for the hip abduction-adduction angle and at all gait cycle increments 0%-90% for the ankle dorsi-plantar flexion angle. Plots of the hip flexion-extension and knee flexion-extension angles also show that the VCM model produced a small angle offset, displaying slightly higher flexion angles than BB (Figures 4.4 and 4.6). The estimation of segment axes and joint centres is the first step in determining the joint angles and it is therefore likely that their estimation will be one of the causes of the differences observed.

In the VCM model, the hip joint centre position is estimated based on a hip joint centering algorithm developed by Davis *et al.* at the Newington Childrens' Hospital in 1981 through radiographic examinations of 25 hips. The hip joint centre calculation for VCM is based on three constants θ, β and C, where C is a function of leg length. The hip joint centre estimation also includes a measure of the ASIS breadth and is described by Davis *et al.* (1991), (chapter two). The knee joint centre is then calculated based on the position of the hip joint centre, the lateral femoral epicondyle marker and the knee width.

The BB model estimates the hip joint centre using methods described by Vaughan *et al.* (1999). This method requires that three orthogonal axes are defined in the segment and then estimation equations, which make use of the ASIS breadth, are used to approximate the hip joint centre. The knee joint centre is also calculated by defining three orthogonal axes and makes use of the knee width measurement and the lateral femoral epicondyle marker position The knee joint centre estimation in BB does not take the hip joint centre position into account as the VCM model does.

The differences in the hip joint centre between BB and VCM is plotted in Figure 5.2. In the case of VCM the ASIS breadth and leg length are incorporated into the estimation, while in the BB model the leg length is not incorporated. In VCM the hip joint centre is used to calculate the knee joint centre, while in BB there is no direct link between the hip joint position and knee joint position.

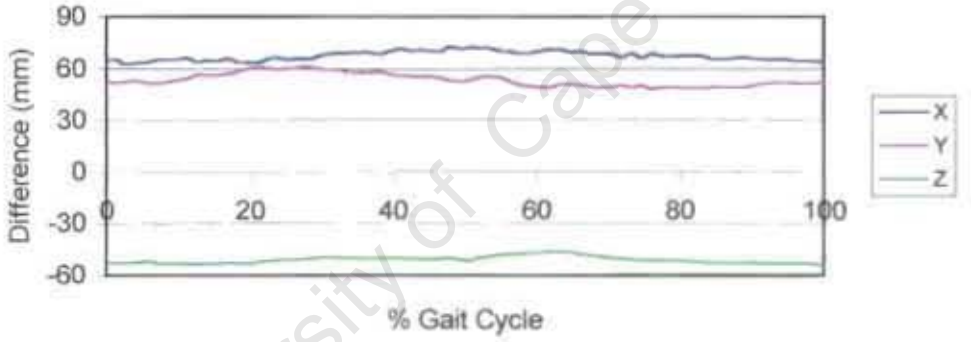

Figure 5.2 Difference in the hip joint centre position between BB and VCM, anterior (X), medial (Y) and superior (Z) is positive

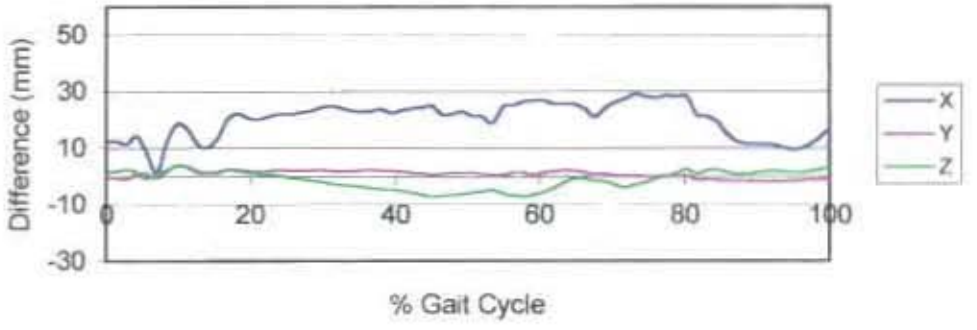

Figure 5.3 Difference in the knee joint centre position between BB and VCM, anterior (X), medial (Y) and superior (Z) is positive

In Figure 5.2 an absolute difference of more than 50 mm can be seen between BB and VCM for all orientations X, Y and Z. This places the hip joint centre in BB about 60 mm anterior, 60 mm medial and 50 mm inferior to that of VCM. In Figure 5.3 the difference in the position of the knee joint centre can be seen to be close to 30 mm in the anterior-posterior axis, with the BB model placing this joint centre anterior to the VCM model. The difference in ankle joint centre between BB and VCM (Figure 5.4) is seen to be more than 15mm in the anterior-posterior axis.

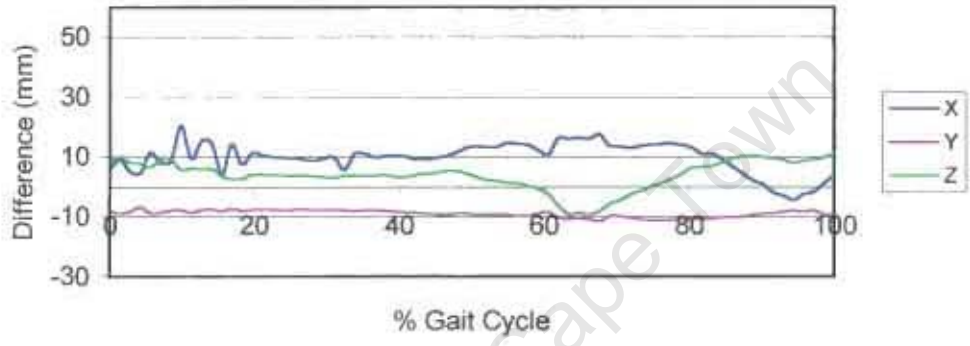

Figure 5.4 Difference in the ankle joint centre position between BB and VCM, anterior (X), medial (Y) and superior (Z) is positive

The increased flexion angles observed in the VCM model compared to the BB model are most likely a result of these differences observed in the joint centre positions (Figures 5.2, 5.3 and 5.4).

Significant differences ($p<0.01$) are observed, between BB and VCM, for the hip abduction-adduction angle (Table 4.1 and Figure 4.5). VCM calculates the hip abduction-adduction angle to have a higher adduction angle than BB. The difference in hip joint centre position as seen in Figure 5.2, means that VCM places the hip joint centre about 50 mm lateral to that of BB and therefore will calculate a larger adduction angle.

Plots of the knee abduction adduction angles (Figure 4.7) display visible differences between BB and the other 3 models, with the difference only being significant ($p<0.01$) at 80% of the gait cycle for the comparison between BB and VCM. The

differences between BB and VCM may also be as a result of the different knee joint centre estimation procedures.

The ankle flexion-extension angle as discussed above, exhibits the greatest difference between BB and VCM. The ankle flexion-extension angle calculated in VCM shows less plantar flexion and more dorsiflexion than that calculated in BB. This offset is probably as a result of the foot segment axis definitions, but the differences observed in the ankle joint centre (Figure 5.4) will also affect these angles.

These differences in joint centre estimation may also have an influence on the joint moment calculations and may be the cause of the increased flexion moment offset for the hip and ankle and the decreased flexion moment offset for the knee. The joint moments are calculations of the joint force multiplied by the lever arm. If the joint centres are different, the lever arms are different and this will result in a change in joint moment.

5.3 Joint Angle Calculations

In addition to the joint centre estimation and segment orientation, a further influence on the results may be the algorithms used by the different models to calculate the joint angles. VCM uses methods described by Kadaba *et al.* (1990) and Davis *et al.* (1991), while the other models use methods described by Vaughan *et al.* (1999).

VCM and the other models calculate the joint angles as the rotation of the distal segment relative to the proximal one, although the relationships used to describe these angles are different to those used by the other three models. This variation may also account for the angle offset and statistical differences observed between BB and VCM.

VCM estimates the joint angles by calculating the dot product of the distal segment on the proximal segment for all three rotations: flexion-extension, abduction-adduction and internal-external rotation. BB, GL and PP calculate an abduction-addduction axis through the joint about which the angle rotations are occuring. The abduction-

adduction angle in BB is also calculated as the dot product of the proximal segment on the distal segment and not the other way round as in VCM.

However the effect of the angle calculations is assumed to be small in comparison to the influence of joint centre estimation and segment axis definition. The angles are generally calculated in the same manner, as the rotation of the distal segment on the proximal one.

5.4 Euler Angle Calculations

The Euler angle calculations in all the models are needed to calculate the angular velocities and accelerations, which are in turn needed to calculate the resultant joint moments. The Euler rotations described in VCM, BB, GL and PM are based in general on the work of Chao (1980). Therefore the calculation of Euler angle rotations in the different models have no effect on the joint moments measured.

5.5 Joint Kinetics

5.5.1 Joint Moments

The different methods of calculating joint centres have an effect on the joint moments, because of the length of the lever arm associated with the relevant joint. The difference in joint centre estimation can be seen in Figures 5.2, 5.3 and 5.4, with the largest difference occurring at the hip joint. Davis (1994b) shows that by reducing the error in joint center positioning to zero, the overall uncertainty in the calculated moment, in his example, will drop from 11.634 Nm to 8.33 Nm. This demonstrates that the joint centre position has a large effect on the joint moments.

Figure 5.5 below helps explain how the position of the joint centre may influence the moment calculations for the hip, knee and ankle. If we simplify the inverse dynamics approach for calculating joint moments and estimate the joint moment based on a crude approach of force × lever arm, it can be seen how a change in lever arm will result in a change in joint moment.

In Figure 5.5, it can be seen how the position of the joint centres (HJC, KJC and AJC) affect the length of the lever arm. If the force is constant, then the longer the lever arm the greater the moment.

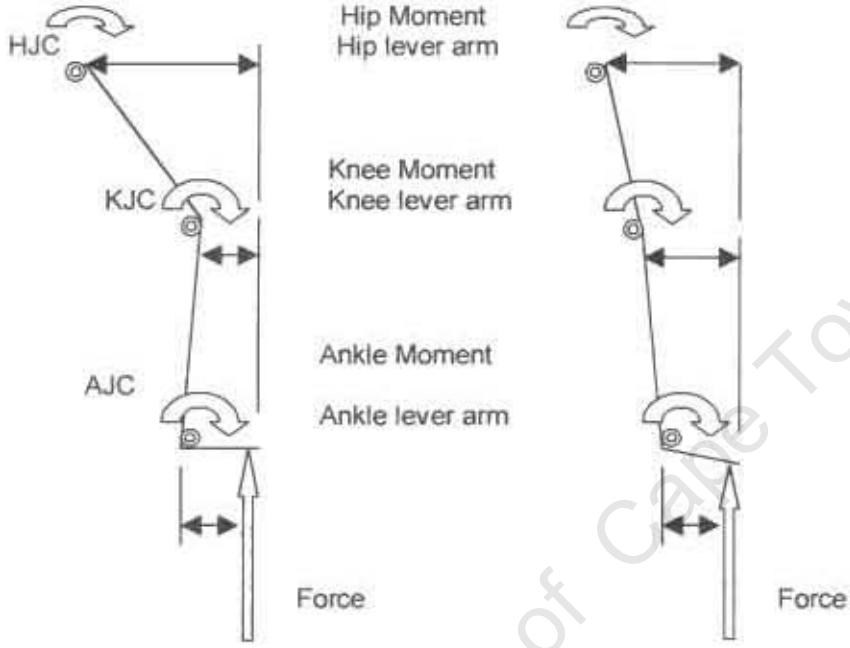

Figure 5.5 The influence of joint centre position on the joint moment lever arm.

The different joint centre estimation algorithms and therefore the different joint centre positions mean that the lever arms in the VCM model are different to those in the BB model. In Figure 5.5 it can be seen how a longer lever arm will lead to a larger flexion moment. The hip joint centre in VCM is placed approximately 50 mm posterior to that in BB, and will therefore calculate a higher flexion moment at the hip. This can be seen in Figure 4.9 where the VCM model has a higher flexion moment than the BB model throughout the stance phase of the gait cycle. This change in lever arm will also affect the knee and ankle joint moments. The knee and ankle joint centres in BB are placed anterior to those in VCM, resulting in a decreased knee extension and ankle plantar flexion moment (Figures 4.10 and 4.11).

5.5.2 The Effects of BSP estimation

As discussed above, the prediction of body segment parameters also has an effect on the joint moments and is the most likely cause of the significant differences calculated between BodyBuilder and Peak Motus 2000 in the knee and hip flexion-extension moments during the swing phase of the gait cycle. Both PM and VCM use the same prediction equations and similar differences are noted between BB and PM and between BB and VCM. Davis (1994a) explains that BSP estimation has very little influence on the joint moment calculations during the stance phase of gait. However during the swing phase the BSP and acceleration parameters have the greatest influence on the joint moments. The differences between BB and VCM in joint moments during the stance phase are therefore assumed to be, mainly, as a result of the joint centre estimation, while the body segment estimations contribute to the differences observed in the swing phase.

5.6 Filtering Techniques

Filtering algorithms are used by each of the gait analysis models to smooth out the high frequency noise from the marker trajectory signal. This high frequency noise is usually a result of marker oscillation and skin movement. Each of the four models uses a different filtering technique.

BB uses a five-point weighted average filter (Lynn and Fuerst, 1989), while GL uses a low-pass digital filter described by Vaughan (1982). VCM uses a Bezier spline interpolation filter (Hamming, 1983). PM uses a fourth order low pass Butterworth filter as well as a cubic spline and fast fourier transform, described by Jackson (1979), depending on the nature of the data to be filtered.

It can reasonably be assumed that the different filters will have some effect on all the gait parameters which are calculated in this study. All the parameters are calculated from the initial marker positions described by the Helen Hayes Hospital marker set (Figures 1.1 and 1.2).

The effects of the different filtering algorithms can be observed in Figure 5.6. It is assumed that the only difference between BB and GL is the differentiation algorithms and the filtering techniques. Therefore, in observing the differences between BB and GL, the effects of the different filters are now explored.

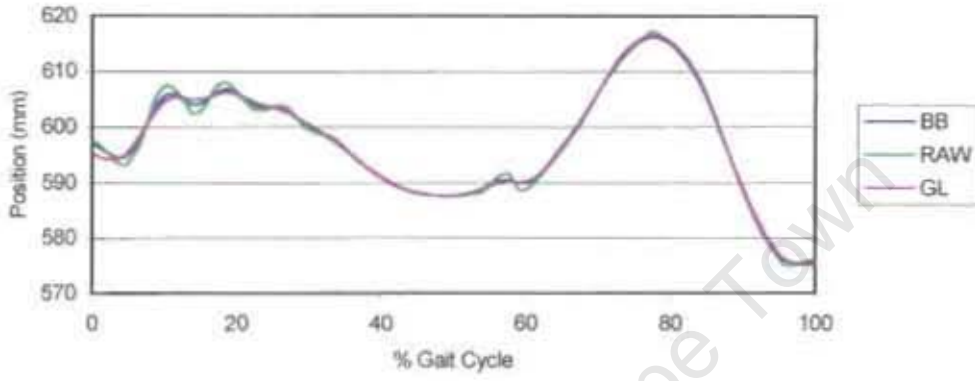

Figure 5.6 Plot of right thigh wand trajectory: Raw data, filtered in BB and filtered in GL

BodyBuilder and GaitLab 2.0 are only found to be statistically different ($0.05>p>0.01$) at the 0% increment of the pelvic obliquity angle. Similar small differences, which may be attributed to filtering algorithms, can be seen in all the other gait parameters compared. In particular for the knee flexion-extension angle it is noticed that the BB model seems to have a slightly attenuated knee flexion angle in the swing phase (75% of gait cycle) and a greater flexion angle after heel strike. The different filtering procedures in BB and GL lead to slightly different marker trajectories (Figure 5.6) which will cause these small differences in joint parameters. Another filtering artifact can be observed between BB and GL at about 95% of the gait cycle where GL produces a smaller hip flexion moment and higher knee flexion moment than BB. This may be accounted for by the endpoint errors caused by the GL filters when there are not extra digitised frames available. Vaughan (1982) describes similar endpoint problems and augments the data artificially to overcome them, but he also suggests digitizing extra frames as an alternative.

An angle offset exists between BB and GL for both the hip and knee abduction-adduction angles. The hip shows more abduction and the knee more adduction in GL than in BB. As all the other estimations and calculations in BB and GL are exactly the same, this difference is a result of the filtering techniques. The abduction-adduction angle takes place about the orthogonal floating axis (Vaughan *et al.*, 1999) and the segment axis is defined using the wand markers which are most affected by oscillation (Figure 5.6). The GL filter, smooths this wand marker vibration differently to BB and the floating axis is therefore not defined exactly the same way in both models, resulting in the angle offsets observed. Since no wand markers are used on the foot this does not apply to the ankle angles. Of course this difference will also be observed in the comparison of BB to the other two models. The high variation in knee abduction-adduction angles calculated also means that these differences are not significant (Figure A.7 in Appendix A).

The filtering techniques used in Vicon Clinical Manager also had small effects on the differences observed. Once again the most obvious is the significant difference ($p<0.01$) observed at the 0% increment of the pelvic obliquity angle. Endpoint errors, similar to those of GL, are also observed in the hip and knee moment calculations. In the case of the VCM model, the different filtering technique serves to increase the differences, which are caused by the different segment axis definitions, joint centre estimations and body segment estimations. The larger differences tend to occur at peaks of flexion or extension and abduction or adduction. This may also be attributed to the different filtering technique as the signal is attenuated depending on the filter characteristics.

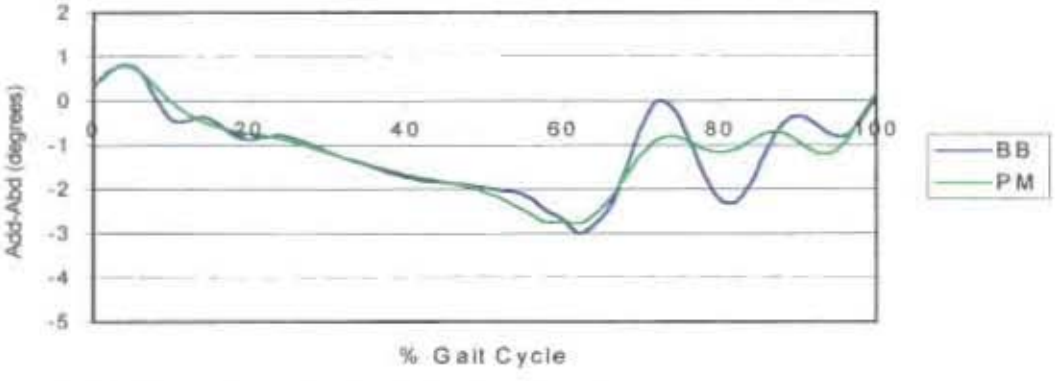

Figure 5.7 BB vs PM for the knee abduction-adduction angle.

The Peak Motus 2000 gait analysis package shows the largest differences based on the filtering algorithm. It can be seen in all the plots of the gait parameters that PM smooths the data more than the other three models. This is assumed to be a result of the 4th order Butterworth filter that is used to filter the raw displacement data. The best example of this increased smoothing can be seen in the plot of BB vs PM for the knee abduction-adduction angle and which has been reproduced below (Figure 5.7). It can immediately be seen that between 70% and 90% of the cycle the PM data have been smoothed far more than that of BB.

The significant differences calculated between BB and PM for the hip and knee flexion-extension moments have partly been accounted for by the estimation of body segment parameters and once again it is assumed that the filtering techniques add to this difference. Large endpoint filter errors in PM can also be seen in the hip and knee moments and these are in fact significant for the hip moment at 90% of the gait cycle. It can also be seen again that the significant differences occur at peaks of flexion or extension, which may be as a result of the filter attenuation.

In chapter three, the filtering of the raw analogue data is discussed. A three point weighted average filter is used to filter the raw force plate data before it are processed in each of the software packages. A three point weighted average filter (Lynn and Fuerst, 1989) results in one frame of data at the beginning and one frame at the end of the data series being eliminated because the data are interpolated. The displacement data are then filtered in each gait analysis package and once again, depending on the filter, a number of data frames at the beginning and end of the data series are lost. This loss in frames, leads to the large endpoint errors which can be seen in the comparison of BB with the other three models.

5.6.1 Differentiation

To obtain the segment velocities and accelerations, which are used in the calculation of joint moments it is necessary to differentiate the segment centre of gravity position with respect to time. Both linear and angular accelerations are important in calculating kinetic gait parameters based on Newton's laws and equations 3.15 and 3.16 in chapter three.

Different methods are used to differentiate the segment centre of gravity positions and Euler angle calculations with respect to time. VCM uses a weighted least squares differentiation technique (Lynnn and Fuerst, 1989), while GL uses finite difference methods derived from Taylor series expansions (Vaughan *et al.*, 1999). PM uses a quintic spline processor which is adopted from Hermann Woltring's GCVSPL routine and BB uses a simple differentiation method over two 60 Hz time frames.

These differences may have a small effect on the results of the different models moment outputs. However the differentiation techniques are in general the same and the smoothing algorithms are the only aspects that may affect the moment calculations. These small differences may be observed when studying the plots of BB vs GL for the hip, knee and ankle flexion-extension moments (Figures 4.4, 4.6 and 4.8). As no significant differences are calculated between BB and GL for the flexion-extension moments, these differences are assumed to be negligible.

5.7 Statistical Analysis

5.7.1 Variation of Data

The effect of the variability of the BodyBuilder model means on the statistical significance of a comparison must be noted. Often a visible difference will be deemed to be statistically non-significant because the standard deviation is large for that particular parameter at that particular point in the cycle. Appendix A includes plots of the subject means for the BodyBuilder model (plus and minus one standard deviation for all 11 parameters) and should be viewed as a helpful tool in distinguishing between significant and non-significant results.

When viewing the knee abduction-adduction angle (Figure 4.7) it is evident that the four models have different although not significantly different results. A closer inspection is made of the mean of the BodyBuilder model with its standard deviations in Figure 5.8. The standard deviation is large in this case and therefore only one significant difference is evident between BB and the other models (at 80% of the cycle between BB and VCM as highlighted by Figure 4.7).

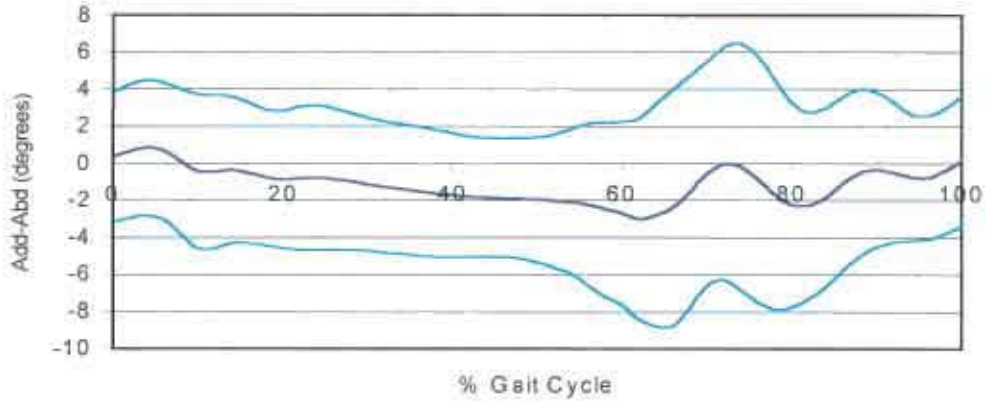

Figure 5.8 Subject mean ±1SD of the knee abduction-adduction angle for the BodyBuilder model

The large variability in gait data have also been noted by Kadaba *et al.* (1989). They report large variability particularly in the pelvic angles, hip abduction-adduction and knee varus-valgus angles. As in Figure 3.8 the variability in their knee varus-valgus angle also increases during the swing phase of the cycle. The variability reported by Kadaba *et al.* (1989) and the data reported on the Clinical Gait Analysis website (http://guardian.curtin.edu.au/cga/data/index.html), compare with the data presented in Appendix A.

5.7.2 Limitations of Statistical Analysis Procedure

A possible limitation of the statistical analysis, which may affect the results is that the models are only compared at 10% increments and therefore significant differences which may exist between these points are missed. It is felt however that repeated measures analysis of variance and Scheffés post-hoc analysis at 10% increments is sufficient to represent the entire gait cycle.

This limitation is evident when viewing the plots of the knee flexion-extension angle at 75% (Figure 4.6) and that of the hip and knee flexion-extension moments at 95% (Figures 4.9 and 4.10). At these points in the gait cycle one would have expected some sort of significant difference to be calculated. Calculating the differences at only 70% and 80% for the knee angle may have enabled this increased flexion angle seen in the knee to be accounted for as not significant when in fact it is significant.

Although Scheffés post-hoc analysis is a conservative post-hoc test for significance between means, it is possible that because of the large number of statistical comparisons that the alpha level should have been adjusted to prevent an error-rate problem. The Bonferroni test, which makes a very conservative analysis of a large number of group means, may be preferred. It is however felt that as the data fit the criteria for an analysis of variance that an alpha adjustment is not necessary.

5.8 Summary of Conclusions

5.8.1 BodyBuilder vs Vicon Clinical Manager

The significant differences observed between BB and VCM are assumed to be a result of a combination of a few different aspects. The aspects, which play a large role in the differences, are the estimation of body segment parameters, the definition of segment axes and the estimation of joint centres. The calculation of joint angles, the method of differentiation and the filtering techniques play minor roles and may only increase the differences, which have already been established.

The significant differences observed for the ankle flexion-extension angle do raise some concerns when considering a clinical observation. At heelstrike the BodyBuilder model displays about 5^0 of plantar flexion, while the Vicon Clinical Manager model suggests that the ankle is in about 3^0 of dorsiflexion. This difference may result in a different clinical diagnosis and must therefore be taken into account when comparing the output from different gait models.

The significantly different hip and knee flexion-extension moments should also be noted when making a clinical diagnosis or treatment decision.

5.8.2 BodyBuilder vs GaitLab 2.0

A significant difference is only observed at 0% of the gait cycle for the pelvic obliquity angle. Any differences found between the two models can only be associated with the filtering techniques and differentiation algorithms, as all the other estimations and calculations, which make up the gait parameters analysed are exactly

the same. It is therefore unlikely that a different clinical diagnosis or treatment decision could be made with GaitLab 2.0 model and the BodyBuilder model.

5.8.3 BodyBuilder vs Peak Motus 2000

Significant differences between these two models are only noted in the hip and knee flexion-extension moments. This difference is assumed to be a result of the different methods of estimating the body segment parameters and the different filtering techniques. The body segment estimation procedure is based on the same data as that from VCM, and similar moment differences are observed between BB and these two models. Differentiation algorithms and filtering techniques could also cause differences between BB and PM. It is noted that the PM filter does smooth the gait data parameters more than any of the other models.

The significant differences displayed in the hip and knee flexion-extension moment calculations may result in different clinical diagnoses and must therefore also be taken into account.

5.8.4 Miscellaneous Effects

A possible shortfall of the statistical analysis performed in this study is the fact that the models are only compared at 10% intervals and therefore any statistical differences falling outside of these increments may have been missed. An error-rate problem may also have been avoided by adjusting the alpha level for significance.

The VCM software package also suggests the use of a knee alignment device (KAD) for determining the placement of the wand markers. However as this study did not compare subjects and trials, it is decided that the use of the KAD is unnecessary.

Chapter 6

Recommendations

6.1 Conclusions

The discussion is summarised in the previous chapter and it is obvious that some significant differences can be found between BodyBuilder and Vicon Clinical Manager and between BodyBuilder and Peak Motus 2000. These differences are a result of the different model algorithms used by the gait analysis packages. This study is able to test for the effects of these different algorithms by maintaining a common marker set and processing the same subject data using the four different model algorithms.

As expected, the results from the BodyBuilder model and the GaitLab 2.0 model are found to match the closest, with filtering and differentiation algorithms being the only differences between the models.

From the results of this thesis, it is not possible to distinguish which model is more accurate. The study only serves to point out the differences that can be made by using the different methods to calculate joint angles and moments and also the different methods used to filter the raw displacement data.

Gait clinicians who wish to compare their data with data which have been processed by a different gait analysis package at another laboratory, must take these significant differences into account. The angle offsets displayed by VCM, especially for the hip abduction-adduction and ankle flexion-extension angles, must be accounted for, when comparing data.

6.2 Recommendations

There are at least three other commercial software packages that utilise the Helen Hayes Hospital marker set. These include: Motion Analysis Corporation; Qualisys; and Bioengineering Technology and Systems. It is therefore recommended that the output parameters from these packages should be compared to a common

BodyBuilder or GaitLab 2.0 model. Motion Analysis Corporation had offered to process the data collected in this study, using their Orthotrak II software. However this analysis was unfortunately not completed by the company.

In this study a repeated measures analysis of variance is performed at 10% gait cycle increments. The comparison of data would be more complete if the data could be compared at every one of the 51 gait cycle increments. It is recommended that a statistical test is performed on the results which can compare the data at all 51 time increments. This however requires a PC with high processing capabilities. A Bonferroni post-hoc analysis may also have been performed to ensure that no error-rate problems exist in the comparison of the group means.

One of the problems, which is encountered when attempting to compare data, is the data formats that are required by each gait analysis package. In this study three different formats are used, namely C3D, DST and ASCII. In order to compare the same set of data with different gait analysis packages it is recommended that a conversion program such as Rdata 2 (by Edmund Cramp from Motion Lab Systems, Appendix D) is used. Perhaps in the future a common file format may be decided on, and will allow for easier distribution and comparison of gait data.

The gait clinician needs to realise that differences do exist between the different gait analysis programs and they should be wary of these differences when comparing data captured at different laboratories and with different gait analysis software packages. The significant differences in angle and moment calculations make it possible that differing clinical or operative decisions can be made on the basis of the differences observed between the gait analysis packages. However the actual angle and moment differences are small in magnitude (mean of $6,72^0$ for the ankle flexion-extension angle).

Davis *et al.* (1997) and Kadaba *et al.* (1990) suggest that the effective use of movement analysis in a professional context depends on a universal agreement on variable definitions, conventions and terminology, which will allow for a direct interpretation and comparison of data obtained at different laboratories. If the motion analysis community could standardise models and filtering techniques in the gait

analysis packages, gait analysis may be accepted as a diagnostic tool and not just an evaluation tool (Brand and Crowninshield, 1981).

Competition between the different motion analysis software vendors is likely to delay this sort of a standardisation as no company wants to lose money by converting their software to accept a common model and filtering technique Each company must believe that their model produces results that are accurate and correct. Since no study has been able to confirm which models give superior results, this will continue to be a debate.

A study which could accurately advise which model gives results that are closest to the true gait parameters, would be an invaluable asset in promoting gait analysis as a well respected diagnostic tool.

Appendix A

Variation of Gait Data Parameters

Subjects from age 8 to age 50 were used in this study. Therefore a large variation in subject height and weight was observed. The BodyBuilder model was compared with the other three models and the results can be seen in chapter four. However, in order to properly understand the results, it is necessary to view the figures presented below which plot the subject mean of the parameters for the BodyBuilder model plus and minus one standard deviation.

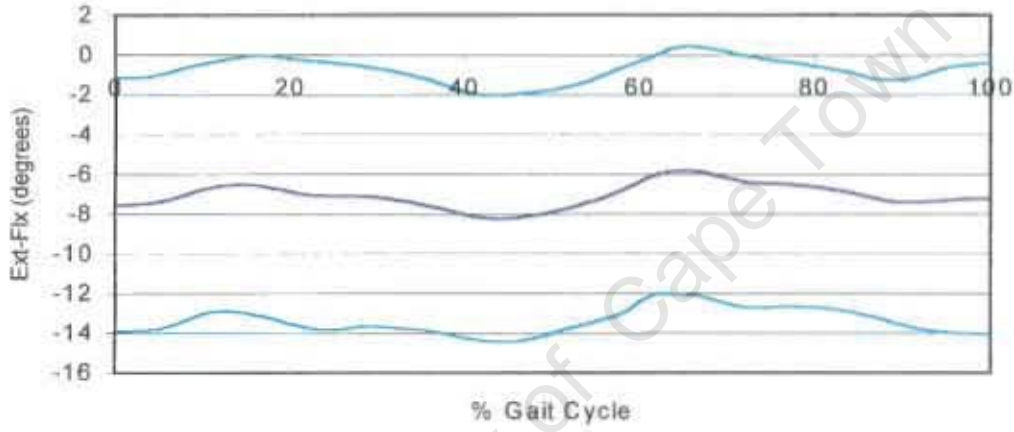

Figure A.1 Subject mean ±1SD of pelvic tilt angle for the BodyBuilder model

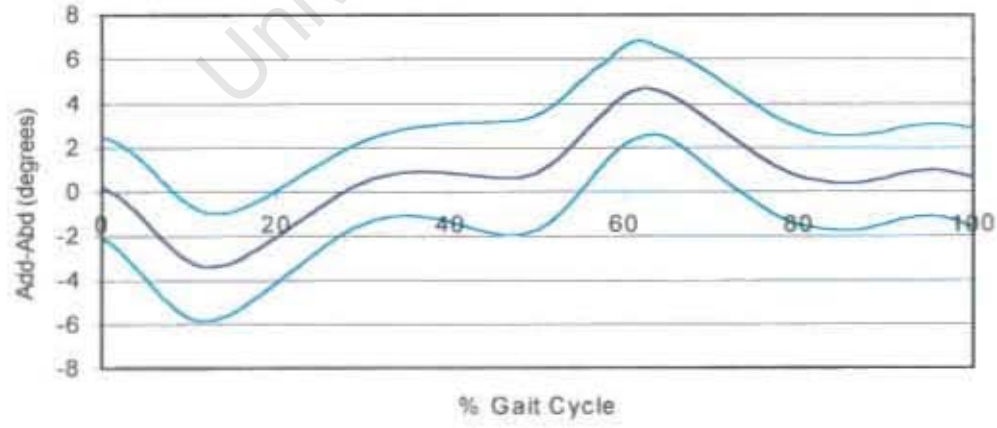

Figure A.2 Subject mean ±1SD of the pelvic obliquity angle for the BodyBuilder model

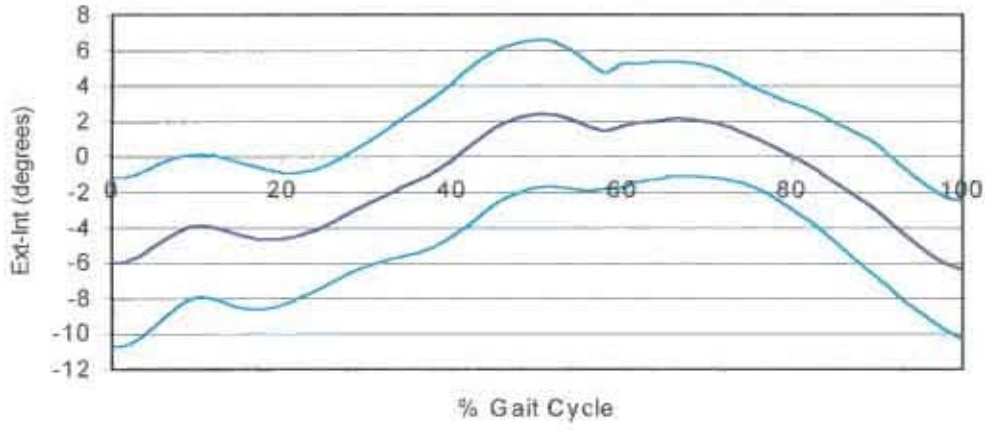

Figure A.3 Subject mean ±1SD of the pelvic rotation angle for the BodyBuilder model

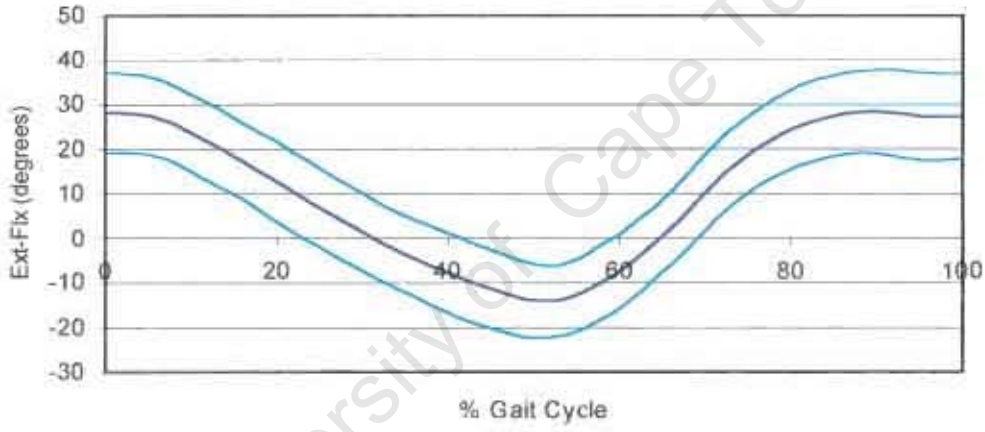

Figure A.4 Subject mean ±1SD of the hip flexion-extension angle for the BodyBuilder model

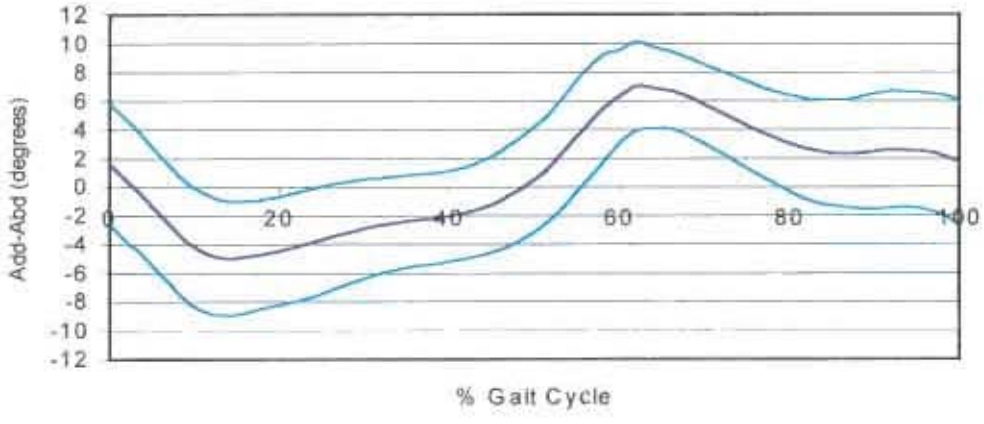

Figure A.5 Subject mean ±1SD of the hip abduction-adduction angle for the BodyBuilder model

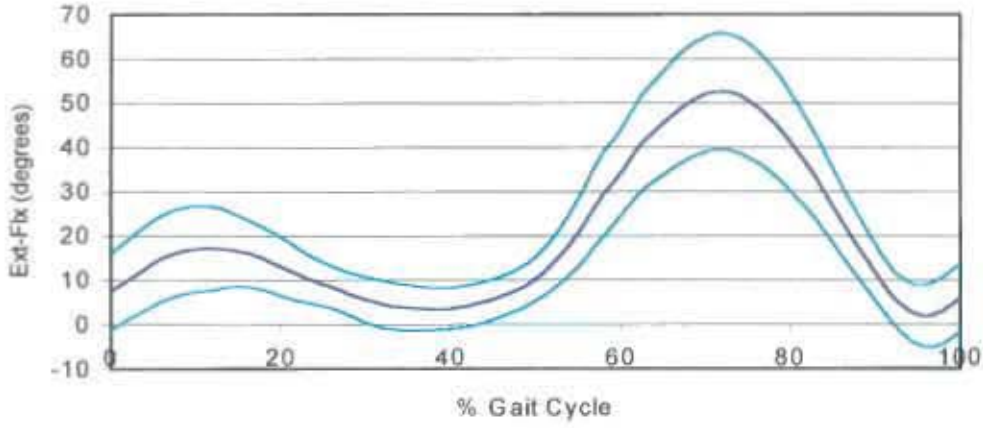

Figure A.6 Subject mean ±1SD of the knee flexion-extension angle for the BodyBuilder model

Figure A.7 Subject mean ±1SD of the knee abduction-adduction angle for the BodyBuilder model

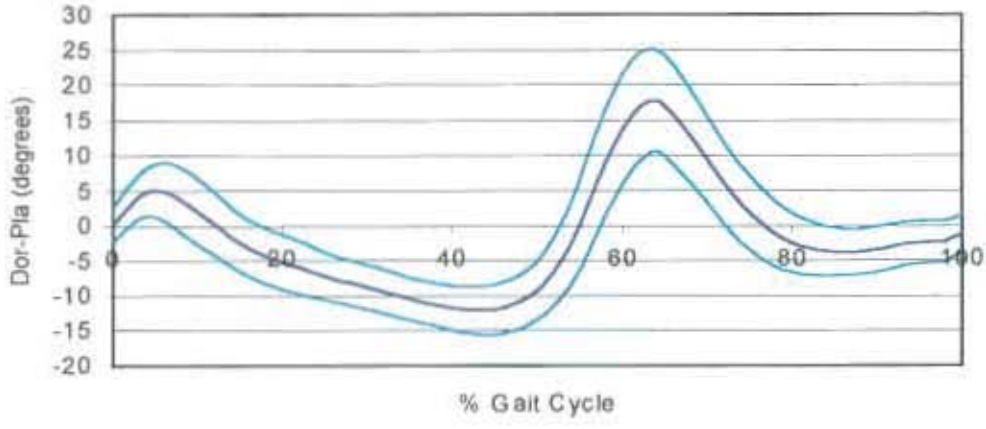

Figure A.8 Subject mean ±1SD of the ankle flexion-extension angle for the BodyBuilder model

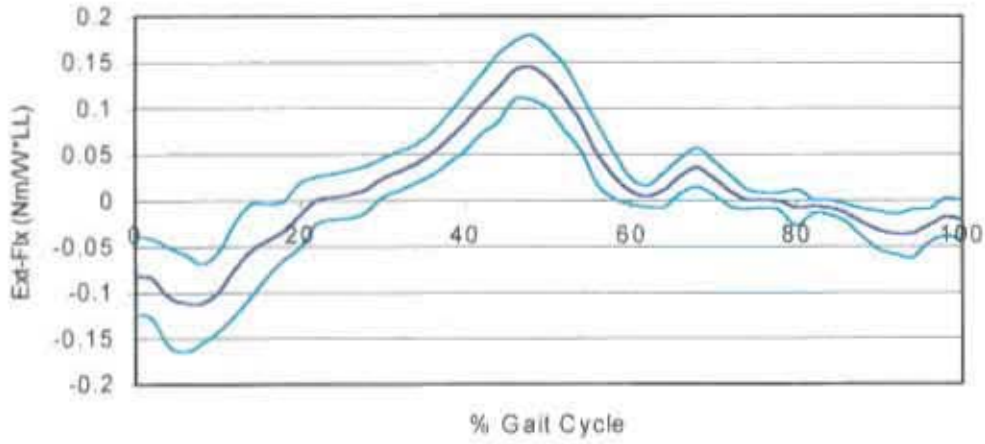

Figure A.9 Subject mean ±1SD of the hip flexion-extension moment for the BodyBuilder model

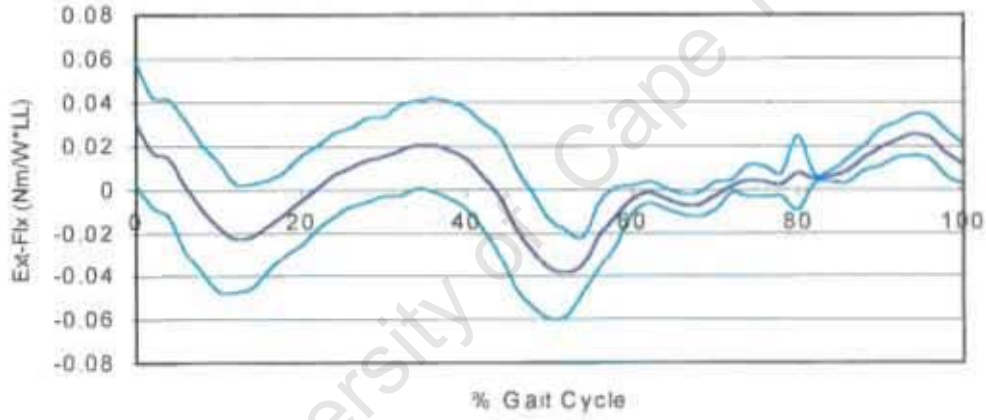

Figure A.10 Subject mean ±1SD of the knee flexion-extension moment for the BodyBuilder model

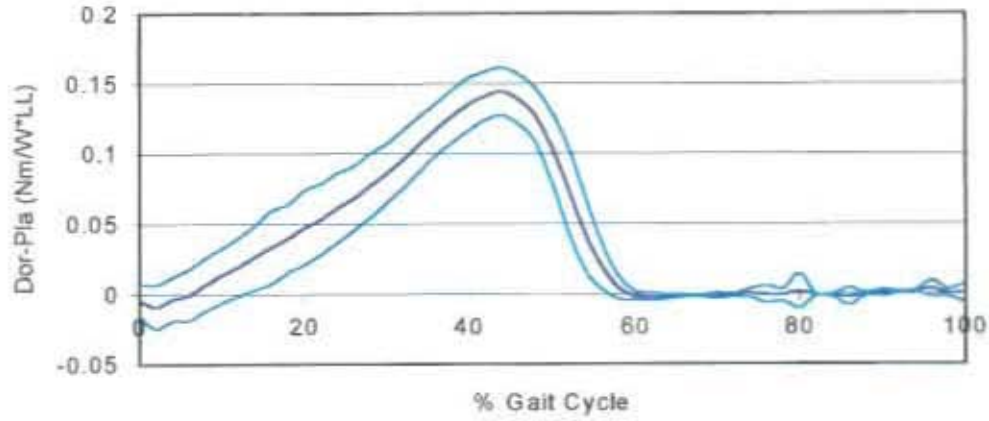

Figure A.11 Subject mean ±1SD of the ankle dorsi-plantar flexion moment for the BodyBuilder model

Appendix B

Source Code for the BodyBuilder Model

The BodyBuilder model used to process the data is written in Body Language, which is the modelling language associated with the BodyBuilder software package from Oxford Metrics. The model has been described in detail in chapter three. The model code is included below.

```
{* GaitLab 2.0 BodyBuilder model*}
{* For use with Gaitlab Marker and Parameter File *}
{*=============================================*}
{* Macro for cross product *}
MACRO CrossProduct ( First, Second, Result )
     Result = ( First(2)*Second(3)-First(3)*Second(2),
     First(3)*Second(1)-First(1)*Second(3),
     First(1)*Second(2)-First(2)*Second(1))
ENDMACRO
{*=============================================*}
{*Macro for Dot Product*}
MACRO DotProduct (One,Two,DotProd)
     DotProd = (1(One)*1(Two)+2(One)*2(Two)+3(One)*3(Two))
ENDMACRO
{*=============================================*}
{*Macro Filter procedure, 5-point weighted average*}
MACRO Filter (Param, F1)
     F1 = (param[-2] + 3*param[-1] + 4*param[0] + 3*param[1]
     + param[2])/12
ENDMACRO

{*Segment Masses *}
{*==============*}

MRThigh =
0.1032*$BodyMass+12.76*$RightThighLength2*($RMidThighCirc2*$RM
idThighCirc2)-1.023
MLThigh =
0.1032*$BodyMass+12.76*$LeftThighLength2*($LMidThighCirc2*$LMi
dThighCirc2)-1.023
MRCalf =
0.0226*$BodyMass+31.33*$RightCalfLength2*($RightCalfCirc2*$Rig
htCalfCirc2)+0.016
MLCalf =
0.0226*$BodyMass+31.33*$LeftCalfLength2*($LeftCalfCirc2*$LeftC
alfCirc2)+0.016
MRFoot =
0.0083*$BodyMass+254.5*$RightFootLength2*$RMalleolusHeight2*$R
MalleolusWidth2-0.065
```

```
MLFoot =
0.0083*$BodyMass+254.5*$LeftFootLength2*$LMalleolusHeight2*$LM
alleolusWidth2-0.065

{*Moments of Inertia*}
{*==================*}
{*Thigh*}
I_FlxExtRThigh =
0.00762*$BodyMass*($RightThighLength2*$RightThighLength2+0.076
*$RMidThighCirc2*$RMidThighCirc2)+0.01153
I_FlxExtLThigh =
0.00762*$BodyMass*($LeftThighLength2*$LeftThighLength2+0.076*$
LMidThighCirc2*$LMidThighCirc2)+0.01153
I_AbdAddRThigh =
0.00726*$BodyMass*($RightThighLength2*$RightThighLength2+0.076
*$RMidThighCirc2*$RMidThighCirc2)+0.01186
I_AbdAddLThigh =
0.00726*$BodyMass*($LeftThighLength2*$LeftThighLength2+0.076*$
LMidThighCirc2*$LMidThighCirc2)+0.01186
I_IntExtRThigh =
0.00151*$BodyMass*($RMidThighCirc2*$RMidThighCirc2)+0.00305
I_IntExtLThigh =
0.00151*$BodyMass*($LMidThighCirc2*$LMidThighCirc2)+0.00305

{*Calf*}
I_FlxExtRCalf =
0.00347*$BodyMass*($RightCalfLength2*$RightCalfLength2+0.076*$
RightCalfCirc2*$RightCalfCirc2)+0.00511
I_FlxExtLCalf =
0.00347*$BodyMass*($LeftCalfLength2*$LeftCalfLength2+0.076*$Le
ftCalfCirc2*$LeftCalfCirc2)+0.00511
I_AbdAddRCalf =
0.00387*$BodyMass*($RightCalfLength2*$RightCalfLength2+0.076*$
RightCalfCirc2*$RightCalfCirc2)+0.00138
I_AbdAddLCalf =
0.00387*$BodyMass*($LeftCalfLength2*$LeftCalfLength2+0.076*$Le
ftCalfCirc2*$LeftCalfCirc2)+0.00138
I_IntExtRCalf =
0.00041*$BodyMass*($RightCalfCirc2*$RightCalfCirc2)+0.00012
I_IntExtLCalf =
0.00041*$BodyMass*($LeftCalfCirc2*$LeftCalfCirc2)+0.00012

{*Foot*}
I_FlxExtRFoot =
0.00023*$BodyMass*(4*$RMalleolusHeight2*$RMalleolusHeight2+3*$
RightFootLength2*$RightFootLength2)+0.00022
I_FlxExtLFoot =
0.00023*$BodyMass*(4*$LMalleolusHeight2*$LMalleolusHeight2+3*$
LeftFootLength2*$LeftFootLength2)+0.00022
I_AbdAddRFoot =
0.00021*$BodyMass*(4*$RightFootBreadth2*$RightFootBreadth2+3*$
RightFootLength2*$RightFootLength2)+0.00067
I_AbdAddLFoot =
0.00021*$BodyMass*(4*$LeftFootBreadth2*$LeftFootBreadth2+3*$Le
ftFootLength2*$LeftFootLength2)+0.00067
```

```
I_IntExtRFoot =
0.00141*$BodyMass*($RmalleolusHeight2*$RmalleolusHeight2+$Righ
tFootBreadth2*$RightFootBreadth2)-0.00008
I_IntExtLFoot =
0.00141*$BodyMass*($LMalleolusHeight2*$LMalleolusHeight2+$Left
FootBreadth2*$LeftFootBreadth2)-0.00008

{*Filter Procedure. 5-point weighted average filter*}
{*================================================*}
Filter (RASI,RASI)
Filter (LASI,LASI)
Filter (SACR,SACR)
Filter (RTHI,RTHI)
Filter (LTHI,LTHI)
Filter (RHEE,RHEE)
Filter (RKNE,RKNE)
Filter (RTOE,RTOE)
Filter (LHEE,LHEE)
Filter (LTOE,LTOE)
Filter (RTIB,RTIB)
Filter (LKNE,LKNE)
Filter (LTIB,LTIB)
Filter (RANK,RANK)
Filter (LANK,LANK)

{*Joint Centre Estimations*}
{*========================*}

{*Pelvis*}
     Vpel = (LASI-RASI)/(ABS(LASI-RASI))
OneA = RASI-SACR
TwoA = LASI-SACR
CrossProduct( OneA, TwoA, UpA)
     Wpel = UpA/(ABS(UpA))
CrossProduct( Vpel, Wpel, Upel)
     Upel = Upel
RHJC = SACR + 0.598*$AsisBreadth*Upel -
0.344*$AsisBreadth*Vpel - 0.290*$AsisBreadth*Wpel
LHJC = SACR + 0.598*$AsisBreadth*Upel +
0.344*$AsisBreadth*Vpel - 0.290*$AsisBreadth*Wpel

{*Knee*}
     VRcalf = (RANK-RKNE)/(ABS(RANK-RKNE))
     VLcalf = (LANK-LKNE)/(ABS(LANK-LKNE))
One = RTIB-RKNE
Two = RANK-RKNE
Three = LTIB-LKNE
Four = LANK-LKNE
CrossProduct(One, Two, Up)
CrossProduct(Three, Four, Down)

     WRcalf = Up/(ABS(Up))
     WLcalf = Down/(Abs(Down))

CrossProduct(WRcalf, VRcalf, URcalf)
CrossProduct(VLcalf, WLcalf, ULcalf)
```

```
      URcalf = URcalf
      ULcalf = ULcalf

RKJC = RKNE + 0.5*($MarkerDiameter + $RightKneeDiam)*URcalf
LKJC = LKNE - 0.5*($MarkerDiameter + $LeftKneeDiam)*WLcalf

{*Foot*}
      URfoot = (RTOE-RHEE)/(ABS(RTOE-RHEE))
      ULfoot = (LTOE-LHEE)/(ABS(LTOE-LHEE))

One1 = RTOE-RANK
Two1 = RHEE-RANK
Three1 = LTOE-LANK
Four1 = LHEE-LANK

CrossProduct(One1, Two1, Up1)
CrossProduct (Three1, Four1, Down1)

      WRfoot = Up1/(ABS(Up1))
      WLfoot = Down1/(ABS(Down1))

CrossProduct(WRfoot, URfoot, VRfoot)
CrossProduct(WLfoot, ULfoot, VLfoot)

      VLfoot = VLfoot
      VRfoot = VRfoot

RAJC = RANK + 0.016*$RightFootLength*URfoot +
0.392*$RMalleolusHeight*VRfoot + 0.478*$RMalleolusWidth*WRfoot
LAJC = LANK + 0.016*$LeftFootLength*ULfoot +
0.392*$LMalleolusHeight*VLfoot - 0.478*$LMalleolusWidth*WLfoot

RToeP = RANK + 0.742*$RightFootLength*URfoot +
1.074*$RMalleolusHeight*VRfoot -
0.187*$RightFootBreadth*WRfoot
LToeP = LANK + 0.742*$LeftFootLength*ULfoot +
1.074*$LMalleolusHeight*VLfoot + 0.187*$LeftFootBreadth*WLfoot


OUTPUT (RHJC,LHJC,RKJC,LKJC,RAJC,LAJC)

{*Centres of Gravity*}
{*==================*}

RThighCG = (RHJC+0.39*(RKJC-RHJC))
LThighCG = (LHJC+0.39*(LKJC-LHJC))
RCalfCG = (RKJC+0.42*(RAJC-RKJC))
LCalfCG = (LKJC+0.42*(LAJC-LKJC))
RFootCG = (RHEE+0.44*(RToeP-RHEE))
LFootCG = (LHEE+0.44*(LToeP-LHEE))


{*Reference Frame, ijk*}
{*====================*}
```

```
{*Pelvis*}
iPel = WPel
jPel = Upel
kPel = VPel

PelF = (LASI+RASI)/2
PelO = (PelF+SACR)/2
Pelvis = [PelO,LASI-RASI,PelF-SACR,yzx]
{*Thighs*}
      iRThigh = (RHJC-RKJC)/(ABS(RHJC-RKJC))
      iLThigh = (LHJC-LKJC)/(ABS(LHJC-LKJC))

One2 = RTHI-RHJC
Two2 = RKJC-RHJC
Three2 = LTHI-LHJC
Four2 = LKJC-LHJC

CrossProduct(One2,Two2,Up2)
CrossProduct(Three2, Four2,Down2)

      jRThigh = Up2/(ABS(Up2))
      jLThigh = Down2/(ABS(Down2))

CrossProduct(iRThigh,jRThigh,kRThigh)
CrossProduct(iLThigh,jLThigh,kLThigh)

      kRThigh = kRThigh
      kLThigh = kLThigh


{*Calves*}
      iRCalf = (RKJC-RAJC)/(ABS(RKJC-RAJC))
      iLCalf = (LKJC-LAJC)/(ABS(LKJC-LAJC))

One3 = RKNE-RKJC
Two3 = RAJC-RKJC
Three3 = LKNE-LKJC
Four3 = LAJC-LKJC

CrossProduct(One3,Two3,Up3)
CrossProduct(Three3,Four3,Down3)

      jRCalf = Up3/(ABS(Up3))
      jLCalf = Down3/(ABS(Down3))

CrossProduct(iRCalf,jRCalf,kRCalf)
CrossProduct(iLCalf,jLCalf,kLCalf)

      kRCalf = kRCalf
      kLCalf = kLCalf

{*Feet*}
      iRFoot = (RHEE-RToeP)/(ABS(RHEE-RToeP))
      iLFoot = (LHEE-LToeP)/(ABS(LHEE-LToeP))

One4 = RAJC-RHEE
```

```
Two4 = RToeP-RHEE
Three4 = LAJC-LHEE
Four4 = LToeP-LHEE

CrossProduct(One4,Two4,Up4)
CrossProduct(Three4, Four4,Down4)

      kRFoot = Up4/(ABS(Up4))
      kLFoot = Down4/(ABS(Down4))

CrossProduct(kRFoot,iRFoot,jRFoot)
CrossProduct(kLFoot,iLFoot,jLFoot)

      jRFoot = jRFoot
      jLFoot = jLFoot



{*Angular Kinematics*}
{*==================*}

CrossProduct(kPel,iRThigh,Solution1)
lRHip = Solution1/ABS(Solution1)
CrossProduct(kPel,iLThigh,Solution2)
lLHip = Solution2/ABS(Solution2)
CrossProduct(kRThigh,iRCalf,Solution3)
lRKnee = Solution3/ABS(Solution3)
CrossProduct(kLThigh,iLCalf,Solution4)
lLKnee = Solution4/ABS(Solution4)
CrossProduct(kRCalf,iRFoot,Solution5)
lRAnkle = Solution5/ABS(Solution5)
CrossProduct(kLCalf,iLFoot,Solution6)
lLAnkle = Solution6/ABS(Solution6)

{*a=flexion/extension, b=abduction/adduction,
c=internal/external rotation*}

{*Pelvis Rotations*}

PelvisAngle = <Pelvis,xyz>
Output(PelvisAngle)

{*Right Hip Angles*}
DotProduct(lRHip,iPel,Dot)
      aRHip = ASIN(Dot)
DotProduct(kPel,iRThigh,Dot1)
      bRHip = ASIN(Dot1)
DotProduct(lRHip,kRThigh,Dot2)
      cRHip = -ASIN(Dot2)

{*Left Hip Angles*}
DotProduct(lLHip,iPel,Dot3)
      aLHip = ASIN(Dot3)
DotProduct(kPel,iLThigh,Dot4)
      bLHip = -ASIN(Dot4)
DotProduct(lLHip,kLThigh,Dot5)
```

```
      cLHip = ASIN(Dot5)

{*Right Knee Angles*}
DotProduct(lRKnee,iRThigh,Dot6)
      aRKnee = -ASIN(Dot6)
DotProduct(kRThigh,iRCalf,Dot7)
      bRKnee = ASIN(Dot7)
DotProduct(lRKnee,kRCalf,Dot8)
      cRKnee = -ASIN(Dot8)

{*Left Knee Angles*}
DotProduct(lLKnee,iLThigh,Dot9)
      aLKnee = -ASIN(Dot9)
DotProduct(kLThigh,iLCalf,Dot10)
      bLKnee = -ASIN(Dot10)
DotProduct(lLKnee,kLCalf,Dot11)
      cLKnee = ASIN(Dot11)

{*Right Ankle Angles*}
DotProduct(lRAnkle,jRCalf,Dot12)
      aRAnkle = ASIN(Dot12)
DotProduct(kRCalf,iRFoot,Dot13)
      bRAnkle = ASIN(Dot13)
DotProduct(lRAnkle,kRFoot,Dot14)
      cRAnkle = -ASIN(Dot14)

{*Left Ankle Angles*}
DotProduct(lLAnkle,jLCalf,Dot15)
      aLAnkle = ASIN(Dot15)
DotProduct(kLCalf,iLFoot,Dot16)
      bLAnkle = -ASIN(Dot16)
DotProduct(lLAnkle,kLFoot,Dot17)
      cLAnkle = ASIN(Dot17)


RHipAngle = {aRHip,bRHip,cRHip}
LHipAngle = {aLHip,bLHip,cLHip}
RKneeAngle = {aRKnee,bRKnee,cRKnee}
LKneeAngle = {aLKnee,bLKnee,cLKnee}
RAnkleAngle = {aRAnkle,bRAnkle,cRAnkle}
LAnkleAngle = {aLAnkle,bLAnkle,cLAnkle}

OUTPUT (RHipAngle, RAnkleAngle, RKneeAngle)
{*Output (LKneeAngle, RAnkleAngle, LAnkleAngle)*}


{*Angular Velocities and Accelerations*}
{*====================================*}

I = {1,0,0}
J = {0,1,0}
K = {0,0,1}

CrossProduct(K,kPel,Answer1)
LPel = Answer1/ABS(Answer1)
CrossProduct(K,kRThigh,Answer2)
```

```
LRThigh = Answer2/ABS(Answer2)
CrossProduct(K,kLThigh,Answer3)
LLThigh = Answer3/ABS(Answer3)
CrossProduct(K,kRCalf,Answer4)
LRCalf = Answer4/ABS(Answer4)
CrossProduct(K,kLCalf,Answer5)
LLCalf = Answer5/ABS(Answer5)
CrossProduct(K,kRFoot,Answer6)
LRFoot = Answer6/ABS(Answer6)
CrossProduct(K,kLFoot,Answer7)
LLFoot = Answer7/ABS(Answer7)


{*Euler Angles*}
CrossProduct(I,LPel,Cross1)
DotProduct(Cross1,K,Thei1)
CrossProduct(K,kPel,Cross2)
Dotproduct(Cross2,LPel,Theta1)
CrossProduct(LPel,iPel,Cross3)
DotProduct(Cross3,kPel,Psi1)
TheiPel = (ASIN(Thei1))*Pi/180
ThetaPel = (ASIN(Theta1))*Pi/180
PsiPel = (ASIN(Psi1))*Pi/180

CrossProduct(I,LRThigh,Cross4)
DotProduct(Cross4,K,Thei2)
CrossProduct(K,kRThigh,Cross5)
Dotproduct(Cross5,LRThigh,Theta2)
CrossProduct(LRThigh,iRThigh,Cross6)
DotProduct(Cross6,kRThigh,Psi2)
TheiRThigh = (ASIN(Thei2))*Pi/180
ThetaRThigh = (ASIN(Theta2))*Pi/180
PsiRThigh = (ASIN(Psi2))*Pi/180

CrossProduct(I,LLThigh,Cross7)
DotProduct(Cross7,K,Thei3)
CrossProduct(K,kLThigh,Cross8)
Dotproduct(Cross8,LLThigh,Theta3)
CrossProduct(LLThigh,iLThigh,Cross9)
DotProduct(Cross9,kLThigh,Psi3)
TheiLThigh = (ASIN(Thei3))*Pi/180
ThetaLThigh = (ASIN(Theta3))*Pi/180
PsiLThigh = (ASIN(Psi3))*Pi/180

CrossProduct(I,LRCalf,Cross10)
DotProduct(Cross10,K,Thei4)
CrossProduct(K,kRCalf,Cross11)
Dotproduct(Cross11,LRCalf,Theta4)
CrossProduct(LRCalf,iRCalf,Cross12)
DotProduct(Cross12,kRCalf,Psi4)
TheiRCalf = (ASIN(Thei1))*Pi/180
ThetaRCalf = (ASIN(Theta1))*Pi/180
PsiRCalf = (ASIN(Psi1))*Pi/180

CrossProduct(I,LLCalf,Cross13)
DotProduct(Cross13,K,Thei5)
```

```
CrossProduct(K,kLCalf,Cross14)
Dotproduct(Cross14,LLCalf,Theta5)
CrossProduct(LLCalf,iLCalf,Cross15)
DotProduct(Cross15,kLCalf,Psi5)
TheiLCalf = (ASIN(Thei5))*Pi/180
ThetaLCalf = (ASIN(Theta5))*Pi/180
PsiLCalf = (ASIN(Psi5))*Pi/180

CrossProduct(I,LRFoot,Cross16)
DotProduct(Cross16,K,Thei6)
CrossProduct(K,kRFoot,Cross17)
Dotproduct(Cross17,LRFoot,Theta6)
CrossProduct(LRFoot,iRFoot,Cross18)
DotProduct(Cross18,kRFoot,Psi6)
TheiRFoot = (ASIN(Thei6))*Pi/180
ThetaRFoot = (ASIN(Theta6))*Pi/180
PsiRFoot = (ASIN(Psi6))*Pi/180

CrossProduct(I,LLFoot,Cross19)
DotProduct(Cross19,K,Thei7)
CrossProduct(K,kLFoot,Cross20)
Dotproduct(Cross20,LLFoot,Theta7)
CrossProduct(LLFoot,iLFoot,Cross21)
DotProduct(Cross21,kLFoot,Psi7)
TheiLFoot = (ASIN(Thei7))*Pi/180
ThetaLFoot = (ASIN(Theta7))*Pi/180
PsiLFoot = (ASIN(Psi7))*Pi/180


{*Angular Velocities*}
TheiPelVel = (TheiPel[1]-TheiPel[-1])/(2*FrameTimeLength)
ThetaPelVel = (ThetaPel[1]-ThetaPel[-1])/(2*FrameTimeLength)
PsiPelVel = (PsiPel[1]-PsiPel[-1])/(2*FrameTimeLength)
OmegaPelx =
TheiPelVel*SIN(ThetaPel)*SIN(PsiPel)+ThetaPelVel*COS(Psipel)
OmegaPely = TheiPelVel*SIN(ThetaPel)*COS(PsiPel)-
ThetaPelVel*SIN(PsiPel)
OmegaPelz = TheiPelVel*COS(ThetaPel)+PsiPelVel

TheiRThighVel = (TheiRThigh[1]-TheiRThigh[-
1])/(2*FrameTimeLength)
ThetaRThighVel = (ThetaRThigh[1]-ThetaRThigh[-
1])/(2*FrameTimeLength)
PsiRThighVel = (PsiRThigh[1]-PsiRThigh[-
1])/(2*FrameTimeLength)
OmegaRThighx =
TheiRThighVel*SIN(ThetaRThigh)*SIN(PsiRThigh)+ThetaRThighVel*C
OS(PsiRThigh)
OmegaRThighy = TheiRThighVel*SIN(ThetaRThigh)*COS(PsiRThigh)-
ThetaRThighVel*SIN(PsiRThigh)
OmegaRThighz = TheiRThighVel*COS(ThetaRThigh)+PsiRThighVel

TheiLThighVel = (TheiLThigh[1]-TheiLThigh[-
1])/(2*FrameTimeLength)
ThetaLThighVel = (ThetaLThigh[1]-ThetaLThigh[-
1])/(2*FrameTimeLength)
```

```
PsiLThighVel = (PsiLThigh[1]-PsiLThigh[-
1])/(2*FrameTimeLength)
OmegaLThighx =
TheiLThighVel*SIN(ThetaLThigh)*SIN(PsiLThigh)+ThetaLThighVel*C
OS(PsiLThigh)
OmegaLThighy = TheiLThighVel*SIN(ThetaLThigh)*COS(PsiLThigh)-
ThetaLThighVel*SIN(PsiLThigh)
OmegaLThighz = TheiLThighVel*COS(ThetaLThigh)+PsiLThighVel

TheiRCalfVel = (TheiRCalf[1]-TheiRCalf[-
1])/(2*FrameTimeLength)
ThetaRCalfVel = (ThetaRCalf[1]-ThetaRCalf[-
1])/(2*FrameTimeLength)
PsiRCalfVel = (PsiRCalf[1]-PsiRCalf[-1])/(2*FrameTimeLength)
OmegaRCalfx =
TheiRCalfVel*SIN(ThetaRCalf)*SIN(PsiRCalf)+ThetaRCalfVel*COS(P
siRCalf)
OmegaRCalfy = TheiRCalfVel*SIN(ThetaRCalf)*COS(PsiRCalf)-
ThetaRCalfVel*SIN(PsiRCalf)
OmegaRCalfz = TheiRCalfVel*COS(ThetaRCalf)+PsiRCalfVel

TheiLCalfVel = (TheiLCalf[1]-TheiLCalf[-
1])/(2*FrameTimeLength)
ThetaLCalfVel = (ThetaLCalf[1]-ThetaLCalf[-
1])/(2*FrameTimeLength)
PsiLCalfVel = (PsiLCalf[1]-PsiLCalf[-1])/(2*FrameTimeLength)
OmegaLCalfx =
TheiLCalfVel*SIN(ThetaLCalf)*SIN(PsiLCalf)+ThetaLCalfVel*COS(P
siLCalf)
OmegaLCalfy = TheiLCalfVel*SIN(ThetaLCalf)*COS(PsiLCalf)-
ThetaLCalfVel*SIN(PsiLCalf)
OmegaLCalfz = TheiLCalfVel*COS(ThetaLCalf)+PsiLCalfVel

TheiRFootVel = (TheiRFoot[1]-TheiRFoot[-
1])/(2*FrameTimeLength)
ThetaRFootVel = (ThetaRFoot[1]-ThetaRFoot[-
1])/(2*FrameTimeLength)
PsiRFootVel = (PsiRFoot[1]-PsiRFoot[-1])/(2*FrameTimeLength)
OmegaRFootx =
TheiRFootVel*SIN(ThetaRFoot)*SIN(PsiRFoot)+ThetaRFootVel*COS(P
siRFoot)
OmegaRFooty = TheiRFootVel*SIN(ThetaRFoot)*COS(PsiRFoot)-
ThetaRFootVel*SIN(PsiRFoot)
OmegaRFootz = TheiRFootVel*COS(ThetaRFoot)+PsiRFootVel

TheiLFootVel = (TheiLFoot[1]-TheiLFoot[-
1])/(2*FrameTimeLength)
ThetaLFootVel = (ThetaLFoot[1]-ThetaLFoot[-
1])/(2*FrameTimeLength)
PsiLFootVel = (PsiLFoot[1]-PsiLFoot[-1])/(2*FrameTimeLength)
OmegaLFootx =
TheiLFootVel*SIN(ThetaLFoot)*SIN(PsiLFoot)+ThetaLFootVel*COS(P
siLFoot)
OmegaLFooty = TheiLFootVel*SIN(ThetaLFoot)*COS(PsiLFoot)-
ThetaLFootVel*SIN(PsiLFoot)
OmegaLFootz = TheiLFootVel*COS(ThetaLFoot)+PsiLFootVel
```

```
{*Angular Acceleration*}
TheiPelAcc = (TheiPelVel[1]-TheiPelVel[-
1])/(2*FrameTimeLength)
ThetaPelAcc = (ThetaPelVel[1]-ThetaPelVel[-
1])/(2*FrameTimeLength)
PsiPelAcc = (PsiPelVel[1]-PsiPelVel[-1])/(2*FrameTimeLength)
AlphaPelx =
TheiPelAcc*SIN(ThetaPel)*SIN(PsiPel)+TheiPelVel*ThetaPelVel*CO
S(ThetaPel)*SIN(PsiPel)+TheiPelVel*PsiPelVel*SIN(ThetaPel)*COS
(PsiPel)+ThetaPelAcc*COS(PsiPel)-
ThetaPelVel*PsiPelVel*SIN(PsiPel)
AlphaPely =
TheiPelAcc*SIN(Thetapel)*COS(PsiPel)+TheipelVel*ThetaPelVel*CO
S(ThetaPel)*COS(Psipel)+TheiPelVel*PsiPelVel*SIN(ThetaPel)*SIN
(PsiPel)-ThetaPelAcc*SIN(PsiPel)-
ThetaPelVel*PsiPelVel*COS(PsiPel)
AlphaPelz = TheiPelAcc*COS(ThetaPel)-
TheiPelVel*ThetaPelVel*SIN(ThetaPel)+PsiPelAcc

TheiRThighAcc = (TheiRThighVel[1]-TheiRThighVel[-
1])/(2*FrameTimeLength)
ThetaRThighAcc = (ThetaRThighVel[1]-ThetaRThighVel[-
1])/(2*FrameTimeLength)
PsiRThighAcc = (PsiRThighVel[1]-PsiRThighVel[-
1])/(2*FrameTimeLength)
AlphaRThighx =
TheiRThighAcc*SIN(ThetaRThigh)*SIN(PsiRThigh)+TheiRThighVel*Th
etaRThighVel*COS(ThetaRThigh)*SIN(PsiRThigh)+TheiRThighVel*Psi
RThighVel*SIN(ThetaRThigh)*COS(PsiRThigh)+ThetaRThighAcc*COS(P
siRThigh)-
ThetaRThighVel*PsiRThighVel*SIN(PsiRThigh)
AlphaRThighy =
TheiRThighAcc*SIN(ThetaRThigh)*COS(PsiRThigh)+TheiRThighVel*Th
etaRThighVel*COS(ThetaRThigh)*COS(PsiRThigh)+TheiRThighVel*Psi
RThighVel*SIN(ThetaRThigh)*SIN(PsiRThigh)-
ThetaRThighAcc*SIN(PsiRThigh)-
ThetaRThighVel*PsiRThighVel*COS(PsiRThigh)
AlphaRThighz = TheiRThighAcc*COS(ThetaRThigh)-
TheiRThighVel*ThetaRThighVel*SIN(ThetaRThigh)+PsiRThighAcc

TheiLThighAcc = (TheiLThighVel[1]-TheiLThighVel[-
1])/(2*FrameTimeLength)
ThetaLThighAcc = (ThetaLThighVel[1]-ThetaLThighVel[-
1])/(2*FrameTimeLength)
PsiLThighAcc = (PsiLThighVel[1]-PsiLThighVel[-
1])/(2*FrameTimeLength)
AlphaLThighx =
TheiLThighAcc*SIN(ThetaLThigh)*SIN(PsiLThigh)+TheiLThighVel*Th
etaLThighVel*COS(ThetaLThigh)*SIN(PsiLThigh)+TheiLThighVel*Psi
LThighVel*SIN(ThetaLThigh)*COS(PsiLThigh)+ThetaLThighAcc*COS(P
siLThigh)-ThetaLThighVel*PsiLThighVel*SIN(PsiLThigh)
AlphaLThighy =
TheiLThighAcc*SIN(ThetaLThigh)*COS(PsiLThigh)+TheiLThighVel*Th
etaLThighVel*COS(ThetaLThigh)*COS(PsiLThigh)+TheiLThighVel*Psi
```

```
LThighVel*SIN(ThetaLThigh)*SIN(PsiLThigh)-
ThetaLThighAcc*SIN(PsiLThigh)-
ThetaLThighVel*PsiLThighVel*COS(PsiLThigh)
AlphaLThighz = TheiLThighAcc*COS(ThetaLThigh)-
TheiLThighVel*ThetaLThighVel*SIN(ThetaLThigh)+PsiLThighAcc

TheiRCalfAcc = (TheiRCalfVel[1]-TheiRCalfVel[-
1])/(2*FrameTimeLength)
ThetaRCalfAcc = (ThetaRCalfVel[1]-ThetaRCalfVel[-
1])/(2*FrameTimeLength)
PsiRCalfAcc = (PsiRCalfVel[1]-PsiRCalfVel[-
1])/(2*FrameTimeLength)
AlphaRCalfx =
TheiRCalfAcc*SIN(ThetaRCalf)*SIN(PsiRCalf)+TheiRCalfVel*ThetaR
CalfVel*COS(ThetaRCalf)*SIN(PsiRCalf)+TheiRCalfVel*PsiRCalfVel
*SIN(ThetaRCalf)*COS(PsiRCalf)+ThetaRCalfAcc*COS(PsiRCalf)-
ThetaRCalfVel*PsiRCalfVel*SIN(PsiRCalf)
AlphaRCalfy =
TheiRCalfAcc*SIN(ThetaRCalf)*COS(PsiRCalf)+TheiRCalfVel*ThetaR
CalfVel*COS(ThetaRCalf)*COS(PsiRCalf)+TheiRCalfVel*PsiRCalfVel
*SIN(ThetaRCalf)*SIN(PsiRCalf)-ThetaRCalfAcc*SIN(PsiRCalf)-
ThetaRCalfVel*PsiRCalfVel*COS(PsiRCalf)
AlphaRCalfz = TheiRCalfAcc*COS(ThetaRCalf)-
TheiRCalfVel*ThetaRCalfVel*SIN(ThetaRCalf)+PsiRCalfAcc

TheiLCalfAcc = (TheiLCalfVel[1]-TheiLCalfVel[-
1])/(2*FrameTimeLength)
ThetaLCalfAcc = (ThetaLCalfVel[1]-ThetaLCalfVel[-
1])/(2*FrameTimeLength)
PsiLCalfAcc = (PsiLCalfVel[1]-PsiLCalfVel[-
1])/(2*FrameTimeLength)
AlphaLCalfx =
TheiLCalfAcc*SIN(ThetaLCalf)*SIN(PsiLCalf)+TheiLCalfVel*ThetaL
CalfVel*COS(ThetaLCalf)*SIN(PsiLCalf)+TheiLCalfVel*PsiLCalfVel
*SIN(ThetaLCalf)*COS(PsiLCalf)+ThetaLCalfAcc*COS(PsiLCalf)-
ThetaLCalfVel*PsiLCalfVel*SIN(PsiLCalf)
AlphaLCalfy =
TheiLCalfAcc*SIN(ThetaLCalf)*COS(PsiLCalf)+TheiLCalfVel*ThetaL
CalfVel*COS(ThetaLCalf)*COS(PsiLCalf)+TheiLCalfVel*PsiLCalfVel
*SIN(ThetaLCalf)*SIN(PsiLCalf)-ThetaLCalfAcc*SIN(PsiLCalf)-
ThetaLCalfVel*PsiLCalfVel*COS(PsiLCalf)
AlphaLCalfz = TheiLCalfAcc*COS(ThetaLCalf)-
TheiLCalfVel*ThetaLCalfVel*SIN(ThetaLCalf)+PsiLCalfAcc

TheiRFootAcc = (TheiRFootVel[1]-TheiRFootVel[-
1])/(2*FrameTimeLength)
ThetaRFootAcc = (ThetaRFootVel[1]-ThetaRFootVel[-
1])/(2*FrameTimeLength)
PsiRFootAcc = (PsiRFootVel[1]-PsiRFootVel[-
1])/(2*FrameTimeLength)
AlphaRFootx =
TheiRFootAcc*SIN(ThetaRFoot)*SIN(PsiRFoot)+TheiRFootVel*ThetaR
FootVel*COS(ThetaRFoot)*SIN(PsiRFoot)+TheiRFootVel*PsiRFootVel
*SIN(ThetaRFoot)*COS(PsiRFoot)+ThetaRFootAcc*COS(PsiRFoot)-
ThetaRFootVel*PsiRFootVel*SIN(PsiRFoot)
```

```
AlphaRFooty =
TheiRFootAcc*SIN(ThetaRFoot)*COS(PsiRFoot)+TheiRFootVel*ThetaR
FootVel*COS(ThetaRFoot)*COS(PsiRFoot)+TheiRFootVel*PsiRFootVel
*SIN(ThetaRFoot)*SIN(PsiRFoot)-ThetaRFootAcc*SIN(PsiRFoot)-
ThetaRFootVel*PsiRFootVel*COS(PsiRFoot)
AlphaRFootz = TheiRFootAcc*COS(ThetaRFoot)-
TheiRFootVel*ThetaRFootVel*SIN(ThetaRFoot)+PsiRFootAcc

TheiLFootAcc = (TheiLFootVel[1]-TheiLFootVel[-
1])/(2*FrameTimeLength)
ThetaLFootAcc = (ThetaLFootVel[1]-ThetaLFootVel[-
1])/(2*FrameTimeLength)
PsiLFootAcc = (PsiLFootVel[1]-PsiLFootVel[-
1])/(2*FrameTimeLength)
AlphaLFootx =
TheiLFootAcc*SIN(ThetaLFoot)*SIN(PsiLFoot)+TheiLFootVel*ThetaL
FootVel*COS(ThetaLFoot)*SIN(PsiLFoot)+TheiLFootVel*PsiLFootVel
*SIN(ThetaLFoot)*COS(PsiLFoot)+ThetaLFootAcc*COS(PsiLFoot)-
ThetaLFootVel*PsiLFootVel*SIN(PsiLFoot)
AlphaLFooty =
TheiLFootAcc*SIN(ThetaLFoot)*COS(PsiLFoot)+TheiLFootVel*ThetaL
FootVel*COS(ThetaLFoot)*COS(PsiLFoot)+TheiLFootVel*PsiLFootVel
*SIN(ThetaLFoot)*SIN(PsiLFoot)-ThetaLFootAcc*SIN(PsiLFoot)-
ThetaLFootVel*PsiLFootVel*COS(PsiLFoot)
AlphaLFootz = TheiLFootAcc*COS(ThetaLFoot)-
TheiLFootVel*ThetaLFootVel*SIN(ThetaLFoot)+PsiLFootAcc



{*Angular Momentum*}
{*================*}

HRThighx = I_IntExtRThigh*AlphaRThighx+(I_FlxExtRThigh-
I_AbdAddRThigh)*OmegaRThighz*OmegaRThighy
HRThighy = I_AbdAddRThigh*AlphaRThighy+(I_IntExtRThigh-
I_FlxExtRThigh)*OmegaRThighx*OmegaRThighz
HRThighz = I_FlxExtRThigh*AlphaRThighz+(I_AbdAddRThigh-
I_IntExtRThigh)*OmegaRThighy*OmegaRThighx

HLThighx = I_IntExtLThigh*AlphaLThighx+(I_FlxExtLThigh-
I_AbdAddLThigh)*OmegaLThighz*OmegaLThighy
HLThighy = I_AbdAddLThigh*AlphaLThighy+(I_IntExtLThigh-
I_FlxExtLThigh)*OmegaLThighx*OmegaLThighz
HLThighz = I_FlxExtLThigh*AlphaLThighz+(I_AbdAddLThigh-
I_IntExtLThigh)*OmegaLThighy*OmegaLThighx

HRCalfx = I_IntExtRCalf*AlphaRCalfx+(I_FlxExtRCalf-
I_AbdAddRCalf)*OmegaRCalfz*OmegaRCalfy
HRCalfy = I_AbdAddRCalf*AlphaRCalfy+(I_IntExtRCalf-
I_FlxExtRCalf)*OmegaRCalfx*OmegaRCalfz
HRCalfz = I_FlxExtRCalf*AlphaRCalfz+(I_AbdAddRCalf-
I_IntExtRCalf)*OmegaRCalfy*OmegaRCalfx

HLCalfx = I_IntExtLCalf*AlphaLCalfx+(I_FlxExtLCalf-
I_AbdAddLCalf)*OmegaLCalfz*OmegaLCalfy
```

```
HLCalfy = I_AbdAddLCalf*AlphaLCalfy+(I_IntExtLCalf-
I_FlxExtLCalf)*OmegaLCalfx*OmegaLCalfz
HLCalfz = I_FlxExtLCalf*AlphaLCalfz+(I_AbdAddLCalf-
I_IntExtLCalf)*OmegaLCalfy*OmegaLCalfx

HRFootx = I_IntExtRFoot*AlphaRFootx+(I_FlxExtRFoot-
I_AbdAddRFoot)*OmegaRFootz*OmegaRFooty
HRFooty = I_AbdAddRFoot*AlphaRFooty+(I_IntExtRFoot-
I_FlxExtRFoot)*OmegaRFootx*OmegaRFootz
HRFootz = I_FlxExtRFoot*AlphaRFootz+(I_AbdAddRFoot-
I_IntExtRFoot)*OmegaRFooty*OmegaRFootx

HLFootx = I_IntExtLFoot*AlphaLFootx+(I_FlxExtLFoot-
I_AbdAddLFoot)*OmegaLFootz*OmegaLFooty
HLFooty = I_AbdAddLFoot*AlphaLFooty+(I_IntExtLFoot-
I_FlxExtLFoot)*OmegaLFootx*OmegaLFootz
HLFootz = I_FlxExtLFoot*AlphaLFootz+(I_AbdAddLFoot-
I_IntExtLFoot)*OmegaLFooty*OmegaLFootx



{*Dynamics of Joints*}
{*====================*}

{*Velociy and Accelerations of Segment Centres of Gravity*}

RFootCGVel = (RFootCG[1]-RFootCG[-1])/((2*FrameTimeLength))
RFootCGAcc = (RFootCGVel[1]-RFootCGVel[-
1])/(1000*(2*FrameTimeLength))
LFootCGVel = (LFootCG[1]-LFootCG[-1])/((2*FrameTimeLength))
LFootCGAcc = (LFootCGVel[1]-LFootCGVel[-
1])/(1000*(2*FrameTimeLength))
RCalfCGVel = (RCalfCG[1]-RCalfCG[-1])/(2*FrameTimeLength)
RCalfCGAcc = (RCalfCGVel[1]-RCalfCGVel[-
1])/(1000*(2*FrameTimeLength))
LCalfCGVel = (LCalfCG[1]-LCalfCG[-1])/(2*FrameTimeLength)
LCalfCGAcc = (LCalfCGVel[1]-LCalfCGVel[-
1])/(1000*(2*FrameTimeLength))
RThighCGVel = (RThighCG[1]-RThighCG[-1])/(2*FrameTimeLength)
RThighCGAcc = (RThighCGVel[1]-RThighCGVel[-
1])/(1000*(2*FrameTimeLength))
LThighCGVel = (LThighCG[1]-LThighCG[-1])/(2*FrameTimeLength)
LThighCGAcc = (LThighCGVel[1]-LThighCGVel[-
1])/(1000*(2*FrameTimeLength))


{* Show the force vectors *}
if EXIST( ForcePlate1 )
      Force1 = ForcePlate1(1)
      Moment1 = ForcePlate1(2)
      Centre1 = ForcePlate1(3)

      if Force1(3 ) < 10
            Force1 = Force1*0
            Moment1 = Moment1*0
```

```
            Point1 = Centre1
      else
            Force1 = (Force1[-1]+2*(Force1[0])+Force1[1])/4
            Moment1 = (Moment1[-1]+2*(Moment1[0])+Moment1[1])/4
            Point1 = Centre1 + {-Moment1(2)/Force1(3),
Moment1(1)/Force1(3), -Centre1(3) }

      endif

endif

output(force1)


{*Forces and Moments*}
{*==================*}

{*RAnkle*}
FRAnkleX = MRFoot*RFootCGAcc(1)-Force1(1)
FRAnkleY = MRFoot*RFootCGAcc(2)-Force1(2)
FRAnkleZ = MRFoot*(RFootCGAcc(3)+9.81)-Force1(3)
FRAnkle = FRAnkleX*I+FRAnkleY*J+FRAnkleZ*K

{*Moment Arms*}

PPlate1 = Point1(1)*I+Point1(2)*J+0*K
PPRFoot = (RAJC-RFootCG)/1000
PDRFoot = (PPlate1-RFootCG)/1000

CrossProduct(PPRFoot,FRAnkle,Mom1)
CrossProduct(PDRFoot,Force1,Mom2)

TPlate1 = (0*I+0*J+Moment1(3)*K)/1000
MResRFoot = TPlate1+Mom1+Mom2

DotProduct(iRFoot,MResRFoot,Ank1)
DotProduct(jRFoot,MResRFoot,Ank2)
DotProduct(kRFoot,MResRFoot,Ank3)

MRAnkleX = HRFootx-Ank1
MRAnkleY = HRFooty-Ank2
MRAnkleZ = HRFootz-Ank3

MRAnkle = MRAnkleX*iRFoot+MRAnkleY*jRFoot+MRAnkleZ*kRFoot


DotProduct(FRAnkle,iRFoot,FRAnklePrxDis)
DotProduct(FRAnkle,kRCalf,FRAnkleMedLat)
DotProduct(FRAnkle,lRAnkle,FRAnkleAntPos)
DotProduct(MRAnkle,iRFoot,MRAnkleInvEve)
DotProduct(MRAnkle,kRCalf,MRAnklePlaDor)
DotProduct(-MRAnkle,lRAnkle,MRAnkleVarVal)

FRAnkle1 = {FRAnklePrxDis,FRankleMedLat,FRAnkleAntPos}
MRAnkle1 = {MRAnkleInvEve,MRAnklePlaDor,MRAnkleVarVal}
```

```
{*RKnee*}
FRKneeX = MRCalf*RCalfCGAcc(1)+FRAnkleX
FRKneeY = MRCalf*RCalfCGAcc(2)+FRAnkleY
FRKneeZ = MRCalf*(RCalfCGAcc(3)+9.81)+FRAnkle(3)

FRKnee = FRKneeX*I+FRKneeY*J+FRKneeZ*K


{*Moment Arms*}
PPRCalf = (RKJC-RCalfCG)/1000
PDRCalf = (RAJC-RcalfCG)/1000

CrossProduct(PDRCalf,FRAnkle,Mom3)
CrossProduct(PPRCalf,FRKnee,Mom4)
MResRCalf = -MRAnkle-Mom3+Mom4

DotProduct(iRCalf,MResRCalf,Calf1)
DotProduct(jRCalf,MResRCalf,Calf2)
DotProduct(kRCalf,MResRCalf,Calf3)

MRKneeX = HRCalfx-Calf1
MRKneeY = HRCalfy-Calf2
MRKneeZ = HRCalfz-Calf3

MRKnee = MRKneeX*iRCalf+MRKneeY*jRCalf+MRKneeZ*kRCalf

DotProduct(FRKnee,iRCalf,FRKneePrxDis)
DotProduct(FRKnee,kRThigh,FRKneeMedLat)
DotProduct(FRKnee,lRKnee,FRKneeAntPos)
DotProduct(MRKnee,iRCalf,MRKneeIntExt)
DotProduct(MRKnee,kRThigh,MRKneeFlxExt)
DotProduct(-MRKnee,lRKnee,MRKneeAbdAdd)

FRKnee1 = {FRKneePrxDis,FRKneeMedLat,FRKneeAntPos}
MRKnee1 = {MRKneeIntExt,MRKneeFlxExt,MRKneeAbdAdd}


{*RHip*}
FRHipX = MRThigh*RThighCGAcc(1)+FRKneeX
FRHipY = MRThigh*RThighCGAcc(2)+FRKneeY
FRHipZ = MRThigh*(RThighCGAcc(3)+9.81)+FRKnee(3)

FRHip = FRHipX*I+FRHipY*J+FRHipZ*K

{*Moment Arms*}
PPRThigh = (RHJC-RThighCG)/1000
PDRThigh = (RKJC-RThighCG)/1000

CrossProduct(PDRThigh,FRKnee,Mom5)
CrossProduct(PPRThigh,FRHip,Mom6)
MResRThigh = -MRKnee-Mom5+Mom6

DotProduct(iRThigh,MResRThigh,Thigh1)
DotProduct(jRThigh,MResRThigh,Thigh2)
DotProduct(kRThigh,MResRThigh,Thigh3)
```

```
MRHipX = HRThighx-Thigh1
MRHipY = HRThighy-Thigh2
MRHipZ = HRThighz-Thigh3

MRHip = MRHipX*iRThigh+MRHipY*jRThigh+MRHipZ*kRThigh

DotProduct(FRHip,iRThigh,FRHipPrxDis)
DotProduct(FRHip,kPel,FRHipMedLat)
DotProduct(FRHip,lRHip,FRHipAntPos)
DotProduct(MRHip,iRThigh,MRHipIntExt)
DotProduct(-MRHip,kPel,MRHipFlxExt)
DotProduct(-MRHip,lRHip,MRHipAbdAdd)

FRHip1 = {FRHipPrxDis,FRHipMedLat,FRHipAntPos}
MRHip1 = {MRHipIntExt,MRHipFlxExt,MRHipAbdAdd}

Output(MRAnkle1,MRKnee1,MRHip1)

{* Model End *}
{*============*}
```

Appendix C

The MatLab Interpolation Procedure

Vicon Clinical Manager automatically interpolates the data to 51 gait cycle increments, from 0% to 100% in 2% steps. In order to compare the data from the different gait analysis software packages, it was necessary to interpolate all the data to include 51 time increments in the gait cycle.

MatLab code was used to interpolate the data. The program code is listed in this appendix.

```
%MatLab Interpolation program
%Input data
% Input 11 gait parameters from one subject
%RAM- Ankle Moment, RKM-Knee Moment, RHM-Hip Moment
%RAA-Ankle Flx-Ext Angle, RKAA-Knee Abd-Add Angle
%RKA-Knee Flx-Ext Angle, RHAA-Hip Abd-Add Angle
%RHA-Hip Flx-Ext Angle, PAZ-Pelvic Rot, PAY-Pelvic Obl, PAX-
Pelvic Tilt

RAM = [..];
RKM = [..];
RHM= [..];
RAA=[..];
RKAA=[..];
RKA=[..];
RHAA=[..];
RHA=[..];
PAZ=[..];
PAY=[..];
PAX=[..];

%Determine number of field to interpolate
S = size(RAM,1);
P = 1/(S-1)*100;
percent = [0:2:100]';
```

```
pold = [0:P:100]';

%Cubic spline interpolation and output
RAMnew = interp1(pold,RAM,percent,'spline')
RKMnew = interp1(pold,RKM,percent,'spline')
RHMnew = INTERP1(pold,RHM,percent,'spline')
RAAnew = interp1(pold,RAA,percent,'spline')
RKAAnew = interp1(pold,RKAA,percent,'spline')
RKAnew = interp1(pold,RKA,percent,'spline')
RHAAnew = interp1(pold,RHAA,percent,'spline')
RHAnew = interp1(pold,RHA,percent,'spline')
PAZnew = interp1(pold,PAZ,percent,'spline')
PAYnew = interp1(pold,PAY,percent,'spline')
PAXnew = interp1(pold,PAX,percent,'spline')
```

Appendix D

Details of Gait Analysis Software Vendors

Details of the companies who supply gait analysis software and related software, which was used in this study are listed below. The software name is listed first followed by the vendors name and contact details.

GaitLab 2.0, Copyright 1999 by Christopher L Vaughan

Address: Kiboho Publishers
P.O. Box 769
Howard Place, Western Cape 7450
South Africa
email: GaitCD@kiboho.co.za
Website: http://www.kiboho.co.za/GaitCD

Vicon Clinical Manager and Vicon BodyBuilder software, Oxford Metrics Limited

Address: 14, Minns Estate, West Way
Oxford OX2 0JB, United Kingdom
Tel: +44(0) 1865 261800
Fax: +44(0) 1865 240527
email: support@metrics.co.uk
Website: http://www.vicon.com

Peak Motus 2000, Peak Performance Technologies Inc.

Address: 7388 South Revere parkway,
Suite 603 Englewood,
Colorado, 80112 USA
Tel: (303)799-8686
Fax: (303)799-8690
email: peakinfo@peakperform.com
Website: http://www.peakperform.com

GaitEliClinic, Bioengineering Technology and Systems

Address: Via C. Colombo
1-A 20094 Corsico Milan
Italy
Tel: +39-024587521
Fax: +39-0245867074
email: bts@bts.it
Website: http://www.bts.it

Orthotrak II, Motion Analysis Corporation

Address: Motion Analysis Corporation
3617 westwind Blvd.
Santa Rosa, CA 95403
Tel: (707) 579-6500
Fax: (707) 526-0629
email: Info@MotionAnalysis.com
Website: http://www.motionanalysis.com

Qgait, Qualisys

Address: Goteborgsvagen 74,
433 63 Savedalen
SWEDEN
Tel: 031-336 94 00
Fax: 031-336 94 20
email: sales@qualisys.se
Website: http://www.qualisys.se

Rdata2, Motion Lab Systems

Address: 4326 Pine Park Drive,
Baton Rouge,
LA 70809-2397
USA

Tel: +1 (225) 928-4248

Fax: +1 (225) 928-4248

email: Sales@emgsrus.com

Website; http://www.emgsrus.com

References

Barnes S, Oggero E, Pagnacco G, Berme N (1997) Simulation of human movement: goals, model formulation, solution techniques and considerations, (edited by Allard P, Cappozzo A, Lundberg A, Vaughan CL) *Three Dimensional Analysis of Human Locomotion*, John Wiley and Sons, New York, Chapter 14, pp: 281-306.

Barth W, Reinschmidt C, Stussi E (1998) Comparison of different techniques to determine orientation, angular velocity and acceleration of a rigid body, with special consideration of end point errors, conference proceedings, *Fifth International Symposium on the 3D Analysis of Human Movement*, Chattanooga, Tennessee, USA pp: 58-61.

Brand RA, Crowninshield RD (1981) Comment on criteria for patient evaluation tools. *Journal of Biomechanics,* 14:655.

Brigham E.O. (1974) *The Fast Fourier Transform*, Prentice-Hall, Englewood Cliffs, NJ.

Cappello A, Cappozzo A, della Croce U, Leardini A (1997) Bone position and orientation reconstruction using external markers, (edited by Allard P, Cappozzo A, Lundberg A, Vaughan CL) *Three Dimensional Analysis of Human Locomotion*, John Wiley and Sons, New York, Chapter 8, pp: 147-171.

Cappozzo A, Paul JP (1997) Instrumental observations of human movement: historical development, (edited by Allard P, Cappozzo A, Lundberg A, Vaughan CL) *Three Dimensional Analysis of Human Locomotion*, John Wiley and Sons, New York, Chapter 1, pp: 1-25.

Cappozzo A, della Croce U, Lucchetti L (1997) Gait Data: Terminology and Definitions, (edited by Allard P, Cappozzo A, Lundberg A, Vaughan CL) *Three Dimensional Analysis of Human Locomotion*, John Wiley and Sons, New York, Chapter 7, pp: 129-146.

Chandler RF, Clauser CE, McConville JT, Reynolds HM & Young JW (1975), *Investigation of inertial properties of the human body* (Aerospace Medical Research Laboratory Tech. Rep No. 74-137) Dayton, OH: Wright-Patterson Air Force Base, AMRL. (Prepared for U.S. Department of Transportation, National Highway Traffic Safety, Administration, Contract No. DOT-HS-017-2-315-1A; National Technical Information Service No. AD-A016 485).

Chao EYS (1980) Justification of triaxial goniometer for the measurement of joint rotation. *Journal of Biomechanics,* 13:989-1006.

Daly EL, Bourke GJ, McGilvray J (1991) *Interpretation and Uses of Medical Statistics*, Blackwell Scientific Publications, pp:245-248.

Davis B. (1994a) Re: BSP parameters and human gait. *Biomch-L Archives*, May 1994, http://isb.ri.ccf.org/biomch-l/archives/biomch-l-1994-05/00109.html.

Davis B. (1994b) Errors in BSP data. *Biomch-L Archives,* June 1994, http://isb.ri.ccf.org/biomch-l/archives/biomch-l-1994-06/00013.html.

Davis RB, Õunpuu S, Tyburski D, Gage JR (1991) A gait analysis data collection and reduction technique. *Human Movement Science,* 10:575-587.

Davis RB, Õunpuu S, Deluca PA (1997) Gait data: Reporting, Archiving and Sharing, (edited by Allard P, Cappozzo A, Lundberg A, Vaughan CL) *Three Dimensional Analysis of Human Locomotion*, John Wiley and Sons, New York, Chapter 19, pp: 173-189.

Dempster WT, Gabel WC, Felts WJL (1959) The anthropometry of manual workspace for the seated subject. *American Journal of Physiological Anthropometry,* 17:289-317.

Fioretti S, Cappozzo A, Lucchetti L (1997) Joint Kinematics, (edited by Allard P, Cappozzo A, Lundberg A, Vaughan CL) *Three Dimensional Analysis of Human Locomotion*, John Wiley and Sons, New York, Chapter 9, pp: 173-189.

Furnée H (1997) Real time motion capture systems, (edited by Allard P, Cappozzo A, Lundberg A, Vaughan CL) *Three Dimensional Analysis of Human Locomotion*, John Wiley and Sons, New York, Chapter 5, pp: 85-108.

Grabiner MD, Feuerbach JW, Lundin TM, Davis BL (1995) Visual guidance to force plates does not influence ground reaction force variability. *Journal of Biomechanics*, 28 (9): 1115-1117.

Grood ES, Suntay WJ (1983) A joint coordinate system for the clinical description of three-dimensional motions: Application to the knee. *ASME Journal of Biomechanical Engineering,* 105: 136-144.

Growney E, Meglan D, Johnson M, Cahalan T, An K (1997) Repeated measures of adult normal walking using a video tracking system. *Gait & Posture*, 6 (2): 147-162.

Hamming R.W (1983) *Digital Filters*, Prentice-Hall, Englewood Cliffs, NJ.

Heshler C, Milner M (1978) An optimality criterion for processing electromyographic (EMG) signals relating to human locomotion. *Transactions in Biomedical Engineering*, 25: 413-420.

Jackson K.M (1979) Fitting of mathematical functions to biomechanical data. *IEEE Transactions on Biomedical Engineering*, pp: 122-124.

Kadaba MP, Ramakrishnan HK, Wootten ME, Gainey J, Gorton G, Cochran GVB (1989) Repeatability of kinematic, kinetic and electromyographic data in normal adult gait. *Journal of Orthopaedic Research,* 7(6):849-860.

Kadaba MP, Ramakrishnan HK, Wootten ME (1990) Measurement of lower extremity kinematics during level walking. *Journal of Orthopaedic Research,* 8:383-392.

Lynn PA, Fuerst W (1989) *Introductory Signal Processing with Computer Applications*, John Wiley and Sons, New York, Chapter 2, pp: 41-50.

Miller I, Freund JE (1985) *Probability and statistics for engineers* third edition, Prentice Hall Inc., Englewood Cliffs, NJ.

Rose J, Gamble JG (1994) *Human Walking* second edition, Williams and Wilkins, London.

Siegler S, Liu W (1997) Inverse dynamics in human locomotion, (edited by Allard P, Cappozzo A, Lundberg A, Vaughan CL) *Three Dimensional Analysis of Human Locomotion*, John Wiley and Sons, New York, Chapter 10, pp: 191-209.

Vaughan CL (1996) Are joint torques the Holy Grail of human gait analysis? *Human Movement Science,* 15:423-443.

Vaughan CL, Davis BL, O'Connor J (1992) *Dynamics of Human Gait*, Human Kinetics Publishers, Champaign IL.

Vaughan CL, Davis BL, O'Connor J (1999*) Dynamics of Human Gait,* (Second Edition), Kiboho Publishers, Cape Town, SA.

Vaughan CL (1982) Smoothing and differentiation of displacement-time data: An application of splines and digital filtering. *International Journal of Bio-Medical Computing*, 13:375-386.

Vaughan CL (1983) Forces and moments at the hip, knee and ankle joints. *Annual Report of the Oxford orthopaedic Engineering Centre*, 10:17-18.

Walker RM, Faulkner JC (1983) *An Introduction to Newtonian Mechanics*, Juta & Company, Ltd., Johannesburg, SA.

Whittle M (1991). *Gait Analysis: An Introduction*, Butterworth-Heinemann, Ltd., Oxford, England.

Whittle MW, Ferris KJ (1993) Effects of walkway carpeting on gait analysis data, conference proceedings, *East Coast Clinical Gait Analysis Meeting*, Mayo Clinic, Rochester, Minnesota, USA, May 5-8, 1993, http://guardian.curtin.edu.au/cga/faq/carpet.html.

Winter, DA (1991) *The biomechanics & motor control of human gait: normal, elderly & pathological*, 2nd edition, University of Waterloo Press, Waterloo, Ont., Canada.

Woltring HJ (1994) 3-D attitude representation of human joints: A standardisation proposal, *Journal of Biomechanics*, 27(12) 1399-1414.